ECOGRAPHY

LandsatTS: an R package to facilitate retrieval, cleaning, cross-calibration, and phenological modeling of Landsat time-series data

Journal:	*Ecography*
Manuscript ID	Draft
Wiley - Manuscript type:	Software Note
Keywords:	Landsat, NDVI, spectral index, sensor calibration, greening, browning
Abstract:	The Landsat satellites provide decades of near-global surface reflectance measurements that are increasingly used to assess interannual changes in terrestrial ecosystem function. These assessments often rely on spectral indices related to vegetation greenness and productivity (e.g., NDVI). Nevertheless, multiple factors impede multi-decadal assessments of spectral indices using Landsat satellite data, including ease of data access and cleaning, as well as lingering issues with cross-sensor calibration and challenges with irregular timing of cloud-free acquisitions. To help address these problems, we developed the LandsatTS package for R. This software package facilitates sample-based time series analysis of surface reflectance and spectral indices derived from Landsat sensors. The package includes functions that enable the extraction of the full Landsat 5, 7, and 8 records from Collection 2 for point sample locations or small study regions using the Google Earth Engine accessed directly from R. Moreover, the package includes functions for (1) rigorous data cleaning, (2) cross-sensor calibration, (3) phenological modeling, and (4) time series analysis. For an example application, we show how LandsatTS can be used to assess changes in annual maximum vegetation greenness from 2000 to 2022 across the Noatak National Preserve in northern Alaska, USA. Overall, this software provides a suite of functions to enable broader use of Landsat satellite data for assessing and monitoring terrestrial ecosystem function during recent decades across local to global geographic extents.

SCHOLARONE™
Manuscripts

Abstract

The Landsat satellites provide near-global surface reflectance measurements since the early 1980s that are increasingly used to assess interannual changes in terrestrial ecosystem function. These assessments often rely on spectral indices related to vegetation greenness and productivity (e.g., NDVI). Nevertheless, multiple factors impede multi-decadal assessments of spectral indices using Landsat satellite data, including ease of data access and cleaning, as well as lingering issues with cross-sensor calibration and challenges with irregular timing of cloud-free acquisitions. To help address these problems, we developed the *LandsatTS* package for R. This software package facilitates sample-based time series analysis of surface reflectance and spectral indices derived from Landsat sensors. The package includes functions that enable the extraction of the full Landsat 5, 7, and 8 records from Collection 2 for point sample locations or small study regions using the Google Earth Engine accessed directly from R. Moreover, the package includes functions for (1) rigorous data cleaning, (2) cross-sensor calibration, (3) phenological modeling, and (4) time series analysis. For an example application, we show how *LandsatTS* can be used to assess changes in annual maximum vegetation greenness from 2000 to 2022 across the Noatak National Preserve in northern Alaska, USA. Overall, this software provides a suite of functions to enable broader use of Landsat satellite data for assessing and monitoring terrestrial ecosystem function during recent decades across local to global geographic extents.

For Review Only

Background

Satellite remote sensing is crucial for assessing and monitoring how Earth's terrestrial ecosystems have changed during recent decades (National Academies of Sciences 2018). The Landsat satellites are particularly valuable in this regard because they are the longest continuously running satellite program and were designed for terrestrial ecosystem monitoring at moderate spatial resolution (Wulder et al. 2019). The first Landsat satellite (Landsat 1) was launched in 1972 as a partnership between NASA and the US Geological Survey (USGS) and since that time a series of additional satellites have been launched, with the most recent being Landsat 9 in 2021. The Landsat satellites carry multispectral sensors that provide surface reflectance measurements used for a wide range scientific and land management applications (Wulder et al. 2019). These include global monitoring of forest canopy cover change (Hansen et al. 2013, Sexton et al. 2013), land cover and use change (Potapov et al. 2022) and surface water extent change (Pekel et al. 2016), as well as regional- to biome-scale assessments of how disturbance, land-use and climate change are impacting terrestrial ecosystems (e.g., Wulder et al. 2004, Powell et al. 2010, Ju and Masek 2016, Wang and Friedl 2019). Hence, the Landsat program has become a cornerstone of Earth surface monitoring. Yet there are challenges that hinder use of these data by ecologists, land managers, and other non-remote sensing specialists.

Here we present the *LandsatTS* (i.e., *Landsat Time Series*) software package for R that enables users to extract, process, and analyze time series of Landsat surface reflectance measurements for sample locations anywhere on Earth. *LandsatTS* enables extraction of Landsat 5, 7, and 8 surface reflectance measurements from the full Landsat Collection 2 dataset on Google Earth Engine (GEE; Gorelick et al. 2017). Furthermore, *LandsatTS* includes functions that facilitate (1) data cleaning, (2) cross-sensor calibration, (3) phenological modeling, and (4) time series analysis of vegetation greenness (Figure 1, Table 1). This software grew out of research projects focused on vegetation dynamics across northern high-latitude ecosystems (Berner et al. 2020, Berner and Goetz 2022) and is implemented within the free, open-source, and widely used R statistical computing environment (R Core Team 2021).

It has become easier to access and process Landsat data since the archive was made publicly available in 2008 (Wulder et al. 2012) and a copy of the archive subsequently hosted on GEE (Gorelick et al. 2017). The GEE cloud-computing platform enables users to access and process Landsat data using JavaScript and Python application program interfaces (APIs), as well as with R through the *rgee* package (Aybar et al. 2020). R is very popular among ecologists (Lai et al. 2019), yet other existing R packages only provide tools for processing individual Landsat scenes. For instance, *landsat* includes functions for radiometric and topographic correction of Landsat scenes (Goslee 2011), while *landsat8* includes functions for computing top of atmosphere reflectance, radiance, and/or brightness temperature on Landsat scenes (dos Santos 2017). Thus, the *rgee* package makes it easier for ecologists use the GEE platform and work with Landsat data. Nevertheless, it remains non-trivial to not only extract Landsat time series data using *rgee*, but also to thoroughly clean the extracted data to ensure that only high-quality measurements are used in analyses. *LandsatTS* therefore provides new tools for sample-based extraction of full Landsat data records using *rgee* to access the GEE. Furthermore, *LandsatTS* includes tools to rigorously clean Landsat data using both pixel-level CFmask flags (e.g., cloud, water; Zhu et al. 2015) and scene-level criteria (e.g., cloud cover, solar zenith angle). Consequently, *LandsatTS* helps further broaden the community of researchers who can utilize Landsat data for robust spatiotemporal analyses of terrestrial ecosystem dynamics.

Landsat time series analyses that use measurements from multiple sensors are hindered by systematic biases in spectral bands and indices among the Landsat 5 Thematic Mapper (TM), Landsat 7 Enhanced Thematic Mapper Plus (ETM+), and Landsat 8 Operational Land Imager (OLI) sensors (Ju and Masek 2016, Roy et al. 2016, Berner et al. 2020, Berner and Goetz 2022). If unaccounted for, these biases can introduce pronounced artificial trends into combined time series, such as spurious increases over time in spectral indices of vegetation greenness including the widely used Normalized Difference Vegetation Index (NDVI) (Sulla-Menashe et al. 2017). Prior approaches for cross-sensor calibration focused on linear corrections for individual spectral bands and select spectral indices (e.g., NDVI) using regional data (e.g., continental USA) from Landsat Collection 1 (e.g., Ju and Masek 2016, Roy et al. 2016). While valuable, these published cross-sensor calibration models do not account for potential non-linearities, may not be suitable for other regions, and may not be appropriate for the newer Landsat Collection 2 dataset. Therefore, *LandsatTS* includes functions to cross-calibrate spectral bands and indices among Landsat 5, 7, and 8 using either random forest machine learning or polynomial regression models. These models are fit using the user's dataset. However, if the user's dataset is too small to fit these models, then, if appropriate, the user can choose to fit models using pre-processed and staged Landsat data that were sampled from across the Arctic tundra and boreal forest biomes. Flexible implementation of cross-sensor calibration in the *LandsatTS* workflow enables the user to generate high quality time-series that are free from sensor-specific biases that can otherwise induce spurious trends.

Vegetation phenology controls ecosystem processes (e.g., photosynthesis) and is often assessed using spectral indices (e.g., NDVI) derived from satellite measurements (Helman 2018, Zeng et al. 2020). Nevertheless, efforts to assess vegetation phenology using the Landsat satellites are complicated by multiple factors that include (1) irregular timing of clear-sky acquisitions within a growing season and (2) changes in the annual number of clear-sky acquisitions across years as new satellites were launched. These challenges are especially acute in regions with short, cloudy growing seasons such as the Arctic, where the median number of clear-sky growing season measurements increased from 2 per year in 1995 to 7 per year in 2015

For Review Only

(Berner et al. 2020). Annual maximum vegetation greenness is an important metric of vegetation phenology related to productivity (Berner et al. 2020, Zeng et al. 2020, Boyd et al. 2021), yet this metric is sensitive to the timing and number of measurements made in a growing season. Consequently, simple calculations of this metric tend to be artificially low early in the Landsat record but less so during later years when more measurements are available, which can introduce a spurious positive trend into a time series (Berner et al. 2020). To address this issue, *LandsatTS* includes tools to estimate annual maximum vegetation greenness based on site-specific phenological modeling that iteratively fits cubic splines to vegetation greenness time series. Users interested in other aspects of vegetation phenology (e.g., timing of spring onset or fall senescence) could extract and process Landsat data using *LandsatTS*, but then capitalize on tools provided by other R packages, such as the new *phenofit* package that provides state-of-the-art tools for fitting phenological models (Kong et al. 2022). More broadly, while *LandsatTS* provides tools focused on generating high-quality vegetation greenness times series, it also enables users to undertake other analyses that rely on cleaned and cross-calibrated Landsat data.

LandsatTS includes an integrated suite of tools that were originally developed to assess long-term changes in vegetation greenness within the rapidly warming Arctic tundra and boreal forest biomes (Berner et al. 2020, Berner and Goetz 2022). This software implements a sample-based approach that we found is well-suited for assessing vegetation dynamics and evaluating ecological hypotheses in these cold northern biomes, while substantially reducing computational burden compared with wall-to-wall analyses. The sample-based approach is conducive to rigorous propagation of uncertainty using Monte Carlo simulations (Berner et al. 2020, Berner and Goetz 2022), which is important for improving confidence in remote sensing analyses but seldom carried out because of computational constraints (Myers-Smith et al. 2020). Furthermore, the sample-based approach has helped validate and interpret vegetation dynamics inferred from spectral indices by enabling comparisons between satellite and field measurements across widely distributed site networks (Boyd et al. 2019, Berner et al. 2020, Boyd et al. 2021, Walker et al. 2021). These tools have also been used to assess high-latitude vegetation responses to insect outbreaks (Boyd et al. 2019, Boyd et al. 2021), wildfires (Gaglioti et al. 2021), and permafrost degradation (Verdonen et al. 2020), as well as for syntheses focused on high-latitude disturbance regimes (Foster et al. 2022) and Arctic shrubification (Mekonnen et al. 2021). Among other applications, these tools could further be used to complement field-based ecosystems monitoring in protected areas, evaluate ecosystem impacts of extreme weather events (e.g., droughts), and improve local to global mapping efforts by enabling users to develop regression models for cross-sensor calibration. In summary, *LandsatTS* enables ecologists and other researchers to extract and process Landsat time series that can then be used to analyze vegetation phenology or for other user-defined applications. Below, we provide (1) an example application focused on vegetation dynamics across the Noatak National Preserve, USA, (2) instructions for package installation, and (3) descriptions of each function.

For Review Only

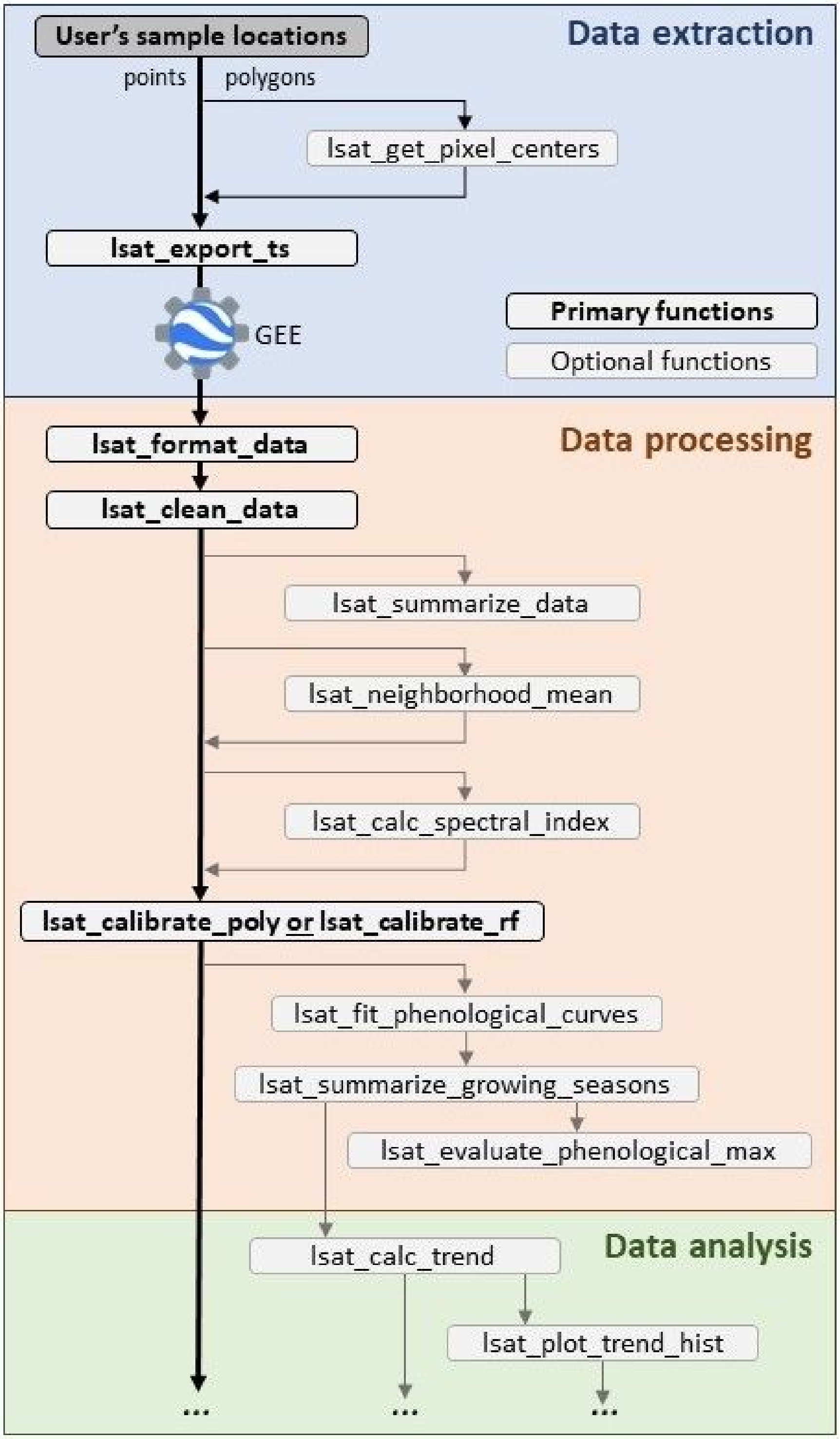

Figure 1. Schematic illustrating functions and typical workflow of the *LandsatTS* package. Each function is described in the main text and Table 1. *LandsatTS* has primary been used for assessments of interannual variability and trends in vegetation greenness. However, *LandsatTS* facilitates other Landsat time series analyses by providing tools for general data extraction and processing.

Table 1. Function names and descriptions. These are listed in the order typically used.

Step	Function	Description
Data extraction	lsat_get_pixel_centers	(*Optional*) Retrieve point coordinates of all Landsat 8 pixel centers that fall within a polygon.
	lsat_export_ts	Export full Landsat surface reflectance time series for a set of point coordinates using GEE accessed from R.
Data processing	lsat_format_data	Prepare data exported from GEE, including parsing satellite names and renaming and scaling bands.
	lsat_clean_data	Filter out measurements based on presence of clouds, water, shadows, oblique view angles, and other criteria.
	lsat_summarize_data	(*Optional*) Summarize data availability at each site, such as total number and years of observations.
	lsat_neighborhood_mean	(*Optional*) For buffered sites, compute band-wise mean surface reflectance across grid cells within the buffer.
	lsat_calc_spectral_index	Calculate a variety of widely used spectral indices, such as the Normalized Difference Vegetation Index (NDVI).
	lsat_calibrate_rf	Cross-calibrate bands or spectral indices from Landsat 5/8 to match Landsat 7 using Random Forest models.
	lsat_calibrate_poly	Cross-calibrate bands or spectral indices from Landsat 5/8 to match Landsat 7 using polynomial regression.
	lsat_fit_phenological_curves	Characterize seasonal land surface phenology at each site by iteratively fitting flexible cubic splines.
	lsat_summarize_growing_seasons	Estimate various phenological metrics from fitted cubic splines, such as annual maximum vegetation greenness.
	lsat_evaluate_phenological_max	(*Optional*) Evaluate estimates of annual maximum vegetation greenness with measurement availability.
Data analysis	lsat_calc_trend	Calculate temporal trends using non-parametric Mann-Kendall trend tests and Theil-Sen slope indicators.
	lsat_plot_trend_hist	Plots a histogram of trends across sample sites

Example application: Vegetation greenness trends in the Noatak National Preserve, USA

Here we provide an example analysis of interannual changes in vegetation greenness from 2000 to 2022 within the Noatak National Preserve in northern Alaska, USA (Figure 2). The Noatak National Preserve is a vast wilderness of mountainous Arctic and alpine tundra that encompasses the largest undisturbed watershed in North America. The preserve is about 2.6 million hectares of roadless lands that were designated in 1980 to maintain ecological integrity, protect habitat and archeological resources, and provide opportunities for scientific research. Recent ecological research found climate warming substantially increased growth rates of white spruce (*Picea glauca*) and led to rapid expansion of trees and tall shrubs into tundra over the past half century in parts of the preserve (Suarez et al. 1999, Terskaia et al. 2020, Dial et al. 2022). The impacts of climate change are increasingly evident in the Noatak National Preserve and underscore the importance of sustained and cost-effective ecological monitoring and assessment.

Annual maximum vegetation greenness is related to tundra aboveground biomass and productivity, making it an important ecological metric that can be monitored using satellite remote sensing (Jia et al. 2003, Raynolds et al. 2012, Berner et al. 2018, Bhatt et al. 2021). We therefore demonstrate how multidecadal changes in annual maximum vegetation greenness can be readily assessed across the preserve using Landsat satellite data. In this section, we guide the reader through the analysis code with example output figures and tables that are generated by the *LandsatTS* functions.

For Review Only

Part 1: Export Landsat time series from Google Earth Engine

To start, we create a random sample of points within the Noatak National Preserve and then export Landsat time series for each sample point using GEE (Code Box 1). To facilitate our example, we include the preserve boundary as a simple feature polygon dataset ("noatak.sf") in *LandsatTS*. Users could alternatively read in their own shapefile using *sf::st_read()* or create a collection of spatial points (e.g., field sites) using *sf::st_sf()* (Pebesma 2018). We load the preserve boundary dataset, create a simple random sample of *n* points within the boundary using the *sf::st_sample* function, give each sample a unique identifier, and then create an interactive map showing preserve and sample point locations using *leaflet* (Figure 2) (Cheng et al. 2022). We then initialize GEE and submit a task to GEE that for each sample point exports all Landsat 5, 7, and 8 measurements made between day of year 152 (beginning of June) and 273 (end of September) from 1985 to 2022. For expediency, this example exports data for three random sample points, which took ~11 minutes and yielded ~800 B of data written to a folder called "earth_engine" on the user's Google Drive. Exporting four decades of summer Landsat data for 100 sample points took ~6 hours and yielded ~28 MB of data, while exporting data for 1,000 sample points took ~15 hours with four tasks running in parallel and yielded ~280 MB of data. To facilitate subsequent parts of this example, we include Landsat data for 100 sample points as a dataset ("noatak.dt") in *LandsatTS*. Data export progress can be monitored using the GEE task manager in the web browser (https://code.earthengine.google.com/tasks) or with the R console using the ee_monitoring() function provided by *rgee*. The CSV file(s) containing the raw exports need to be copied from the user's Google Drive to the local machine that will carry out the subsequent processing using *LandsatTS*. The files can be copied manually or using the ee_drive_to_local() function provided by *rgee*. Once the records are available locally, they need to be cleaned and processed into vegetation index time series as detailed in the next section.

Code Box 1: Export Landsat time series from Google Earth Engine

```
 # Load required R packages
require(LandsatTS)
require(sf)
require(rgee)
require(tidyverse)
require(leaflet)

# Load the Noatak National Preserve simple feature polygon
data(noatak.sf)

# Create n random sample points within the Noatak National Preserve
n.pts <- 3
noatak.pts.sf <- st_sample(x = noatak.sf, size = n.pts) %>% st_sf()

# Add unique identifier to each point
noatak.pts.sf$sample_id <- paste0('S_', 1:n.pts)

# Make a basic interactive map showing Noatak National Preserve and sample points
leaflet() %>%
  addProviderTiles('Esri.WorldImagery') %>%
  addCircleMarkers(data = noatak.pts.sf,
                   color = 'white',
                   opacity = 0.9,
                   fillColor = 'fuchsia',
```

```
                   fillOpacity = 0.75,
                   weight = 1,
                   radius = 5) %>%
  addPolygons(data = noatak.sf,
              color = 'white',
              weight = 3) %>%
  addScaleBar(options = scaleBarOptions(imperial = F))

# Initialize Earth Engine
ee_Initialize()

# Extract a time-series of surface reflectance measurements for each Landsat pixel
task_list <- lsat_export_ts(pixel_coords_sf = noatak.pts.sf,
                            start_date = "1985-06-01",
                            end_date = "2022-09-30",
                            start_doy = 152,
                            end_doy = 273,
                            file_prefix = 'noatak',
                            drive_export_dir = 'earth_engine')
```

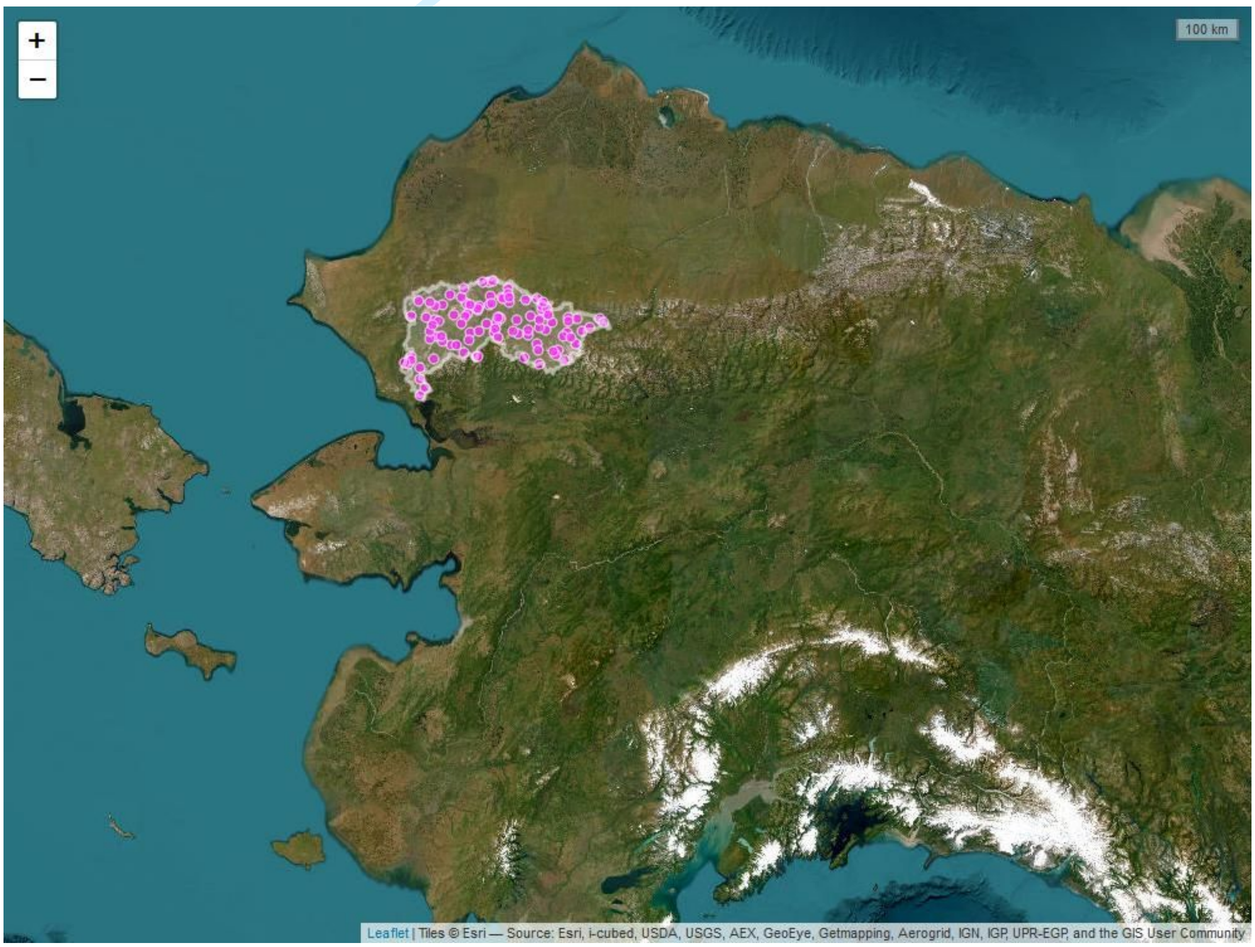

Figure 2. Screenshot of a *leaflet* interactive map showing the Noatak National Preserve boundary in northern Alaska, USA, and 100 random sample points within the preserve. Landsat time series data were extracted for each of these sample points. Base map from ESRI World Imagery.

Part 2: Format, clean, and summarize Landsat data in preparation for analysis

We load the Landsat data into R, format and clean the data, and then examine data availability. Here, we provide Landsat data for the 100 sample points as a dataset in *LandsatTS*; however, the dataset alternatively could be read into R as a data.table using the *fread()* function from the *data.table* package (Dowle and Srinivasan 2021). Once loaded into R, we format the dataset for analysis using *lsat_format_data()*, which formats column names and scales the band values, among other necessary formatting. We then clean the dataset using *lsat_clean_data()* to filter out clouds, snow, and water, as well as radiometric and geometric errors. For these field sites, *lsat_clean_data()* removed 78,625 of 99,600 observations (78.94%), including one sample point located in water. We then check the availability of clear-sky Landsat observations for the remaining 99 sample points using *lsat_summarize_data*(). On average (± 1 SD), each sample point had 212±48 clear-sky observations made between 1985 and 2022. The annual number of observations is typically small before the year 2000, as highlighted by the figure generated by the function (Figure 3).

Code Box 2: Format, clean, and summarize Landsat data in preparation for analysis

```
# Load required R packages
require(LandsatTS)
require(data.table)
require(tidyverse)
require(sf)
require(leaflet)
require(mapview)

# Load Landsat data for Noatak sites, or read in file using data.table::fread().
data(noatak.dt)

# Format the exported data
noatak.dt <- lsat_format_data(noatak.dt)

# Clean the data by filtering out clouds, snow, water, etc.
noatak.dt <- lsat_clean_data(noatak.dt)

# Summarize the availability of Landsat data for each pixel
lsat_summarize_data(noatak.dt)

# Continue to Code Box 3...
```

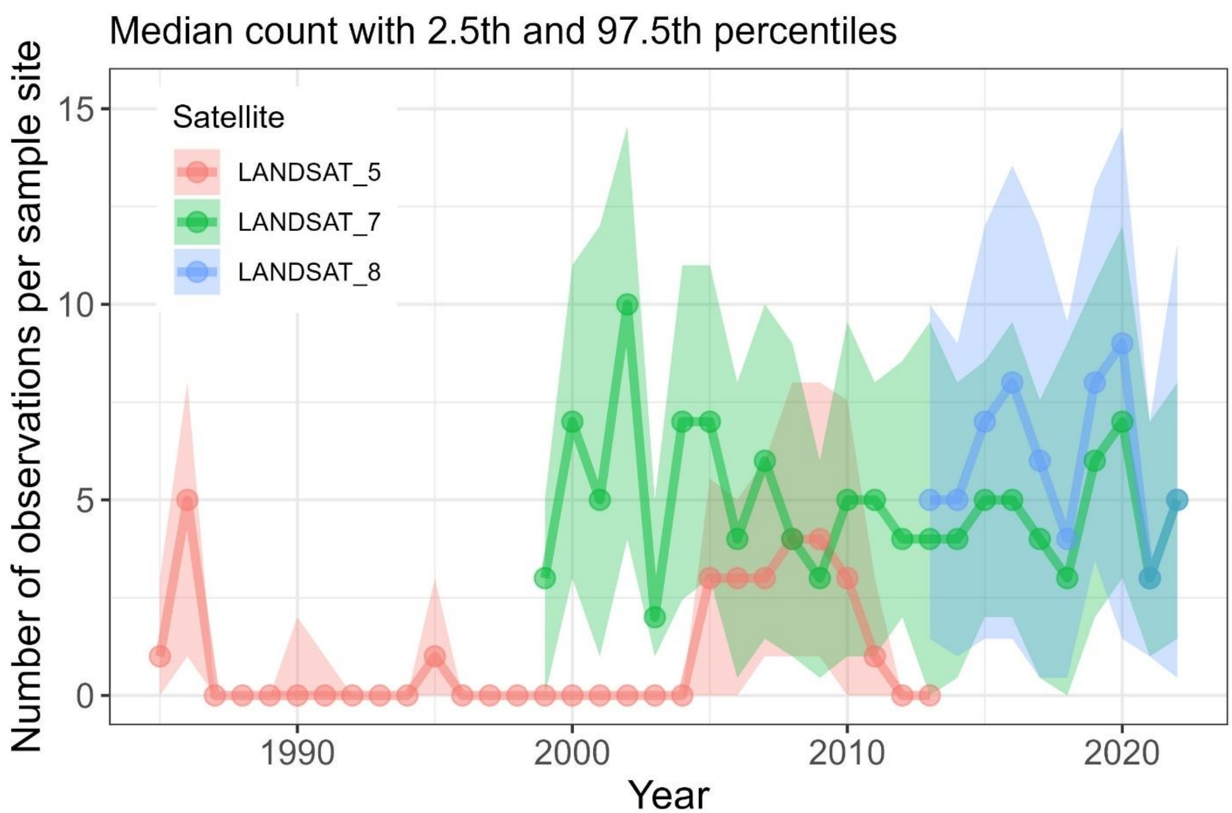

Figure 3. Annual availability of quality screened summer Landsat observations summarized across sample points in the Noatak National Preserve as returned by the function *lsat_summarize_data()*. Summaries are based on observations acquired between day of year 152 (beginning of June) and 273 (end of September). Note the limited availability of observations before the year 2000. Lines with points denote median counts while shaded bands encompass the 2.5th to 97.5th percentiles of counts among sample points.

Part 3: Generate cross-calibrated time series of annual maximum vegetation greenness

To generate time series of annual maximum vegetation greenness for each sample point, we (1) compute NDVI, (2) cross-calibrate NDVI among Landsat sensors, and then (3) estimate annual maximum NDVI (NDVImax) using phenological modeling. First, we calculate NDVI using *lsat_calc_spectral_index()*, which supports calculating a variety of commonly used spectral indices. There are systematic differences in NDVI among Landsat sensors, so next we calibrate NDVI from Landsat 5 TM and Landsat 8 OLI to match Landsat 7 ETM+, which has measurements that temporally overlap with the other two sensors. We cross-calibrate NDVI among sensors using *lsat_calibrate_poly()* to fit and apply polynomial regression models. As the number of field sites in this dataset is rather small, we use a pre-processed dataset of Landsat observations that were randomly sampled from across northern high-latitudes ecosystems and are included for this purpose with *LandsatTS*. The function generates and returns a series of graphs (Figure 4) and tabular data (Table 3) that help with evaluating model performance and can optionally be written to a user-specified directory. As desired, calibration visually (Figure 4) and statistically (Table 3) reduced the bias between Landsat 7 NDVI and Landsat 5 and 8 NDVI.

As a step towards estimating annual $NDVI_{max}$, we fit phenological models to the calibrated NDVI time series using *lsat_fit_phenological_curves()*. The function automatically returns a figure with Landsat observations and fitted phenological curves for nine random sample locations in the dataset (Figure 5). Each phenological curve characterizes the seasonal progression of NDVI using observations pooled over a multi-year period (here a 7-year moving window) and should be smooth and hump-shaped. Beware of phenological curves with long straight lines that could suggest inadequate seasonal distribution of data used when fitting the curves. Phenological models were not fit for three sites that were minimally vegetated (NDVI < 0.15) because it is challenging to extract a meaningful vegetation phenology signal under these conditions. After fitting phenological models for 22 field sites, we then generated growing season summary statistics, including estimates of $NDVI_{max}$, using *lsat_summarize_growing_seasons()*. The *lsat_evaluate_phenological_max()* can be used to output a figure that allows for visually assessing the performance of modelled $NDVI_{max}$ (Figure 6). In the case of the Noatak example dataset, modeled estimates of $NDVI_{max}$ tend to be biased slightly low (~1%) when only one or two observations are available from a growing season (Figure 6), yet there were rarely such few observations during the period from 2000 to 2021 (Figure 3). The final step following the cross-calibration and phenological modelling is the time series analysis.

Code Box 3: Cross-calibration and phenological modelling

```
# ... continuing from Code Box 2

# Compute the Normalized Difference Vegetation Index (NDVI)
noatak.dt <- lsat_calc_spectral_index(noatak.dt, si = 'ndvi')

# Cross-calibrate NDVI among sensors using polynomial regression
noatak.dt <- lsat_calibrate_poly(noatak.dt,
                             band.or.si = 'ndvi',
                             train.with.highlat.data = T,
                             overwrite.col = T)

# Fit phenological models (cubic splines) to each time series
noatak.pheno.dt <- lsat_fit_phenological_curves(noatak.dt, si = 'ndvi')

# Summarize growing season characteristics
noatak.gs.dt <- lsat_summarize_growing_seasons(noatak.pheno.dt, si = 'ndvi')

# Evaluate estimates of annual maximum NDVI
noatak.gs.eval.dt <- lsat_evaluate_phenological_max(noatak.pheno.dt, si = 'ndvi')

# Continue to Code Box 4...
```

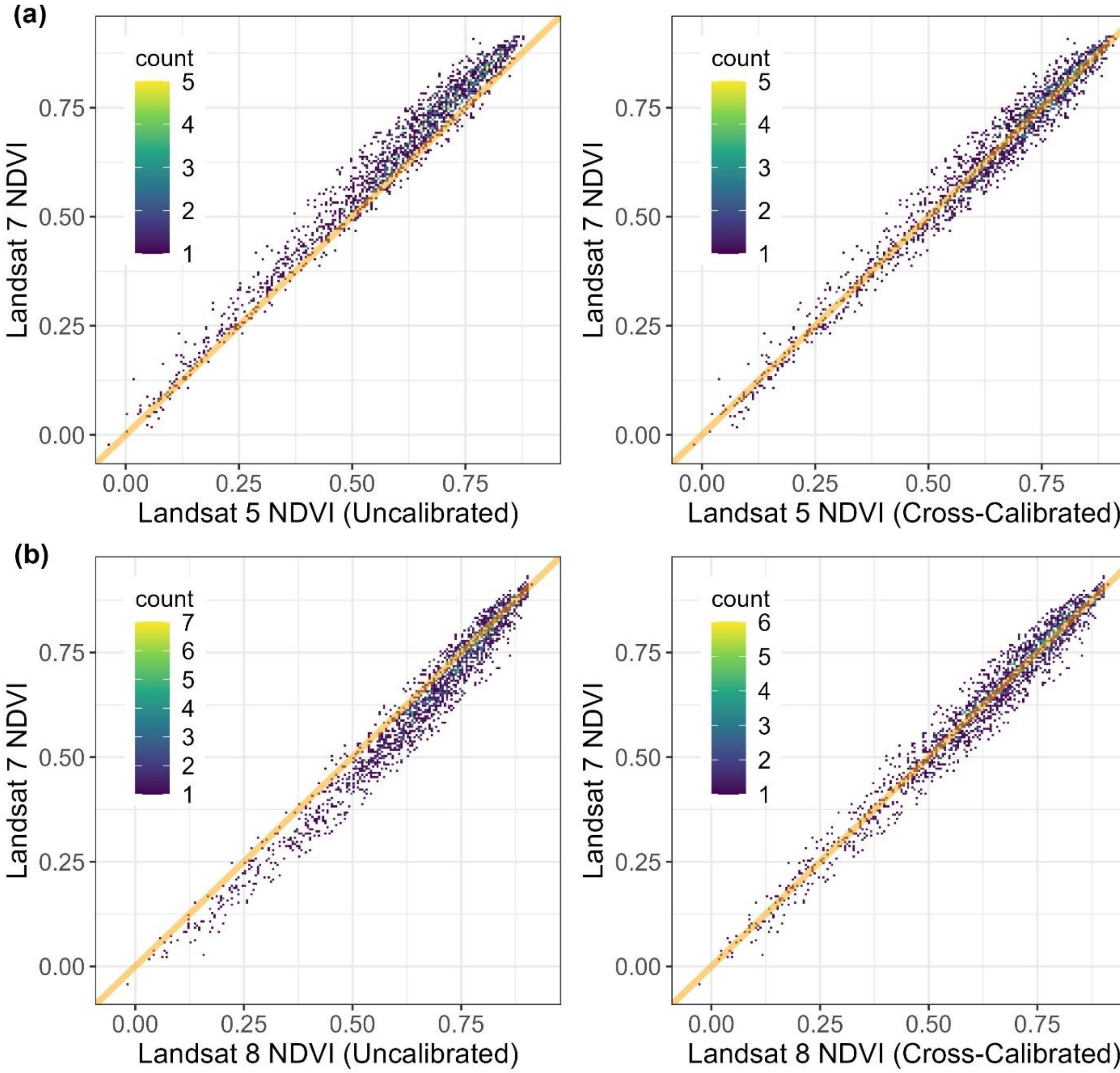

Figure 4. Relationships between Landsat 7 NDVI and both (a) Landsat 5 NDVI and (b) Landsat 8 NDVI using (left panels) original data and (right panels) data that were calibrated using polynomial regression models. Each point is a sample location from the Arctic – Boreal domain with temporally overlapping measurements from pairs of Landsat sensors. Orange diagonal lines depict 1:1 relationships. Model performance metrics are provided in Table 3. Cross-calibration substantially reduces biases between sensors.

Table 3. Summary of original biases, performance of polynomial regression models for cross-sensor calibration, and post-calibration biases in NDVI between Landsat 7 ETM+ and either Landsat 5 TM or Landsat 8 OLI. Each model was trained using 75% of available data selected at random and then cross-validated using the remaining 25% of data.

Satellite sensor	Number of sites		Original Data			Cross-Validated Error Metrics			
	Train	Eval.	RMSE	Median bias	Median % bias	r^2	RMSE	Median bias	Median % bias
Landsat 5 TM	5237	1746	0.052	-0.04	-6.1	0.974	0.032	<0.01	<0.1

Landsat 8 OLI	5927	1976	0.050	0.03	4.9	0.965	0.035	<0.01	<0.1

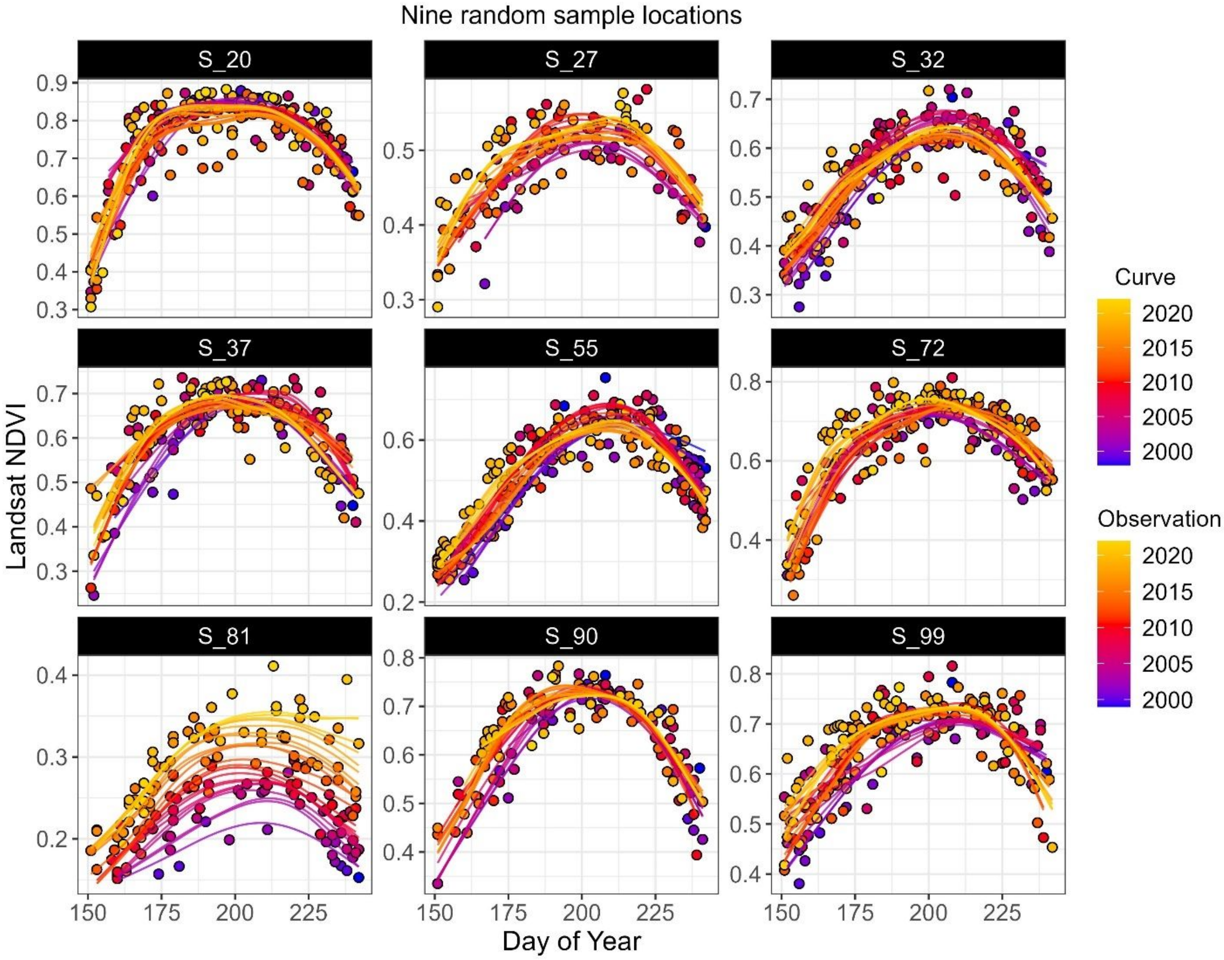

Figure 5. Seasonal progression of Landsat NDVI and phenological curves for nine random sample points in the Noatak National Preserve. Each dot is an observation that is colored by the year of acquisition ranging between 1985 and 2022. Each line represents a phenological curve that was fit to observations pooled over a 7-year window centered on the focal year as indicated by the color of the line. Color coding helps illustrate how individual curves are fit to observations. These figures can visually highlight long-term changes in phenology and can provide a quick visual assessment of how well curves are being fit to observations, especially when the function is run using the parameter *test.run* = TRUE.

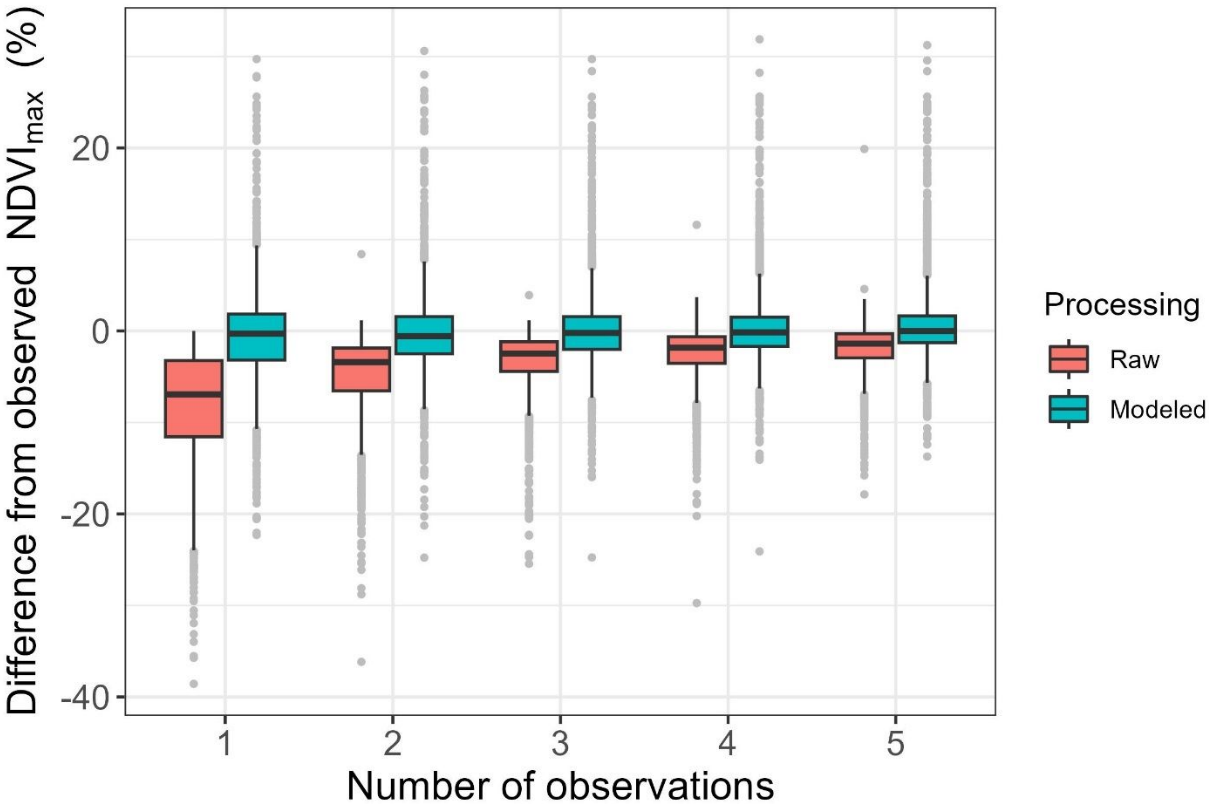

Figure 6. Raw estimates of annual maximum NDVI ($NDVI_{max}$) are biased low when only a few Landsat observations are available from a given growing season, whereas phenologically modeled estimates of $NDVI_{max}$ are minimally impacted by the availability of observations. The figure summarizes how raw and modeled estimates of $NDVI_{max}$ differ from observed $NDVI_{max}$ based on number of observations, as determined using *lsat_evaluate_phenological_max().*

Part 3: Analyze vegetation greenness time series

Finally, we evaluate the interannual trend in $NDVI_{max}$ from 2000 to 2022 for each sample point. We calculate temporal trends using the *lsat_calc_trend()* function that implements and summarizes non-parametric trend assessments (Table 4). Note how we use the "yrs" argument to restrict the time series analysis to the years between 2000-2022 to avoid using the low number of observations in the record prior to the turn of the millennium. We then create a histogram of recent $NDVI_{max}$ trends using *lsat_plot_trend_hist()* (Figure 7) and also create an interactive map showing the trend at each sample point (Figure 8). These figures indicate extensive greening across the study area in recent decades.

Code Box 4: Analyze and visualize vegetation greenness time series

```
# ... continuing from Code Box 3

# Compute temporal trend in annual NDVImax for each sample point
noatak.trend.dt <- lsat_calc_trend(noatak.gs.dt, si = 'ndvi.max', yrs = 2000:2022)

# Plot histogram of trends across sample points
lsat_plot_trend_hist(noatak.trend.dt, xlim = c(-21,21))

```

```
# Create an interactive map showing NDVI trends
colors.dt <- data.table(trend.cat = c("greening","no_trend","browning"),
                        trend.color = c("green","white","brown"))

noatak.trend.dt <- noatak.trend.dt[colors.dt, on = 'trend.cat']

noatak.trend.sf <- st_as_sf(noatak.trend.dt,
                            coords = c("longitude", "latitude"),
                            crs = 4326)

leaflet() %>%
  addProviderTiles('Esri.WorldImagery') %>%
  addPolylines(data = noatak.sf, color = 'white', weight = 3) %>%
  addCircleMarkers(data = noatak.trend.sf,
                   color = 'white',
                   weight = 1,
                   opacity = 0.9,
                   fillColor = ~trend.color,
                   fillOpacity = 0.5,
                   radius = ~sqrt(abs(total.change.pcnt))*3) %>%
  setView(-160, 68, zoom = 7) %>%
  addLegend('bottomright',
            colors = colors.dt$trend.color,
            labels = colors.dt$trend.cat,
            title = 'NDVImax trend',
            opacity = 1)

# End of code examples
```

Table 4. Abridged summary of $NDVI_{max}$ trends from 2000 to 2022 for each sample point (Sample ID) as generated using the function *lsat_calc_trend()*.Trends were assessed for each sample point by removing temporal autocorrelation and then applying a Mann-Kendall trend test (tau statistic and p-value provided). Slopes were calculated using the Theil-Sen slope estimators.

Sample ID	Latitude	Longitude	N	Slope	Intercept	Tau	P-value	Total change	Total change (%)
S_1	67.70765	-157.404	22	0.00109	0.5918	0.181	0.2639	0.025	4.2
S_10	68.23443	-158.416	23	0.00127	0.6144	0.091	0.5728	0.029	4.7
S_11	67.8104	-157.097	21	0.0017	0.6366	0.105	0.5376	0.039	6.1
S_12	67.81419	-160.017	23	0.00155	0.6943	0.108	0.4986	0.036	5.2
S_13	68.12915	-161.226	23	0.00209	0.5268	0.541	< 0.001	0.048	9.1
S_14	68.26632	-157.32	23	0.00067	0.2369	0.403	0.0095	0.015	6.3
S_15	67.87087	-156.911	22	0.00073	0.6307	0.01	0.9759	0.017	2.7
S_16	68.18229	-156.824	23	0.00048	0.6445	0.065	0.693	0.011	1.7
S_17	67.64494	-158.002	23	0.00314	0.6726	0.541	< 0.001	0.072	10.7
S_18	67.94227	-161.809	23	-0.00086	0.7419	-0.152	0.3377	-0.020	-2.7
S_19	67.76848	-162.447	23	0.00623	0.5918	0.784	< 0.001	0.025	4.2

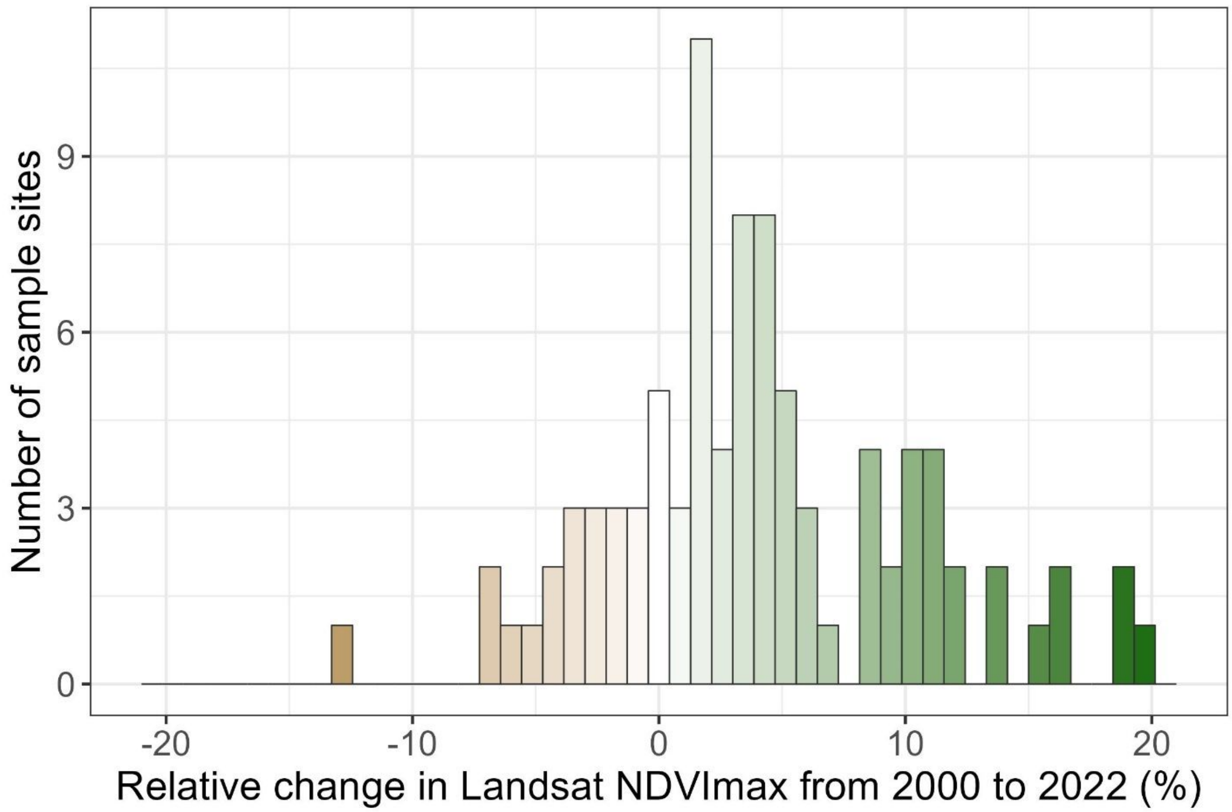

Figure 7. Histogram of relative change in Landsat $NDVI_{max}$ from 2000 to 2022 among sample points across the Noatak National Preserve. Relative changes in percent are calculated based on the Theil-Sen slope and intercept estimates (Table 4).

iew Only

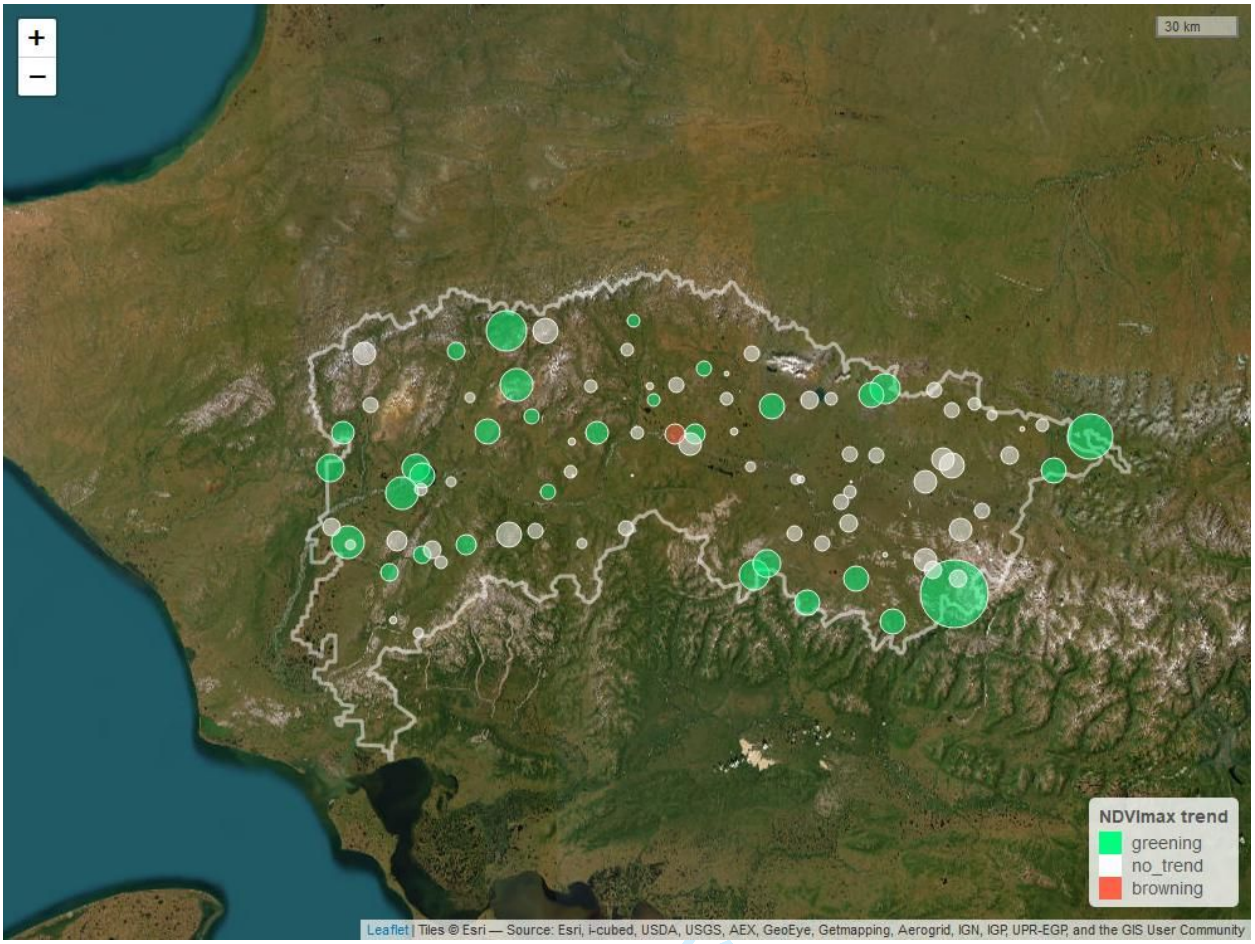

Figure 8. Screenshot of a *leaflet* interactive map showing the trends in $NDVI_{max}$ from 2000 to 2022 for sample points in the Noatak National Preserve. Base map from ESRI World Imagery.

Results and interpretation of the example analysis

Our analysis showed annual maximum vegetation greenness (i.e., $NDVI_{max}$) increased 5.5 ± 10.8% (mean ± 1 SD) from 2000 to 2022 across sample points in the Noatak National Preserve (Figure 7). During these years, vegetation greenness increased by at least 10% at 20% of sample points. Vegetation greenness systematically ($\alpha = 0.10$) increased at 32% of sample points, decreased at 1% of sample points, and exhibited no systematic change at the remaining 67% of sample points. Greening was especially prevalent in western parts of the preserve, as well as along in the northern foothills of the Brooks Range (Figure 8).

These remotely sensed changes suggest tundra productivity and biomass increased in recent decades across large parts of the Noatak National Preserve. These changes are consistent with observed warming-induced expansion of trees and tall shrubs in the preserve (Tape et al. 2006, Terskaia et al. 2020, Dial et al. 2022), as well as with rising summer temperatures increasing the productivity of existing vegetation in this cold tundra environment (Suarez et al. 1999, Berner et al. 2020, Dial et al. 2022). This preserve is also one of the most fire-prone regions in the Arctic and observed greening trends could partially be related to historical fires causing near-surface permafrost thaw, nutrient release, and subsequent shrub proliferation (Gaglioti et al. 2021). Greening in the preserve generally mirrors changes that have been observed more broadly across the Arctic tundra biome, though greening was more prevalent in the preserve than the broader Arctic (32% vs 27% of sample points) (Berner et al. 2020, Mekonnen et al. 2021).

This example analysis was based on Landsat data from 100 random sample points, yet nearly identical results were obtained when the analysis was performed using 1,000 sample points. Further insight into recent ecological changes could be garnered using a higher sample density with samples stratified by land cover type, ecological land unit, management unit, or other factors (e.g., Gaglioti et al. 2021, Berner and Goetz 2022). Nevertheless, Landsat data from even a relatively small random sample (n = 100) enabled robust inference about recent ecological changes that occurred over the past two decades within one of the most remote protected areas in the United States.

Package installation

The R package *LandsatTS* is publicly available through a GitHub code repository. Users will need to have installed the R software environment on their computer. The *LandsatTS* package is operating system agnostic and can be installed from within R using the *install_github()* function from the *devtools* package:

```
devtools::install_github("logan-berner/LandsatTS")
```

The installation will compile the package from source code on the user's computer. As the *LandsatTS* package itself is exclusively written in R code, no additional software is required.

To use the data extraction and preparation functions, users will need an account on GEE, and to have installed and configured the *rgee* package to access GEE from R. Please see the GEE (https://earthengine.google.com/) and *rgee* (https://r-spatial.github.io/rgee/) websites for details on signing up for an account and configuring *rgee*, respectively.

All other external package dependencies are configured and automatically dealt with by *devtools* during the installation. These required packages include (*LandsatTS* tested with version cited): *crayon* v1.4.2 (Csárdi 2021), *data.table* v1.14.2 (Dowle and Srinivasan 2021), *dplyr* v1.0.7 (Wickham et al. 2021), *ggplot2* v3.3.5 (Wickham 2016), *ggpubr* v0.4.0 (Kassambara 2020), *magrittr* v2.0.1 (Bache and Wickham 2020), *mapview* v2.10.0 (Appelhans et al. 2021), *purr* v0.3.4 (Henry and Wickham 2020), *R.utils* v2.11.0 (Bengtsson 2021), *ranger* v0.13.1 (Wright and Ziegler 2017), *sf* v1.0-4 (Pebesma 2018), *stats* v4.1.1 (R Core Team 2021), *stringr* v1.4.0 (Wickham 2019), *tidyr* v1.1.4 (Wickham 2021), *zoo* v1.8.9 (Zeileis and Grothendieck 2005), *zyp* v0.10-1.1 (Bronaugh and Werner 2019).

Function descriptions

Below we provide a description of each function, with further details provided in the package manual that is available both within R and as Supplemental Material.

Export point-coordinate Landsat time series from Google Earth Engine using lsat_export_ts()

The function *lsat_export_ts()* exports Landsat 5, 7 and 8 surface reflectance measurements for each sample location over a user-defined period by querying the Landsat Collection 2 archived on GEE. Sample locations typically represent (1) center coordinates of field sites, (2) a census of all Landsat pixels from a small area of interest, or (3) a random sample from a large region. If the user wishes to extract Landsat data for all pixels in a small area of interest (e.g., 5 km x 5 km), then the central coordinates of each pixel can be obtained using *lstat_get_pixel_centers()* and

For Review Only

then those sample locations are passed to *lsat_export_ts()*. It is important to stress this function only works for sample locations (point coordinates) that must be supplied as a simple feature (*sf*) collection of point geometries.

The function issues one or more tasks to GEE that export the data in the form of comma separated value (CSV) files to the user's Google Drive. The number of tasks issued varies depending on the number of sample locations for which the Landsat record is to be extracted. Data extractions that involve many sample locations are prone to errors and may exceed user limits set by GEE. Therefore, the function will chunk the sample locations into small groups (by default 250 sites) and for each chunk will issue a separate export task to GEE. The function returns a list of *rgee* task objects, which can be used to query the progress of the exports and subsequently retrieve the data from the user's Google Drive.

Please note that *lsat_export_ts()* has not been tested for data extractions exceeding 10^5 Landsat pixels (~90 km^2). It took about two weeks to extract four decades of summer Landsat data for 10^5 pixels sampled from across the boreal forest biome. This data extraction yielded ~41.6 million multispectral measurements that required ~15 Gb of hard drive storage (Berner and Goetz 2022). *LandsatTS* enables large data extractions but is not infinitely scalable.

For Review Only

Optional: Get central coordinates of pixels within a polygon using lsat_get_pixel_centers()

The function *lsat_get_pixel_centers()* facilitates extracting data for all Landsat pixels in a small area of interest (e.g., < 5 km x 5 km) by determining the central coordinates of all Landsat pixels that fall within a user-specified polygon. The user-specified polygon is supplied to the function as a simple feature collection. The function determines the Landsat Worldwide Reference System (WRS) scene whose center is closest to the center of the user-specified polygon. It then extracts the center coordinates for all pixels that overlap with the user-specified polygon from the first Landsat 8 scene on record available on GEE. A buffer can be specified to include additional pixels beyond the polygon boundary. The function returns the pixel centers as a simple feature object that can then be passed to the *lsat_export_ts()* function for the extraction of the Landsat time series. Please note this function is not designed to be used for sampling polygons that would exceed tens of thousands of Landsat pixels. The number of pixels in large polygons can quickly become too difficult to handle in the subsequent export and processing workflow, and such polygons may also extend beyond the area of the Landsat scene (185 km x 180 km) used to determine the pixel centers. For large areas, we recommend a random or regular subsampling of point locations such as done in prior studies (Berner et al. 2020, Berner and Goetz 2022).

Format data for analysis using lsat_format_data ()

The function *lsat_format_data()* takes the GEE exports generated by *lsat_export_ts()* and prepares the data for the subsequent *LandsatTS* workflow. These preprocessing tasks include parsing coordinates and other information, renaming columns, and scaling band values. The GEE exports need to be passed to the function in the form of a *data.table* object. *lsat_format_data()* returns a *data.table* object that can then be passed on to *lsat_clean_data()* for the next step in the processing workflow. Please note that all *LandsatTS* functions handling a *data.table* object require a column called "sample.id" that uniquely identifies each location. If this column is not called "sample.id", please modify accordingly.

Clean surface reflectance data using lsat_clean_data()

The function *lsat_clean_data()* filters measurements to those made under clear-sky conditions. This function allows the user to filter measurements based on pixel quality flags and scene criteria. The USGS provides pixel quality flags based on the CFMask algorithm (Zhu et al. 2015) and information on each scene (e.g., cloud cover). The default settings for *lsat_clean_data()* will filter out measurements flagged as snow or water, as well as measurements acquired at high solar zenith angle (>60°), those with high geolocation uncertainty (>15 m), or those acquired as part of scenes with extensive cloud cover (>80%). Additionally, optional water masking is provided based on maximum surface water extent from the Landsat-based JRC Global Surface Water Dataset (Pekel et al. 2016). The main input supplied to *lsat_clean_data()* is a *data.table* of Landsat records for individual sample locations (specified by a sample.id column) - usually the direct output of *lsat_format_data()* - and returns cleaned records in the form of an updated *data.table*, along with a console message summarizing the number and percentage of measurements removed during cleaning (generally >70%).

Compute neighborhood mean surface reflectance using lsat_neighborhood_mean()

The function *lsat_neighborhood_mean()* computes the mean band-specific reflectance across a neighborhood of pixels for measurements at each period in time. This is helpful when each of the user's sample locations was buffered to include a neighborhood of Landsat pixels (e.g., 3 x 3 pixels). If there are neighborhood pixels with no data (i.e., NA values), then the function omits those pixels and computes the mean across the remaining pixels. The main input to this function is a *data.table* of Landsat records for buffered sample locations. The function returns a new *data.table* with mean reflectance for each band at each point in time at every sample location. If used, the function should be called immediately after *lsat_clean_data()*.

Summarize data availability for each site using lsat_summarize_data()

The function *lsat_summarize_data()* takes a *data.table* of Landsat records and returns a summary *data.table* that provides information on the time period and number of observations available for each sample location. It also generates a figure showing the annual median (2.5th and 97.5th percentile) number of observations available from each satellite summarized across all sample locations. The figure is plotted to the current graphics device and can be saved by calling the function *ggsave()*.

Calculate spectral indices using lsat_calc_spectral_index()

The function *lsat_calc_spectral_index()* calculates a variety of common spectral indices. The function currently supports calculating 15 spectral indices, including the Normalized Difference Vegetation Index (NDVI), 2-band Enhanced Vegetation Index (EVI2), and others (Table 2). Note the function can only compute one spectral index at a time. As an input it requires a *data.table* with Landsat records and a string indicating the spectral index to be calculated. The function then returns the *data.table* updated with a new column containing the spectral index for each observation.

Table 2. Spectral indices that can be computed using the *lsat_calc_spectral_index()* function.

Name	**Abbreviation**	**Formula**	**Citation**

For Review Only

Enhanced Vegetation Index	EVI	$\frac{2.5(NIR - RED)}{NIR + 6 * RED - 7.5 * BLUE + 1}$	Huete et al. (2002)
Enhanced Vegetation Index (2-band)	EVI2	$\frac{2.5 * (NIR - RED)}{NIR + 2.5 * RED + 1}$	Jiang et al. (2008)
Moisture Stress Index	MSI	$\frac{SWIR1}{NIR}$	Rock et al. (1986)
Near Infrared Vegetation Index	NIRv	$\frac{NIR * (NIR - RED)}{NIR + RED}$	Badgley et al. (2017)
Normalized Burn Ratio	NBR	$\frac{NIR - SWIR2}{NIR + SWIR2}$	Key and Benson (1999)
Normalized Difference Infrared Index	NDII	$\frac{NIR - SWIR1}{NIR + SWIR1}$	Hardisky et al. (1983)
Normalized Difference Moisture Index	NDMI	$\frac{NIR - SWIR1}{NIR + SWIR1}$	Gao (1996)
Normalized Difference Vegetation Index (red)	NDVI	$\frac{NIR - RED}{NIR + RED}$	Rouse et al. (1974)
Normalized Difference Vegetation Index (green)	gNDVI	$\frac{NIR - GREEN}{NIR + GREEN}$	Gitelson and Merzlyak (1998)
Normalized Difference Vegetation Index (kernel)	kNDVI	$\tanh\left(\left(\frac{NIR - RED}{NIR + RED}\right)^2\right)$	Camps-Valls et al. (2021)
Normalized Difference Water Index	NDWI	$\frac{GREEN - NIR}{GREEN + NIR}$	McFeeters (1996)
Plant Senescence Reflectance Index	PSRI	$\frac{RED - BLUE}{NIR}$	Merzlyak et al. (1999)
Soil Adjusted Vegetation Index	SAVI	$1.5 * \frac{SWIR1 - RED}{SWIR1 + RED * 0.5} - \frac{SWIR2}{2}$	Huete (1988)
Soil Adjusted Total Vegetation Index	SATVI	$\frac{1.5\ (NIR - RED)}{NIR + RED + 0.5}$	Marsett et al. (2006)
Wide Dynamic Range Vegetation Index	WDRVI	$\frac{NIR - RED}{0.2 *\ NIR + RED}$	Gitelson (2004)

Cross-calibrate spectral data across sensors using lsat_calibrate_rf()

The function *lsat_calibrate_rf()* will calibrate individual bands or spectral indices from Landsat 5 TM and Landsat 8 OLI to match Landsat 7 ETM+ using random forest models following the approach developed by Berner et al. (2020). Further cross-sensor calibration is needed because there are systematic differences in individual bands and spectral indices among Landsat sensors that must be addressed when combining data from multiple sensors (Ju and Masek 2016, Roy et al. 2016, Berner et al. 2020, Berner and Goetz 2022). Here, the Landsat 7 ETM+ is used as a benchmark because it temporally overlaps with the other two sensors. Cross-calibration can only be performed on one band or spectral index at a time and requires having data from 100s to preferably many 1,000s of sample locations to train the random forest models. There is an option for users to train the random forest models using pre-processed Landsat data from ~6000 randomly sampled locations across the Arctic – Boreal domain.

The overall approach involves determining the median spectral reflectance at a sample location during a portion of the growing season using Landsat 7 and Landsat 5/8 data that were collected the same years. A random forest model is then trained to predict Landsat 7 reflectance from Landsat 5/8 reflectance. Random forest models are ensembles of regression trees (Breiman 2001) that here are trained using a fast implementation provided by the *ranger* package (Wright and Ziegler 2017). If the user's dataset includes both Landsat 5 and 8, then the function will train a random forest model for each sensor. The function evaluates model performance using both out-of-bag and cross-validated approaches. Please see Berner et al. (2020) for further details.

For Review Only

The main input to *lsat_calibrate_rf()* is a *data.table* of Landsat records for sample locations and a string specifying the name of the band or spectral index to be cross-calibrated. By default, *lsat_calibrate_rf()* will return a *data.table* with a new column containing the cross-calibrated data. If requested using the *write.output* parameter, the function creates a user-specified output directory that contains (1) trained random forest models, (2) a CSV file with model evaluation metrics, and (3) a multi-panel figure comparing sensors pre- and post-calibration. In any case, model evaluation metrics are returned to the console and the figure plotted in the active graphics device. If the default setting to add a new column with the cross-calibrated data is used, then either use those data in the subsequent functions (e.g., ndvi.xcal) or, once satisfied, manually overwrite the uncalibrated data to simplify subsequent column names.

Cross-calibrate spectral data across sensors using lsat_calibrate_poly()

The function *lsat_calibrate_poly()* behaves similarly to *lsat_calibrate_rf()* but fits polynomial regression models rather than random forest models. The function automatically fits first-, second- and third-order polynomial regression models (i.e., $Y = \beta_0 + \beta_1 X + \beta_2 X^2 + \beta_3 X^3$). It then automatically selects the most parsimonious fit using Bayesian Information Criterion (BIC), applies the most parsimonious model for cross-sensor calibration, and then returns regression model coefficients and cross-validation metrics. Initial testing showed *lsat_calibrate_poly()* and *lsat_calibrate_rf()* produce very similar results ($r^2 = 0.97$), have similar run times, and both effectively mitigate biases among Landsat sensors, yet an advantage of the more recently developed *lsat_calibrate_poly()* function is it generates regression model coefficients that can be more readily applied to other datasets or incorporated into other software (e.g., GEE).

Fit phenological curves to vegetation greenness time series using lsat_fit_phenological_curves()

The function *lsat_fit_phenological_curves()* provides information on the phenological timing of every Landsat observation relative to multi-year estimates of annual maximum vegetation greenness at each sample location. Specifically, the function models seasonal land surface phenology at each sample location using cubic splines iteratively fit to vegetation greenness (e.g., NDVI) time series within successive moving windows. The magnitude and timing of annual maximum vegetation greenness are determined for each period by first pooling observations over years within each moving-window and then fitting cubic splines to observations that have been sorted by day of year. Often there are too few observations from an individual year to fit a reliable phenological curve, therefore the function enables users to pool observations over multiple years when fitting each cure. The default is a 7-year moving-window centered on the focal year, but the width of the moving window can be made shorter or longer if there are many or few observations in the data record. For each time period, a cubic spline is initially fit that describes vegetation greenness for each day of year during the growing season. To screen outliers, each observation of vegetation greenness is compared against the model fitted values for that day of year and if the deviation is greater than a user-specified difference (default is a 30% difference), then the observation is removed, and the cubic spline is re-fit. This is repeated until no observations exceed the user-specified threshold. The phenological status of each remaining observation is then determined relative to the modeled maximum vegetation greenness during the multi-year period. Additional details are provided in Berner et al. (2020).

The function takes as input a *data.table* with irregular time series of vegetation greenness observations at each sample location, as well as several parameters (e.g., moving window width, minimum number of observation needed to fit a cubic spline, cubic spline flexibility). The

For Review Only

function returns a new *data.table* with phenological information for each remaining observation that occurred during a time period with adequate data for modeling surface phenology (i.e., typically fewer observations will be returned than are provided to the function). Among other output, the returned *data.table* provides for each observation the modeled estimates of (1) vegetation greenness for that day of year and for peak summer; (2) vegetation greenness for that day of year as a fraction of annual maximum vegetation greenness; (3) day of year when annual maximum vegetation greenness occurred; and (4) expected difference in vegetation greenness between that day of year and peak summer. The function also returns a figure to the current graphic device that shows seasonal progression of Landsat observations and modeled surface phenology for a random subset of nine sample locations. The user can optionally output a CSV that includes for each sample location the vegetation greenness predicted for each day of year during each period by the cubic splines. Furthermore, the function includes an optional "test run" mode that will run the function on a random subset of nine sample locations and return a figure showing model fits, thus allowing the user to quickly experiment with different parameter settings. Note the function was designed to characterize seasonal phenology in terrestrial ecosystems with a single growing season and thus may not be suitable for use in ecosystems with multiple growing seasons. Also, the function was designed for spectral indices that are typically positive (e.g., NDVI). If using a spectral index that is typically negative (e.g., NDWI) then multiply the index by -1 before running the *lsat_fit_phenological_curves()* and *lsat_summarize_growing_seasons()* functions and then back-transform afterwards.

Derive annual growing season metrics using lsat_summarize_growing_seasons()

The function *lsat_summarize_growing_seasons()* estimates several annual growing season metrics from vegetation greenness time series and modeled land surface phenology derived from Landsat satellite observations. The function's main input is the *data.table* generated by *lsat_fit_phenological_curves()* and user-specified parameters including the name of the spectral index and the phenological cut-off for an observation to be considered part of the growing season. Specifically, an observation is considered to be part of the growing season if the modeled vegetation greenness for that day of year is within a user-specified fraction of modeled annual maximum vegetation greenness (by default 0.75). The function returns a new *data.table* that includes for each sample location the annual mean, median, and 90th percentile vegetation greenness computed from observations during each growing season. The function also returns phenologically modeled estimates of the magnitude and timing (day of year) of annual maximum vegetation greenness. For each sample location, annual maximum vegetation greenness is estimated by first adjusting individual observations by the expected difference in vegetation greenness between that day of year and peak summer, and then taking the median of phenologically adjusted values within each growing season. Please see Berner et al. (2020) for additional details.

Assess estimates of maximum vegetation greenness using lsat_evaluate_phenological_max()

The function *lsat_evaluate_phenological_max()* assesses how estimates of annual maximum vegetation greenness vary with the number of Landsat observations when derived from raw observations and after phenological modeling. Raw estimates of annual maximum vegetation greenness are sensitive to the number of observations available from a growing season, but phenological modeling tends to substantially reduce this dependency (Berner et al. 2020). The main input to the function is a *data.table* with Landsat records and phenological information

For Review Only

generated by *lsat_fit_phenological_curves()*. The function assumes the "actual" annual maximum vegetation greenness at a sample location is captured by having at least a user-specific number of observations (e.g., ≥ 7). For each site, the function extracts years with at least the user-specified number of growing season observations and then repeatedly compares how raw and phenologically modeled estimates of annual maximum vegetation greenness differ from actual annual maximum vegetation greenness as progressively smaller subsets of observations are used. The function returns a figure to the current graphic device that summarizes how raw and modeled estimates of annual maximum vegetation greenness differ from actual conditions when there are between 1 and n-1 Landsat observations from a single growing season. This lets the user determine how much annual estimates of maximum vegetation greenness are impacted by the number of available growing season observations.

Compute interannual trends in vegetation greenness using lsat_calc_trend()

The function *lsat_calc_trend()* computes a temporal trend in annual time series of vegetation greenness for each sample location over a user-specified period. This function pre-whitens each time series (i.e., removes temporal autocorrelation) (Yue et al. 2002) and then computes Mann-Kendall trend tests and Theil-Sen slope indicators as implemented by the *zyp.yuepilon()* function from the *zyp* package (Bronaugh and Werner 2019). The function takes as input a *data.table* with annual time series of vegetation greenness, or other spectral index, for each sample location. The function returns (1) a new *data.table* that summarizes the interannual trend at each sample location; (2) a console message summarizing trends across all sample locations. Specifically, the new *data.table* summarizes for each sample location the trend slope, intercept, Kendall's tau, and p-value, as well as total absolute and relative change in vegetation greenness and other information (e.g., number of years with observations). The console message summarizes the mean (±1 SD) relative change in vegetation greenness across all sample locations, as well as the percentage of samples sites that greened, browned, or had no trend based on a user-specified critical value (default α = 0.10).

Plot histogram of vegetation greenness trends using lsat_plot_trend_hist()

The function *lsat_plot_trend_hist()* creates a histogram depicting the total percent change in vegetation greenness, or other spectral index, among sample locations. The function takes the *data.table* that is output by the function *lsat_calc_trend()* and returns a figure that is plotted to the current graphics device.

Conclusions

The *LandsatTS* package for R facilitates extracting and processing Landsat surface reflectance time series, as well as generating and analyzing metrics of vegetation greenness and other spectral indices. We demonstrated the functionality of this software by analyzing multidecadal changes in vegetation greenness across the Noatak National Preserve, USA, but would like to highlight that these tools are also well suited for sample-based analyses of vegetation dynamics across geographic regions ranging from individual field sites to entire terrestrial biomes (e.g., Berner et al. 2020, Berner and Goetz 2022). To date, *LandsatTS* has been used for ecological studies focused on the Arctic tundra and boreal forest biomes, but many of the functions could be used for studies focused on lower latitude ecosystems, especially ecosystems without a multi-

For Review Only

modal growing season. Overall, this software provides a suite of functions to enable broader use of Landsat satellite data for assessing and monitoring Earth's land surface over the past four decades in a sample-based framework suitable for local to global geographic extents.

References

Appelhans, T., F. Detsch, C. Reudenbach, and S. Woellauer. 2021. mapview: Interactive Viewing of Spatial Data in R. R package version 2.10.0. https://CRAN.R-project.org/package=mapview.

Aybar, C., Q. Wu, L. Bautista, R. Yali, and A. Barja. 2020. rgee: An R package for interacting with Google Earth Engine. Journal of Open Source Software **5**:2272.

Bache, S. M., and H. Wickham. 2020. magrittr: A Forward-Pipe Operator for R. R package version 2.0.1. https://CRAN.R-project.org/package=magrittr.

Badgley, G., C. B. Field, and J. A. Berry. 2017. Canopy near-infrared reflectance and terrestrial photosynthesis. Science Advances **3**:e1602244.

Bengtsson, H. 2021. R.utils: Various Programming Utilities. R package version 2.11.0. https://CRAN.R-project.org/package=R.utils.

Berner, L. T., and S. J. Goetz. 2022. Satellite observations document trends consistent with a boreal forest biome shift. Global Change Biology **28**:3275–3292.

Berner, L. T., P. Jantz, K. D. Tape, and S. J. Goetz. 2018. Tundra plant aboveground biomass and shrub dominance mapped across the North Slope of Alaska. Environmental Research Letters **13**:035002.

Berner, L. T., R. Massey, P. Jantz, B. C. Forbes, M. Macias-Fauria, I. H. Myers-Smith, T. Kumpula, G. Gauthier, L. Andreu-Hayles, B. Gaglioti, P. J. Burns, P. Zetterberg, R. D'Arrigo, and S. J. Goetz. 2020. Summer warming explains widespread but not uniform greening in the Arctic tundra biome. Nature communications **11**:4621.

Bhatt, U. S., D. A. Walker, M. K. Raynolds, J. E. Walsh, P. A. Bieniek, L. Cai, J. C. Comiso, H. E. Epstein, G. V. Frost, and R. Gersten. 2021. Climate drivers of Arctic tundra variability and change using an indicators framework. Environmental Research Letters **16**:055019.

Boyd, M. A., L. T. Berner, P. Doak, S. J. Goetz, B. M. Rogers, D. Wagner, X. J. Walker, and M. C. Mack. 2019. Impacts of climate and insect herbivory on productivity and physiology of trembling aspen (Populus tremuloides) in Alaskan boreal forests. Environmental Research Letters **14**:085010.

Boyd, M. A., L. T. Berner, A. C. Foster, S. J. Goetz, B. M. Rogers, X. J. Walker, and M. C. Mack. 2021. Historic declines in growth portend trembling aspen death during a contemporary leaf miner outbreak in Alaska. Ecosphere **12**:e03569.

Breiman, L. 2001. Random Forests. Machine Learning **45**:5-32.

Bronaugh, D., and A. Werner. 2019. zyp: Zhang + Yue-Pilon trends package. R package version 0.10-1.1. https://CRAN.R-project.org/package=zyp.

Camps-Valls, G., M. Campos-Taberner, Á. Moreno-Martínez, S. Walther, G. Duveiller, A. Cescatti, M. D. Mahecha, J. Muñoz-Marí, F. J. García-Haro, and L. Guanter. 2021. A unified vegetation index for quantifying the terrestrial biosphere. Science Advances **7**:eabc7447.

Cheng, J., B. Karambelkar, and Y. Xie. 2022. leaflet: Create Interactive Web Maps with the JavaScript 'Leaflet' Library. R package version 2.1.1. https://CRAN.R-project.org/package=leaflet.

Csárdi, G. 2021. crayon: Colored Terminal Output. R package version 1.4.2. https://CRAN.R-project.org/package=crayon.

Dial, R. J., C. T. Maher, R. E. Hewitt, and P. F. Sullivan. 2022. Sufficient conditions for rapid range expansion of a boreal conifer. Nature **608**:546-551.

dos Santos, A. 2017. landsat8: Landsat 8 Imagery Rescaled to Reflectance, Radiance and/or Temperature. R package version 0.1-10. https://CRAN.R-project.org/package=landsat8.

For Review Only

Dowle, M., and A. Srinivasan. 2021. data.table: Extension of `data.frame`. R package version 1.14.2. https://CRAN.R-project.org/package=data.table.
Foster, A. C., J. A. Wang, G. V. Frost, S. J. Davidson, E. Hoy, K. W. Turner, O. Sonnentag, H. Epstein, L. T. Berner, A. H. Armstrong, M. Kang, B. M. Rogers, E. Campbell, K. R. Miner, K. M. Orndahl, L. L. Bourgeau-Chavez, D. A. Lutz, N. French, D. Chen, J. Du, T. A. Shestakova, J. K. Shuman, K. Tape, A.-M. Virkkala, C. Potter, and S. Goetz. 2022. Disturbances in North American boreal forest and Arctic tundra: impacts, interactions, and responses. Environmental Research Letters **17**:113001.
Gaglioti, B., L. T. Berner, B. M. Jones, K. M. Orndahl, A. P. Williams, L. Andreu-Hayles, R. D'Arrigo, S. J. Goetz, and D. H. Mann. 2021. Tussocks enduring or shrubs greening: Alternate responses to changing fire regimes in the Noatak River Valley, Alaska. Journal of Geophysical Research: Biogeosciences **126**:e2020JG006009.
Gao, B.-C. 1996. NDWI—A normalized difference water index for remote sensing of vegetation liquid water from space. Remote Sensing of Environment **58**:257-266.
Gitelson, A. A. 2004. Wide dynamic range vegetation index for remote quantification of biophysical characteristics of vegetation. Journal of plant physiology **161**:165-173.
Gitelson, A. A., and M. N. Merzlyak. 1998. Remote sensing of chlorophyll concentration in higher plant leaves. Advances in Space Research **22**:689-692.
Gorelick, N., M. Hancher, M. Dixon, S. Ilyushchenko, D. Thau, and R. Moore. 2017. Google Earth Engine: Planetary-scale geospatial analysis for everyone. Remote Sensing of Environment **202**:18-27.
Goslee, S. 2011. Analyzing remote sensing data in R: The Landsat Package. The Journal of Statistical Software **43**.
Hansen, M. C., P. V. Potapov, R. Moore, M. Hancher, S. A. Turubanova, A. Tyukavina, D. Thau, S. V. Stehman, S. J. Goetz, T. R. Loveland, A. Kommareddy, A. Egorov, L. Chini, C. O. Justice, and J. R. G. Townshend. 2013. High-Resolution Global Maps of 21st-Century Forest Cover Change. science **342**:850.
Hardisky, M., V. Klemas, and M. Smart. 1983. The influence of soil salinity, growth form, and leaf moisture on the spectral radiance of Spartina alterniflora. Photogrammetric Engineering & Remote Sensing **49**:77-83.
Helman, D. 2018. Land surface phenology: What do we really 'see' from space? Science of the Total Environment **618**:665-673.
Henry, L., and H. Wickham. 2020. purrr: Functional Programming Tools. R package version 0.3.4. https://CRAN.R-project.org/package=purrr.
Huete, A., K. Didan, T. Miura, E. P. Rodriguez, X. Gao, and L. G. Ferreira. 2002. Overview of the radiometric and biophysical performance of the MODIS vegetation indices. Remote Sensing of Environment **83**:195-213.
Huete, A. R. 1988. A soil-adjusted vegetation index (SAVI). Remote Sensing of Environment **25**:295-309.
Jia, G. J., H. E. Epstein, and D. A. Walker. 2003. Greening of arctic Alaska, 1981–2001. Geophysical Research Letters **30**:2067.
Jiang, Z., A. R. Huete, K. Didan, and T. Miura. 2008. Development of a two-band enhanced vegetation index without a blue band. Remote Sensing of Environment **112**:3833-3845.
Ju, J., and J. G. Masek. 2016. The vegetation greenness trend in Canada and US Alaska from 1984–2012 Landsat data. Remote Sensing of Environment **176**:1-16.
Kassambara, A. 2020. ggpubr: 'ggplot2' Based Publication Ready Plots. R package version 0.4.0. https://CRAN.R-project.org/package=ggpubr.
Key, C. H., and N. C. Benson. 1999. The Normalized Burn Ratio (NBR): A Landsat TM radiometric measure of burn severity. United States Geological Survey, Northern Rocky Mountain Science Center.(Bozeman, MT).

For Review Only

Kong, D., T. R. McVicar, M. Xiao, Y. Zhang, J. L. Peña-Arancibia, G. Filippa, Y. Xie, and X. Gu. 2022. phenofit: An R package for extracting vegetation phenology from time series remote sensing. Methods in Ecology and Evolution **13**:1508-1527.

Lai, J., C. J. Lortie, R. A. Muenchen, J. Yang, and K. Ma. 2019. Evaluating the popularity of R in ecology. Ecosphere **10**:e02567.

Marsett, R. C., J. Qi, P. Heilman, S. H. Biedenbender, M. C. Watson, S. Amer, M. Weltz, D. Goodrich, and R. Marsett. 2006. Remote sensing for grassland management in the arid southwest. Rangeland Ecology & Management **59**:530-540.

McFeeters, S. K. 1996. The use of the Normalized Difference Water Index (NDWI) in the delineation of open water features. International Journal of Remote Sensing **17**:1425-1432.

Mekonnen, Z. A., W. J. Riley, L. T. Berner, N. J. Bouskill, M. S. Torn, G. Iwahana, A. L. Breen, I. H. Myers-Smith, M. G. Criado, Y. Liu, E. S. Euskirchen, S. J. Goetz, M. C. Mack, and R. F. Grant. 2021. Arctic tundra shrubification: a review of mechanisms and impacts on ecosystem carbon balance. Environmental Research Letters **16**:053001.

Merzlyak, M. N., A. A. Gitelson, O. B. Chivkunova, and V. Y. Rakitin. 1999. Non-destructive optical detection of pigment changes during leaf senescence and fruit ripening. Physiologia plantarum **106**:135-141.

Myers-Smith, I. H., J. T. Kerby, G. K. Phoenix, J. W. Bjerke, H. E. Epstein, J. J. Assmann, C. John, L. Andreu-Hayles, S. Angers-Blondin, P. S. A. Beck, L. T. Berner, U. S. Bhatt, A. D. Bjorkman, D. Blok, A. Bryn, C. T. Christiansen, J. H. C. Cornelissen, A. M. Cunliffe, S. C. Elmendorf, B. C. Forbes, S. J. Goetz, R. D. Hollister, R. de Jong, M. M. Loranty, M. Macias-Fauria, K. Maseyk, S. Normand, J. Olofsson, T. C. Parker, F.-J. W. Parmentier, E. Post, G. Schaepman-Strub, F. Stordal, P. F. Sullivan, H. J. D. Thomas, H. Tømmervik, R. Treharne, C. E. Tweedie, D. A. Walker, M. Wilmking, and S. Wipf. 2020. Complexity revealed in the greening of the Arctic. Nature Climate Change **10**:106-117.

National Academies of Sciences. 2018. Thriving on Our Changing Planet: A Decadal Strategy for Earth Observation from Space. The National Academies Press, Washington, DC.

Pebesma, E. J. 2018. Simple features for R: standardized support for spatial vector data. The R Journal **10**:439-446.

Pekel, J.-F., A. Cottam, N. Gorelick, and A. S. Belward. 2016. High-resolution mapping of global surface water and its long-term changes. Nature **540**:418-422.

Potapov, P., M. C. Hansen, A. Pickens, A. Hernandez-Serna, A. Tyukavina, S. Turubanova, V. Zalles, X. Li, A. Khan, F. Stolle, N. Harris, X.-P. Song, A. Baggett, I. Kommareddy, and A. Kommareddy. 2022. The Global 2000-2020 Land Cover and Land Use Change Dataset Derived From the Landsat Archive: First Results. Frontiers in Remote Sensing **3**.

Powell, S. L., W. B. Cohen, S. P. Healey, R. E. Kennedy, G. G. Moisen, K. B. Pierce, and J. L. Ohmann. 2010. Quantification of live aboveground forest biomass dynamics with Landsat time-series and field inventory data: A comparison of empirical modeling approaches. Remote Sensing of Environment **114**:1053-1068.

R Core Team. 2021. R: A Language and Environment for Statistical Computing. R Foundation for Statistical Computing, Vienna, Austria.

Raynolds, M. K., D. A. Walker, H. E. Epstein, J. E. Pinzon, and C. J. Tucker. 2012. A new estimate of tundra-biome phytomass from trans-Arctic field data and AVHRR NDVI. Remote Sensing Letters **3**:403-411.

Rock, B., J. Vogelmann, D. Williams, A. Vogelmann, and T. Hoshizaki. 1986. Remote detection of forest damage. BioScience **36**:439-445.

Rouse, J., R. Haas, J. Schell, and D. Deering. 1974. Monitoring vegetation systems in the Great Plains with ERTS. NASA special publication **351**:309-317.

For Review Only

Roy, D. P., V. Kovalskyy, H. K. Zhang, E. F. Vermote, L. Yan, S. S. Kumar, and A. Egorov. 2016. Characterization of Landsat-7 to Landsat-8 reflective wavelength and normalized difference vegetation index continuity. Remote Sensing of Environment **185**:57-70.

Sexton, J. O., X.-P. Song, M. Feng, P. Noojipady, A. Anand, and C. Huang. 2013. Global, 30-m resolution continuous fields of tree cover: landsat-based rescaling of MODIS vegetation continuous fields with lidar-based estimates of error. Int J Digit Earth **6**.

Suarez, F., D. Binkley, M. W. Kaye, and R. Stottlemyer. 1999. Expansion of forest stands into tundra in the Noatak National Preserve, northwest Alaska. Ecoscience **6**:465-470.

Tape, K., M. Sturm, and C. Racine. 2006. The evidence for shrub expansion in Northern Alaska and the Pan-Arctic. Global Change Biology **12**:686-702.

Terskaia, A., R. J. Dial, and P. F. Sullivan. 2020. Pathways of tundra encroachment by trees and tall shrubs in the western Brooks Range of Alaska. Ecography **43**:769-778.

Verdonen, M., L. T. Berner, B. C. Forbes, and T. Kumpula. 2020. Periglacial vegetation dynamics in Arctic Russia: decadal analysis of tundra regeneration on landslides with time series satellite imagery. Environmental Research Letters **15**:105020.

Walker, X. J., H. D. Alexander, L. T. Berner, M. A. Boyd, M. M. Loranty, S. M. Natali, and M. C. Mack. 2021. Positive response of tree productivity to warming is reversed by increased tree density at the Arctic tundra-taiga ecotone. Canadian Journal of Forest Research **51**:1323-1338.

Wang, J. A., and M. A. Friedl. 2019. The role of land cover change in Arctic-Boreal greening and browning trends. Environmental Research Letters **14**:125007.

Wickham, H. 2016. ggplot2: Elegant Graphics for Data Analysis. Springer-Verlang New York.

Wickham, H. 2019. stringr: Simple, Consistent Wrappers for Common String Operations. R package version 1.4.0. https://CRAN.R-project.org/package=stringr.

Wickham, H. 2021. tidyr: Tidy Messy Data. R package version 1.1.4. https://CRAN.R-project.org/package=tidyr.

Wickham, H., R. Francois, H. Lionel, and K. Müller. 2021. dplyr: A Grammar of Data Manipulation. R package version 1.0.7. https://CRAN.R-project.org/package=dplyr.

Wright, M. N., and A. Ziegler. 2017. Ranger: a fast implementation of random forests for high dimensional data in C++ and R. Journal of statistical software **77**:1-17.

Wulder, M., R. Skakun, W. Kurz, and J. White. 2004. Estimating time since forest harvest using segmented Landsat ETM+ imagery. Remote Sensing of Environment **93**:179-187.

Wulder, M. A., T. R. Loveland, D. P. Roy, C. J. Crawford, J. G. Masek, C. E. Woodcock, R. G. Allen, M. C. Anderson, A. S. Belward, W. B. Cohen, J. Dwyer, A. Erb, F. Gao, P. Griffiths, D. Helder, T. Hermosilla, J. D. Hipple, P. Hostert, M. J. Hughes, J. Huntington, D. M. Johnson, R. Kennedy, A. Kilic, Z. Li, L. Lymburner, J. McCorkel, N. Pahlevan, T. A. Scambos, C. Schaaf, J. R. Schott, Y. Sheng, J. Storey, E. Vermote, J. Vogelmann, J. C. White, R. H. Wynne, and Z. Zhu. 2019. Current status of Landsat program, science, and applications. Remote Sensing of Environment **225**:127-147.

Wulder, M. A., J. G. Masek, W. B. Cohen, T. R. Loveland, and C. E. Woodcock. 2012. Opening the archive: How free data has enabled the science and monitoring promise of Landsat. Remote Sensing of Environment **122**:2-10.

Yue, S., P. Pilon, B. Phinney, and G. Cavadias. 2002. The influence of autocorrelation on the ability to detect trend in hydrological series. Hydrological processes **16**:1807-1829.

Zeileis, A., and G. Grothendieck. 2005. zoo: S3 Infrastructure for Regular and Irregular Time Series. Journal of statistical software **14**:1-27.

Zeng, L., B. D. Wardlow, D. Xiang, S. Hu, and D. Li. 2020. A review of vegetation phenological metrics extraction using time-series, multispectral satellite data. Remote Sensing of Environment **237**:111511.

For Review Only

Zhu, Z., S. Wang, and C. E. Woodcock. 2015. Improvement and expansion of the Fmask algorithm: cloud, cloud shadow, and snow detection for Landsats 4–7, 8, and Sentinel 2 images. Remote Sensing of Environment **159**:269-277.

For Review Only

AUTHOR RESPONSE TO EDITOR AND REVIEWER FEEDBACK

LandsatTS: an R package to facilitate retrieval, cleaning, cross-calibration, and phenological modeling of Landsat time-series data

Subject Editor (Dr. Michael Borregaard) Comments

The package is purely geographical, and thus somewhat on the edge of what Ecography publishes, but given the widespread use of Landsat data among ecologists it still seems useful. It does mean, however, that the quite complicated installation procedure becomes an issue. Very few of the readers of Ecography are likely to have rgee and google earth engine installed and have an active google earth account. They are not trivial to install, and the reviewer had multiple problems getting the install to work. These procedures should be spelt out much more clearly.

Author response: We thank the Subject Editor for not only considering our manuscript for publication with Ecography, but also providing helpful feedback on both the manuscript and software. Following the feedback obtained, we substantially revised and improved both the manuscript and software. This software helps make the indispensable Landsat satellite record more accessible to ecologists, land managers, and others who don't specialize in satellite remote sensing.

We acknowledge that utilizing the *LandsatTS* package for R requires an account with Google Earth Engine (GEE) and installation of GEE and *rgee* but believe these are not too high of barriers to use. Landsat data are publicly available, but all data providers require an account, whether it's GEE or the USGS. Obtaining a GEE account is free, fast, and provides access to a wide variety of data beyond Landsat. While most users find it straightforward to install GEE and rgee, there can be cases when installation proves to be challenging. Therefore, we point users to GEE and rgee documentation that can help guide them through the installation process. Overall, the *LandsatTS* software can help improve our understand of ecological dynamics around the world by enabling a broader community to utilize the unique Landsat data record.

In extension of this, it is hard to see whether your lsatTS install actually works, as the running example in the paper requires 2 days to download the data! I would definitely like the example in the paper to be one that is immediately runnable, so that a reader can read the paper with a working R session next to them, and also use the example to troubleshoot that their install of the package actually works correctly. Maybe one approach is to split the data acquisition and analysis example into two bits, make the data acquisition smaller and supply the data needed for the example within the package.

Author response: We agree the original example application was a poor choice that took too long to run and so now provide a different example application that more quickly and effectively demonstrates software functionality. The new example application focuses on changes in vegetation greenness from 2000 to 2022 across a random sample of locations in the Noatak National Preserve in northern Alaska, USA. As suggested, we split the data extraction and analysis portions of the example. To demonstrate data export from GEE, the example application randomly selects and exports data for three random locations within the preserve, which takes about six minutes to complete. To demonstrated data analysis, the example application now relies on Landsat data included in the package (n = 100 random locations). The revised example application more efficiently demonstrates functionality of *LandsatTS*.

Much of the description in the paper is a point-by-point description of the functions, making this read less like an article and more like a printed manual page. It might make sense to leave the function descriptions in there, but I suggest having them a little later (maybe after the example) and focusing more on a description of the philosophy of the package, use case and workflow design. The readme of the github repository is useful and contains some good illustrations and could probably be reproduced in the supplementary materials.

For Review Only

Author response: We significantly restructured the manuscript to emphasize the philosophy, workflow, and use case of the package. This included fully restructuring the introduction, modifying the use case, and moving the function descriptions to end of the manuscript. This restructuring much improves the manuscript.

In general, Ecography prefers packages installable directly from CRAN. Are there strong technical reasons for not doing this?
Author response: While having written the code to a high standard and provided thorough documentation, we currently are not able to muster the further time and resources necessary to get this R package onto the CRAN. We did not originally plan to develop this package but rather did so opportunistically once it became apparent there was broader community interest in utilizing these tools. Developing this package has already taken time and resources that were considerably beyond the scope of our funded research projects. Besides resource limitations, there currently are a huge and growing number of R packages, many of which are only available through GitHub. GitHub makes it possible to readily implement software changes and updates, as well as easily install the package from within R, while the update and release process in CRAN is substantially more cumbersome.

In general, the github repo and code is well organized and documented, with a good set of unit tests. As a small comment maybe activating continuous integration on repo pushes would secure long-term consistency of the code base.
Author response: This is an excellent suggestion! For now, we have been running the tests locally before pushes to the main branch as setting up the rgee-GEE access on the GitHub runners provided a large hurdle given our limited knowledge of GitHub actions and how to securely handle the secrets that are required. However, we are keen to engage with this in the future and will aim to implement CI using GitHub actions in the long run – even if just for those functions that don't required GEE access.

Secondly, I do have another concern about the package that I'd like you to address. It seems that the workflow is fairly fixed (some functions are marked as "optional"), and I partly get the impression that this package, especially the analytical part, is intended for a very particular pre-determined workflow, leading to a defined set of analyses/results. It would be good to see discussed how much the package lends itself to a broader set of use cases and frameworks, and how much creativity they allow the researchers using the package.
Author response: We primarily developed this package for generating and analyzing multidecadal time series of vegetation greenness using Landsat data and believe there is considerable interest among the ecological community in conducting similar analyses. That said, the package's data extraction and processing tools also enable users to undertake other analyses that rely on carefully processed Landsat time series data for sample locations. Furthermore, we designed the software so there is a lot of flexibility within functions, such as how splines are fit when characterizing seasonal phenology, or choices between different cross-sensor calibration functions. We updated Figure 1 to better demonstrate different options for utilizing this software, and now also discuss several examples of other possible uses. For instance, part of the introduction now reads:

> These tools have also been used to assess high-latitude vegetation responses to insect outbreaks (Boyd et al. 2019, Boyd et al. 2021), wildfires (Gaglioti et al. 2021), and permafrost degradation (Verdonen et al. 2020), as well as for syntheses focused on high-latitude disturbance regimes (Foster et al. 2022) and Arctic shrubification (Mekonnen et al. 2021). Among other applications, these tools could further be used to complement field-based ecosystems monitoring in protected areas, evaluate ecosystem impacts of extreme weather

For Review Only

> events (e.g., droughts), and improve local to global mapping efforts by enabling users to develop regression models for cross-sensor calibration. In summary, *LandsatTS* enables ecologists and other researchers to extract and process Landsat time series that can then be used to analyze vegetation phenology or for other user-defined applications.

In all these comments amount to quite a bit of restructuring, but I feel confident the authors should be able to meet the comments and submit a version that can eventually be accepted, so it's somewhere between a major and a minor revision.
Author response: We appreciate your feedback and have revised and restructured the manuscript as recommended. The revised manuscript and software is greatly improved.

As two small comments that I just mention for consideration:
1. would it be easier if the package was named LsatTS? This seems more consistent with the acronym
Author response: To improve clarity and discoverability, we changed the name of the package from *lsatTS* to *LandsatTS*.

2. It seems unnecessary to have all functions preceeded by `lsat_`. Any user interested in such explicitness could always use `lsatTS::` instead.
Author response: We agree it is not entirely necessary for function names to be preceded by "lsat_", but this naming convention conveniently groups package functions while adding little to the length of function names. Further, we already have a userbase that is using the current naming convention. Therefore, we have opted to maintain the current naming convention to allow for continuity of the already existing code.

Review 1 Comments
The authors present a novel R package (lsatTS) that offers a range of functions for constructing, cleaning, and analyzing Landsat time series for phenology purposes. The integration with Google Earth Engine and related 3rd-party libraries (i.e., rgee) is a key feature. The authors have written a clear, well-organized overview of the package components and background rationale. There are only a few areas where I thought they could strengthen their description of their work, as described below, followed by comments regarding grammatical errors and minor edits.
Author response: We thank the reviewer for their positive, constructive feedback and have accordingly revised the manuscript and software.

The authors describe several existing R packages for processing Landsat data. However, they do not similarly review existing R packages for phenological analysis, such as "phenology", "phenor", and "phenofit". Explaining how lsatTS complements those packages or provides additional functionality would highlight the novelty and utility of their effort.
Author response: We appreciate the reviewer's suggestion and examined the packages they mentioned. The *phenology* package focuses on animal phenological count data, while *phenor* provides tools for evaluating plant phenology for several datasets. Since the manuscript is already rather long, we chose not to review those two packages; however, we now highlight the new *phenofit* package given its particular relevance. Part of the introduction now reads:

> … To address this issue, *LandsatTS* includes tools to estimate annual maximum vegetation greenness based on site-specific phenological modeling that iteratively fits cubic splines to vegetation greenness time series. Users interested in other aspects of vegetation phenology (e.g., timing of spring onset or fall senescence) could extract and process Landsat data using

For Review Only

> *LandsatTS*, but then capitalize on tools provided by other R packages, such as the new *phenofit* package that provides state-of-the-art tools for fitting phenological models (Kong et al. 2022). More broadly, while *LandsatTS* provides tools focused on generating high-quality vegetation greenness times series, it also enables users to undertake other analyses that rely on cleaned and cross-calibrated Landsat data.

I think the random forest cross-calibration option is intriguing but a little puzzling. What is the benefit of the site-specific process over applying fixed band/index transformations (e.g., those in Roy et al. 2016)? If users do not have enough samples to train random forest models, the authors already provide the option of pre-processed data, which seems like a similar approach. Can the authors make some statement about the advisability of performing the RF step?
Author response: Further cross-sensor calibration is crucial for time series analyses, therefore *LandsatTS* includes tools that enable users to cross-calibrate spectral bands and indices from Landsat 5 and 8 with Landsat 7. Prior approaches for cross-sensor calibration focused on linear corrections for individual spectral bands and select spectral indices (e.g., NDVI) using regional data (e.g., continental USA) from Landsat Collection 1 (e.g., Ju and Masek, 2016;Roy et al., 2016). These published cross-sensor calibration models do not account for potential non-linearities, may not be suitable for other regions, and may not be appropriate for the newer Landsat Collection 2 dataset, thus new tools are needed to facilitate cross-sensor calibration. During revision, we added further rational to the Background section and also developed a new function called *lsat_calibrate_poly()* that enables users to cross-calibrate individual spectral bands and indices using polynomial regression models instead of random forest models. The new function yields results that are similar to the original function, but generates regression models that are more readily re-used and shared. Part of the Background section now reads:

> Landsat time series analyses that use measurements from multiple sensors are hindered by systematic biases in spectral bands and indices among the Landsat 5 Thematic Mapper (TM), Landsat 7 Enhanced Thematic Mapper Plus (ETM+), and Landsat 8 Operational Land Imager (OLI) sensors (Ju and Masek 2016, Roy et al. 2016, Berner et al. 2020, Berner and Goetz 2022). If unaccounted for, these biases can introduce pronounced artificial trends into combined time series, such as spurious increases over time in spectral indices of vegetation greenness including the widely used Normalized Difference Vegetation Index (NDVI) (Sulla-Menashe et al. 2017). Prior approaches for cross-sensor calibration focused on linear corrections for individual spectral bands and select spectral indices (e.g., NDVI) using regional data (e.g., continental USA) from Landsat Collection 1 (e.g., Ju and Masek 2016, Roy et al. 2016). While valuable, these published cross-sensor calibration models do not account for potential non-linearities, may not be suitable for other regions, and may not be appropriate for the newer Landsat Collection 2 dataset. Therefore, *LandsatTS* includes functions to cross-calibrate spectral bands and indices among Landsat 5, 7, and 8 using either random forest machine learning or polynomial regression models. These models are fit using the user's dataset. However, if the user's dataset is too small to fit these models, then, if appropriate, the user can choose to fit models using pre-processed and staged Landsat data that were sampled from across the Arctic tundra and boreal forest biomes. Flexible implementation of cross-sensor calibration in the *LandsatTS* workflow enables the user to generate high quality time-series that are free from sensor-specific biases that can otherwise induce spurious trends.

Currently, the user is able to set a threshold deviation from the cubic spline curve for removing points (last_fit_phenological_curves()). It would be helpful to have the option to specify thresholds that are

For Review Only

distinguished by whether the point is above or below the curve, since typically a lower value is more suspect than a higher one.
Author response: This is a good idea, so we modified the function so users can now set separate thresholds to remove points that are above or below the fitted cubic spline.

It might be prudent to present readers with a small, manageable process instead of one that takes ~2 days to export the files.
Author response: We fully agree that a smaller, more manageable example application is needed. Therefore, we developed a new example application that focuses on changes vegetation greenness from 2000 to 2022 across a network of random sample points in the Noatak National Preserve in northern Alaska, USA. The data extraction portion of this example now takes about six minutes, while the data analysis portion of the example relies on data that are now provided with the package. This example now effectively demonstrates the package's functionality in a far more reasonable amount of time.

I recommend commenting out (or at least drawing attention to!) the rm(list=ls()) command in the code, and setting setwd to a generic folder (see https://www.tidyverse.org/blog/2017/12/workflow-vs-script/)
Author response: We appreciate the reviewer highlighting the workflow vs script distinction and have revised the scripts accordingly.

Minor edits and typos:
L78: Remove hyphen between "widely-used". Not necessary in compound adjectives when the first word is an adverb that ends in -ly. Other instances throughout paper.
Author response: Fixed here and elsewhere throughout the manuscript.

L98: "…provides integrated, sample-based framework…" Insert "an" before "integrated".
Author response: Done

L132: This is a trivial request but it would be useful for the packages to be listed alphabetically.
Author response: Done

L210: Italicize "last_general_prep()"
Author response: Done

L216: "Each…were". Change to "was".
Author response: Done

L244: The Landsat sensors are listed correctly on page 2 (L5 TM, L7 ETM+, L8 OLI), but here L7 and L8 are incorrectly referred to as ETM and ETM+, respectively. See also L248, Table 3.
Author response: Fixed

L278, 280: "moving-windows" incorrectly hyphenated here.
Author response: Fixed

L298: Change "(4) and" to "and (4)"
Author response: Done

L311: Missing period at end of sentence.
Author response: Done

For Review Only

L340: “The function extracts site x years with at least…” I’m unclear whether “site x years” is something I’m misinterpreting (x years of data at a site?) or if it’s a typo. Either way, the meaning could be clearer.
Author response: That is the correct interpretation, but to improve clarity, we modified the sentence to now read, “For each site, the function extracts years with at least the user-specified number of growing season observations…”

L354: “remove” -> “removes”
Author response: Done

L383: “was” -> “were” (Landsat data)
Author response: Done

L402: “…observations in the between…” Remove “in the”.
Author response: Done

L488: Italicize “last”
Author response: Done

L544: “…where there were temporally overlaps measurements from pairs Landsat satellites”. Couple of typos in there.
Author response: Corrected to, “… where there were temporally overlapping measurements from pairs of Landsat satellites.”

L566: “estimate” -> “estimates”
Author response: Done

L573: “…prior TO the turn…”
Author response: Done

L610: “dried” -> “drier”
Author response: Done

L611: “with defoliation” -> “to defoliation”
Author response: Done

Figure 1: Is there any significance to the fact that only some functions are italicized?
Author response: No, that was an accident. For the figure, we remove italics from all text.

Figure 2: (b) appears to show the location of Disko Island rather than the study area per se. A different color scheme for the positive NDVImax values might provide more contrast to the green background of the image.
Author response: This figure no longer appears in the manuscript because we now use a different example application.

Figure 4: Remove decimal from right-hand column “count” legend
Author response: Done.

For Review Only

Figure 5:
- Mention the time frame of the example in the caption.

Author response: Done. We now mention observations were made between 1985 and 2022.

- It's unclear whether the Observation (pts) and Curve legends are supposed to match temporally; the color ramps are identical, but the years are clearly at unequal spacing. Is the reader meant to visually match the color of the points with a similarly colored curve? Otherwise, I'm not sure I understand the point of the color-coding.

Author response: We use these figures for a quick visual assessment of whether there are erroneous curves or observations, as well for visually highlighting long-term changes in phenology. Color coding help illustrate how individual curves are fit to observations. Curves are fit to observations from multiple years, but they are colored based on the focal year. We now also make these points in the figure caption.

- I'm a little confused about some of the curve fitting. In samples like pixel _1838 (top row, middle column) many of the lower-NDVI pre-200 DOY points appear to be ignored, while curves are seemingly well-matched to the higher-NDVI points. Is there a weighting function in the curve-fitting routine that promotes points with higher NDVI?

Author response: The figure originally showed all observations, regardless of whether they were filtered out during the curve fitting routine. The curve fitting routine does not inherently promote observations with higher values; however, anomalous observations tend to have low values that get filtered out. We updated the figure so now it does not show observations that were filtered out as anomalies.

- There seems to be quite a lot of low-NDVI points, which makes me wonder about the noise reduction function in the library.

Author response: The curve fitting process involves iteratively removing points and refitting curves until the remaining points are all within a user-defined threshold of the final curve. However, the figure originally showed all points, regardless of whether they were filtered out during the curve fitting routine. As noted above, we updated the figure, so it now only shows observations that were used for curve fitting, while excluding those that were filtered. Nevertheless, we added another noise reduction step to the routine for initial outlier removal. The function now includes an initial step that, for each site, fits a curve using data pooled across all years and then filters out observations that differ from the curve by more than 100%.

- Overall, I find this figure hard to follow. Personally, I think I would prefer to see a sequence of years with individual phenology curves rather than the kind of consolidated representation shown here. This opinion is not a request to revise the approach! But it would be helpful for the authors to explain their justification for the 11-year aggregation of data.

Author response: We concede its challenging to display the seasonal distribution of observations, interannual changes, and curve fits across multiple decades for multiple sites. While imperfect, this figure does convey a lot of information. As we now further note in the function description, it is generally necessary to pool data across multiple years because there are typically few observations within an individual year. Part of the function description now reads:

> … Often there are too few observations from an individual year to fit a reliable phenological curve, therefore the function enables users to pool observations over multiple years when fitting each cure. The default is a 7-year moving-window centered on the focal year, but the

For Review Only

width of the moving window can be made shorter or longer if there are many or few observations in the data record…

Figure 7: Mention the number of sample locations. Please specify what “grouped by the concomitant temporal trends” means. Were the annual data for all sample locations with a particular trend (browning/greening/no-change) averaged?

Author response: After further consideration, we decided to remove this functionality.

Reference

Ju, J., and Masek, J.G. (2016). The vegetation greenness trend in Canada and US Alaska from 1984–2012 Landsat data. *Remote Sensing of Environment* 176**,** 1-16.

Roy, D.P., Kovalskyy, V., Zhang, H.K., Vermote, E.F., Yan, L., Kumar, S.S., and Egorov, A. (2016). Characterization of Landsat-7 to Landsat-8 reflective wavelength and normalized difference vegetation index continuity. *Remote Sensing of Environment* 185**,** 57-70.

For Review Only

Abstract

The Landsat satellites provide near-global surface reflectance measurements since the early 1980s that are increasingly used to assess interannual changes in terrestrial ecosystem function. These assessments often rely on spectral indices ~~(e.g., NDVI)~~ related to vegetation greenness and productivity~~.~~ (e.g., NDVI). Nevertheless, multiple factors impede multi-decadal assessments of spectral indices using Landsat satellite data, including ease of data access and cleaning, as well as lingering issues with cross-sensor calibration and challenges with irregular timing of cloud-free acquisitions. To help address these problems, we developed the *~~lsatTS~~LandsatTS* package for R. This software package facilitates sample-based time series analysis of surface reflectance and spectral indices derived from Landsat sensors. The package includes functions that enable the extraction of the full Landsat ~~record~~5, 7, and 8 records from Collection 2 for point sample locations or small study regions using the Google Earth Engine accessed directly from R. Moreover, the package includes functions for (1) rigorous data cleaning, (2) cross-sensor calibration ~~with machine learning~~, (3) phenological modeling, and (4) time series analysis. For an example application, we show how *~~lsatTS~~LandsatTS* can be used to assess changes in annual maximum vegetation greenness from 2000 to ~~2020~~2022 across ~~a study area on Disko Island~~the Noatak National Preserve in ~~the Greenlandic Arctic~~northern Alaska, USA. Overall, this software provides a suite of functions to enable broader use of Landsat satellite data for assessing and monitoring terrestrial ecosystem function ~~over the past four~~during recent decades across local to global geographic extents.

Background

~~Ecological monitoring using the Landsat satellites~~

Satellite remote sensing is crucial for assessing and monitoring how Earth's terrestrial ecosystems have changed during recent decades (National Academies of Sciences 2018). The Landsat satellites are particularly valuable in this regard because they are the longest continuously running satellite program and were designed for terrestrial ecosystem monitoring at moderate spatial resolution (Wulder et al. 2019). The first Landsat satellite (Landsat 1) was launched in 1972 as a partnership between NASA and the US Geological Survey (USGS) and since that time a series of additional satellites have been launched, with the most recent being Landsat 9 in 2021. The Landsat satellites carry multispectral sensors that provide surface reflectance measurements used for a wide range scientific and land management applications (Wulder et al. 2019). These include~~, for instance,~~ global monitoring of forest canopy cover change (Hansen et al. 2013, Sexton et al. 2013) ~~and surface water extent~~, land cover and use change (Potapov et al. 2022) and surface water extent change (Pekel et al. 2016), as well as regional- to biome-scale assessments of how disturbance, land-use and climate change are impacting terrestrial ecosystems (~~Pastick~~e.g., Wulder et al. ~~2019~~2004, Powell et al. 2010, Ju and Masek 2016, Wang and Friedl 2019~~, Berner et al. 2020, Berner and Goetz 2022~~). Hence, the Landsat program has become a cornerstone of Earth surface monitoring.

~~Impediments to Landsat time series analyses~~

~~In recent years, it has become easier to access, process, and analyze Landsat data; however,~~Yet there are ~~still~~ challenges that hinder use of these data by ecologists, land managers, and other non-remote sensing specialists. ~~The USGS made the Landsat archive publicly available in 2008 (Woodcock et al. 2008) and in recent years Google has hosted a copy of the archive accessible via the cloud-computing platform~~

For Review Only

Here we present the *LandsatTS* (i.e., *Landsat Time Series*) software package for R that enables users to extract, process, and analyze time series of Landsat surface reflectance measurements for sample locations anywhere on Earth. *LandsatTS* enables extraction of Landsat 5, 7, and 8 surface reflectance measurements from the full Landsat Collection 2 dataset on Google Earth Engine (GEE; Gorelick et al. 2017). ~~These steps have made Landsat~~Furthermore, *LandsatTS* includes functions that facilitate (1) data ~~much more readily available to the end user~~cleaning, (2) cross-sensor calibration, (3) phenological modeling, and ~~enabled~~(4) time series ~~analyses~~analysis of ~~the Normalized Difference Vegetation Index (NDVI) and other spectral indices of "~~vegetation greenness~~" that are related to productivity~~ (Figure 1, Table 1). This software grew out of research projects focused on vegetation dynamics across northern high-latitude ecosystems (~~Tucker 1979, Goetz and Prince 1999,~~ Berner et al. 2020, ~~Camps-Valls et al. 2021~~Berner and Goetz 2022)~~.~~ ~~However, time series analyses that use measurements from multiple sensors are hindered by systematic biases in both individual bands and spectral indices among the Landsat 5 Thematic Mapper (TM), Landsat 7 Enhanced Thematic Mapper Plus (ETM+), and Landsat 8 Operational Land Imager (OLI) sensors (Ju and Masek 2016, Roy et al. 2016, Berner et al. 2020, Berner and Goetz 2022). If unaccounted for, these biases can introduce strong artificial trends into combined time series, such as spurious increases in NDVI over time ("greening") (Sulla-Menashe et al. 2017). Existing approaches for cross-sensor calibration focus on linear corrections (Ju and Masek 2016, Roy et al. 2016), but not all relationships are linear, and corrections are available for a limited number of spectral indices (e.g., NDVI) and often based on regional data. Another potential hindrance when analyzing Landsat time series is the irregular timing of clear-sky acquisitions. This can make it challenging to characterize the NDVI or other spectral indices at a desired phenological stage (e.g., peak summer) and is especially problematic in regions with short growing seasons, such as the rapidly warming Arctic (Berner et al. 2020). Simple calculations of annual maximum NDVI (NDVI$_{max}$) will have a low bias early in the Landsat record, but less so during later years when more observations are available during each growing season. Hence, again, care is needed to avoid the introduction of spurious greening trends into the time series (Berner et al. 2020). In summary, while Landsat data are more readily available than ever before, there are lingering challenges for specialists and non-specialists alike.~~

~~*The lsatTS package*~~

~~We developed the R package *lsatTS* (i.e., *Landsat Time Series*) to facilitate sample-based time series analysis of spectral indices derived from surface reflectance measured by multispectral sensors on several Landsat satellites. Specifically, *lsatTS* includes functions for sample-based extraction of full data records from Landsat 5, 7, and 8 that is accomplished by querying the Landsat Collection 2 data set on GEE (Gorelick et al. 2017) using the application programming interface provided by the *rgee* package in R (Aybar et al. 2020). Further functions included in *lsatTS* facilitate (1) data cleaning, (2) cross-sensor calibration with machine learning, (3) characterization of growing season conditions using phenological modeling, and (4) time series analysis of vegetation greenness (Figure 1, Table 1). Altogether, *lsatTS* offers an integrated framework for Landsat data extraction, processing, and time series analysis for sample locations anywhere on Earth's surface.~~

~~*lsatTS*~~ and is implemented within the free, open-source, and widely~~-~~ used R ~~software~~statistical computing environment (R Core Team 2021). ~~Several R packages currently exist for processing Landsat data, including *landsat* (Goslee 2011) and *landsat8* (dos Santos 2017). *landsat* includes functions for radiometric and topographic correction of Landsat scenes,~~

For Review Only

~~while *landsat8* includes functions for computing top of atmosphere reflectance, radiance, and/or brightness temperature on Landsat scenes. These existing packages provide valuable tools for processing individual Landsat scenes. Nevertheless, *lsatTS* provides fundamentally different functionality that includes an integrated framework for robust time-series analysis of vegetation dynamics at local to global scales.~~

~~*lsatTS* grew out of recent research projects~~It has become easier to access and process Landsat data since the archive was made publicly available in 2008 (Wulder et al. 2012) and a copy of the archive subsequently hosted on GEE (Gorelick et al. 2017). The GEE cloud-computing platform enables users to access and process Landsat data using JavaScript and Python application program interfaces (APIs), as well as with R through the *rgee* package (Aybar et al. 2020). R is very popular among ecologists (Lai et al. 2019), yet other existing R packages only provide tools for processing individual Landsat scenes. For instance, *landsat* includes functions for radiometric and topographic correction of Landsat scenes (Goslee 2011), while *landsat8* includes functions for computing top of atmosphere reflectance, radiance, and/or brightness temperature on Landsat scenes (dos Santos 2017). Thus, the *rgee* package makes it easier for ecologists use the GEE platform and work with Landsat data. Nevertheless, it remains non-trivial to not only extract Landsat time series data using *rgee*, but also to thoroughly clean the extracted data to ensure that ~~assessed changes in~~ only high-quality measurements are used in analyses. *LandsatTS* therefore provides new tools for sample-based extraction of full Landsat data records using *rgee* to access the GEE. Furthermore, *LandsatTS* includes tools to rigorously clean Landsat data using both pixel-level CFmask flags (e.g., cloud, water; Zhu et al. 2015) and scene-level criteria (e.g., cloud cover, solar zenith angle). Consequently, *LandsatTS* helps further broaden the community of researchers who can utilize Landsat data for robust spatiotemporal analyses of terrestrial ecosystem dynamics.

Landsat time series analyses that use measurements from multiple sensors are hindered by systematic biases in spectral bands and indices among the Landsat 5 Thematic Mapper (TM), Landsat 7 Enhanced Thematic Mapper Plus (ETM+), and Landsat 8 Operational Land Imager (OLI) sensors (Ju and Masek 2016, Roy et al. 2016, Berner et al. 2020, Berner and Goetz 2022). If unaccounted for, these biases can introduce pronounced artificial trends into combined time series, such as spurious increases over time in spectral indices of vegetation greenness ~~since the early 1980s for~~ including the widely used Normalized Difference Vegetation Index (NDVI) (Sulla-Menashe et al. 2017). Prior approaches for cross-sensor calibration focused on linear corrections for individual spectral bands and select spectral indices (e.g., NDVI) using regional data (e.g., continental USA) from Landsat Collection 1 (e.g., Ju and Masek 2016, Roy et al. 2016). While valuable, these published cross-sensor calibration models do not account for potential non-linearities, may not be suitable for other regions, and may not be appropriate for the newer Landsat Collection 2 dataset. Therefore, *LandsatTS* includes functions to cross-calibrate spectral bands and indices among Landsat 5, 7, and 8 using either random forest machine learning or polynomial regression models. These models are fit using the user's dataset. However, if the user's dataset is too small to fit these models, then, if appropriate, the user can choose to fit models using pre-processed and staged Landsat data that were sampled from across the Arctic tundra and boreal forest biomes ~~(Berner et al. 2020, Berner and Goetz 2022)~~. Flexible implementation of cross-sensor calibration in the *LandsatTS* workflow enables the user to generate high quality time-series that are free from sensor-specific biases that can otherwise induce spurious trends.

For Review Only

Vegetation phenology controls ecosystem processes (e.g., photosynthesis) and is often assessed using spectral indices (e.g., NDVI) derived from satellite measurements (Helman 2018, Zeng et al. 2020). Nevertheless, efforts to assess vegetation phenology using the Landsat satellites are complicated by multiple factors that include (1) irregular timing of clear-sky acquisitions within a growing season and (2) changes in the annual number of clear-sky acquisitions across years as new satellites were launched. These challenges are especially acute in regions with short, cloudy growing seasons such as the Arctic, where the median number of clear-sky growing season measurements increased from 2 per year in 1995 to 7 per year in 2015 (Berner et al. 2020). Annual maximum vegetation greenness is an important metric of vegetation phenology related to productivity (Berner et al. 2020, Zeng et al. 2020, Boyd et al. 2021), yet this metric is sensitive to the timing and number of measurements made in a growing season. Consequently, simple calculations of this metric tend to be artificially low early in the Landsat record but less so during later years when more measurements are available, which can introduce a spurious positive trend into a time series (Berner et al. 2020). To address this issue, *LandsatTS* includes tools to estimate annual maximum vegetation greenness based on site-specific phenological modeling that iteratively fits cubic splines to vegetation greenness time series. Users interested in other aspects of vegetation phenology (e.g., timing of spring onset or fall senescence) could extract and process Landsat data using *LandsatTS*, but then capitalize on tools provided by other R packages, such as the new *phenofit* package that provides state-of-the-art tools for fitting phenological models (Kong et al. 2022). More broadly, while *LandsatTS* provides tools focused on generating high-quality vegetation greenness times series, it also enables users to undertake other analyses that rely on cleaned and cross-calibrated Landsat data.

LandsatTS includes an integrated suite of tools that were originally developed to assess long-term changes in vegetation greenness within the rapidly warming Arctic tundra and boreal forest biomes (Berner et al. 2020, Berner and Goetz 2022). ~~We found~~ This software implements a sample-based approach ~~was~~that we found is well-suited for assessing vegetation dynamics and evaluating ecological hypotheses ~~for~~in these cold northern biomes, while substantially reducing computational burden compared with wall-to-wall analyses. ~~Moreover, this~~ The sample-based approach ~~enables~~is conducive to rigorous propagation of uncertainty using Monte Carlo simulations (Berner et al. 2020, Berner and Goetz 2022), which is important for improving confidence in remote sensing analyses but seldom carried out because of computational constraints (Myers-Smith et al. 2020). Furthermore, the sample-based approach has helped validate and interpret vegetation dynamics inferred from spectral indices by enabling comparisons between satellite and field measurements across widely distributed site networks (Boyd et al. 2019, Berner et al. 2020, Boyd et al. 2021, Walker et al. 2021) ~~and is conducive to rigorous propagation of uncertainty using Monte Carlo simulations (Berner et al. 2020, Berner and Goetz 2022). Comparisons with field measurements are crucial for validating and interpreting vegetation dynamics inferred from satellites measurements, while uncertainty assessments are crucial for improving confidence in such analyses but are seldom if ever carried out partially because of computational constraints (Myers-Smith et al. 2020). Overall, *lsatTS* provides integrated, sampled-based framework that has recently~~. These tools have also been used to assess high-latitude vegetation responses to ~~climate change (Berner et al. 2020, Berner and Goetz 2022),~~ insect outbreaks (Boyd et al. 2019, Boyd et al. 2021), wildfires (Gaglioti et al. 2021), and permafrost degradation (Verdonen et al. 2020) ~~in cold northern biomes.~~ , as well as for syntheses focused on high-latitude disturbance regimes (Foster et al. 2022) and Arctic shrubification (Mekonnen et al. 2021). Among other applications, these tools could further be

For Review Only

used to complement field-based ecosystems monitoring in protected areas, evaluate ecosystem impacts of extreme weather events (e.g., droughts), and improve local to global mapping efforts by enabling users to develop regression models for cross-sensor calibration. In summary, *LandsatTS* enables ecologists and other researchers to extract and process Landsat time series that can then be used to analyze vegetation phenology or for other user-defined applications. Below, we provide (1) an example application focused on vegetation dynamics across the Noatak National Preserve, USA, (2) instructions for package installation, and (3) descriptions of each function.

~~The following sections detail package installation and summarize the purpose and behavior of each *lsatTS* function. Furthermore, we demonstrate the utility of *lsatTS* with an example application focused on changes in vegetation greenness from 2000 to 2020 across a study area in the Greenlandic Arctic. For a detailed list of function descriptions, including the complete lists of arguments require by each function, please consult the helpfiles provided with the R package or refer to the list of function definitions supplied in the Supplementary Material.~~

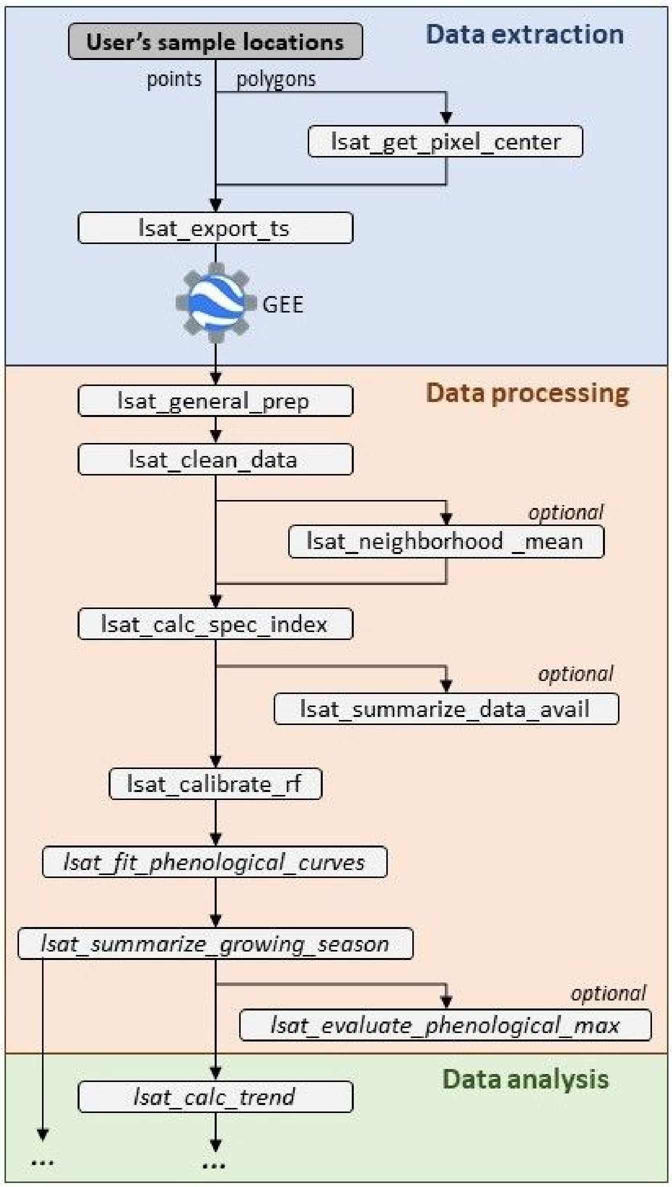

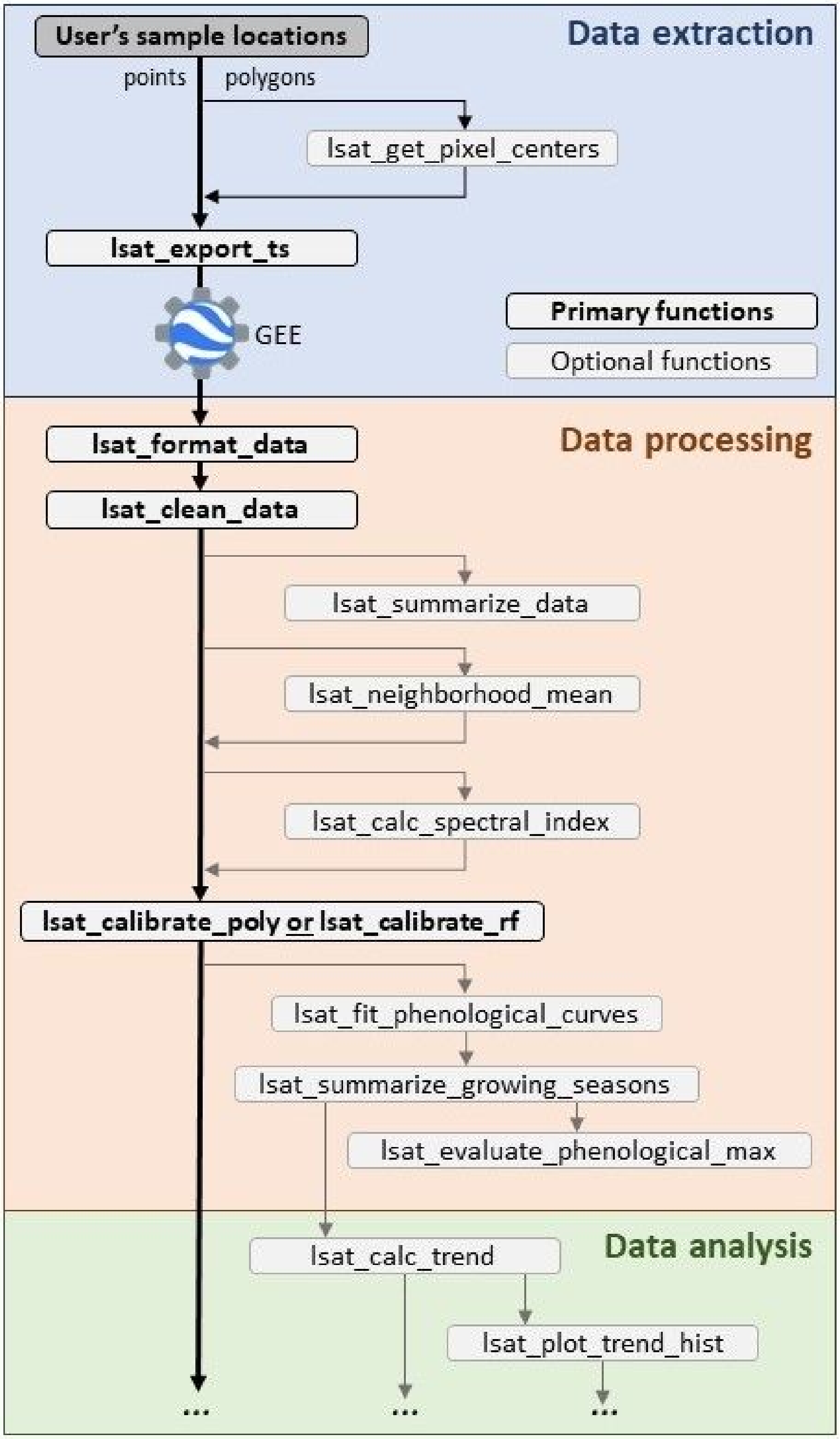

Figure 1. Schematic illustrating functions and typical workflow of the *~~lsatTS~~LandsatTS* package. Each function is described in the main text and Table 1. *~~lsatTS~~LandsatTS* has primary been used for assessments of interannual variability and trends in vegetation greenness. However, *~~lsatTS~~LandsatTS* facilitates other Landsat time series analyses by providing tools for general data extraction and processing.

Table 1. Function names and descriptions. These are listed in the order typically used.

Step	**Function**	**Description**
Data extraction	lsat_get_pixel_centers	(*Optional*) Retrieve point coordinates of all Landsat 8 pixel centers that fall within a polygon.
	lsat_export_ts	Export full Landsat surface reflectance time series for a set of point coordinates using GEE accessed from R.
Data processing	lsat_~~general_prep~~format_data	Prepare data exported from GEE, including parsing satellite names and renaming and scaling bands.
	lsat_clean_data	Filter out measurements based on presence of clouds, water, shadows, oblique view angles, and other criteria.
	lsat_summarize_data~~_avail~~	(*Optional*) Summarize data availability at each site, such as total number and years of observations.
	lsat_neighborhood_mean	(*Optional*) For buffered sites, compute band-wise mean surface reflectance across grid cells within the buffer.
	lsat_calc_~~spec~~spectral_index	Calculate a variety of widely used spectral indices, such as the Normalized Difference Vegetation Index (NDVI).
	lsat_calibrate_rf	Cross-calibrate bands or spectral indices from Landsat 5/8 to match Landsat 7 using Random ~~Forests~~Forest models.
	lsat_calibrate_poly	Cross-calibrate bands or spectral indices from Landsat 5/8 to match Landsat 7 using polynomial regression.
	lsat_fit_phenological_curves	Characterize seasonal land surface phenology at each site by iteratively fitting flexible cubic splines.
	lsat_summarize_growing_seasons	Estimate various phenological metrics from fitted cubic splines, such as annual maximum vegetation greenness.
	lsat_evaluate_phenological_max	(*Optional*) Evaluate estimates of annual maximum vegetation greenness with measurement availability.
Data analysis	lsat_calc_trend	Calculate temporal trends using non-parametric Mann-Kendall trend tests and Theil-Sen slope indicators.
	lsat_plot_trend_hist	Plots a histogram of trends across sample sites

Example application: Vegetation greenness trends in the Noatak National Preserve, USA

Here we provide an example analysis of interannual changes in vegetation greenness from 2000 to 2022 within the Noatak National Preserve in northern Alaska, USA (Figure 2). The Noatak National Preserve is a vast wilderness of mountainous Arctic and alpine tundra that encompasses the largest undisturbed watershed in North America. The preserve is about 2.6 million hectares of roadless lands that were designated in 1980 to maintain ecological integrity, protect habitat and archeological resources, and provide opportunities for scientific research. Recent ecological research found climate warming substantially increased growth rates of white spruce (*Picea glauca*) and led to rapid expansion of trees and tall shrubs into tundra over the past half century in parts of the preserve (Suarez et al. 1999, Terskaia et al. 2020, Dial et al. 2022). The impacts of climate change are increasingly evident in the Noatak National Preserve and underscore the importance of sustained and cost-effective ecological monitoring and assessment.

Annual maximum vegetation greenness is related to tundra aboveground biomass and productivity, making it an important ecological metric that can be monitored using satellite remote sensing (Jia et al. 2003, Raynolds et al. 2012, Berner et al. 2018, Bhatt et al. 2021). We therefore demonstrate how multidecadal changes in annual maximum vegetation greenness can be readily assessed across the preserve using Landsat satellite data. In this section, we guide the reader through the analysis code with example output figures and tables that are generated by the *LandsatTS* functions.

For Review Only

Part 1: Export Landsat time series from Google Earth Engine

To start, we create a random sample of points within the Noatak National Preserve and then export Landsat time series for each sample point using GEE (Code Box 1). To facilitate our example, we include the preserve boundary as a simple feature polygon dataset ("noatak.sf") in *LandsatTS*. Users could alternatively read in their own shapefile using *sf::st_read()* or create a collection of spatial points (e.g., field sites) using *sf::st_sf()* (Pebesma 2018). We load the preserve boundary dataset, create a simple random sample of *n* points within the boundary using the *sf::st_sample* function, give each sample a unique identifier, and then create an interactive map showing preserve and sample point locations using *leaflet* (Figure 2) (Cheng et al. 2022). We then initialize GEE and submit a task to GEE that for each sample point exports all Landsat 5, 7, and 8 measurements made between day of year 152 (beginning of June) and 273 (end of September) from 1985 to 2022. For expediency, this example exports data for three random sample points, which took ~11 minutes and yielded ~800 B of data written to a folder called "earth_engine" on the user's Google Drive. Exporting four decades of summer Landsat data for 100 sample points took ~6 hours and yielded ~28 MB of data, while exporting data for 1,000 sample points took ~15 hours with four tasks running in parallel and yielded ~280 MB of data. To facilitate subsequent parts of this example, we include Landsat data for 100 sample points as a dataset ("noatak.dt") in *LandsatTS*. Data export progress can be monitored using the GEE task manager in the web browser (https://code.earthengine.google.com/tasks) or with the R console using the ee_monitoring() function provided by *rgee*. The CSV file(s) containing the raw exports need to be copied from the user's Google Drive to the local machine that will carry out the subsequent processing using *LandsatTS*. The files can be copied manually or using the ee_drive_to_local() function provided by *rgee*. Once the records are available locally, they need to be cleaned and processed into vegetation index time series as detailed in the next section.

Code Box 1: Export Landsat time series from Google Earth Engine

```
 # Load required R packages
require(LandsatTS)
require(sf)
require(rgee)
require(tidyverse)
require(leaflet)

# Load the Noatak National Preserve simple feature polygon
data(noatak.sf)

# Create n random sample points within the Noatak National Preserve
n.pts <- 3
noatak.pts.sf <- st_sample(x = noatak.sf, size = n.pts) %>% st_sf()

# Add unique identifier to each point
noatak.pts.sf$sample_id <- paste0('S_', 1:n.pts)

# Make a basic interactive map showing Noatak National Preserve and sample points
leaflet() %>%
  addProviderTiles('Esri.WorldImagery') %>%
  addCircleMarkers(data = noatak.pts.sf,
                   color = 'white',
                   opacity = 0.9,
                   fillColor = 'fuchsia',
```

```
                   fillOpacity = 0.75,
                   weight = 1,
                   radius = 5) %>%
  addPolygons(data = noatak.sf,
              color = 'white',
              weight = 3) %>%
  addScaleBar(options = scaleBarOptions(imperial = F))

# Initialize Earth Engine
ee_Initialize()

# Extract a time-series of surface reflectance measurements for each Landsat pixel
task_list <- lsat_export_ts(pixel_coords_sf = noatak.pts.sf,
                            start_date = "1985-06-01",
                            end_date = "2022-09-30",
                            start_doy = 152,
                            end_doy = 273,
                            file_prefix = 'noatak',
                            drive_export_dir = 'earth_engine')
```

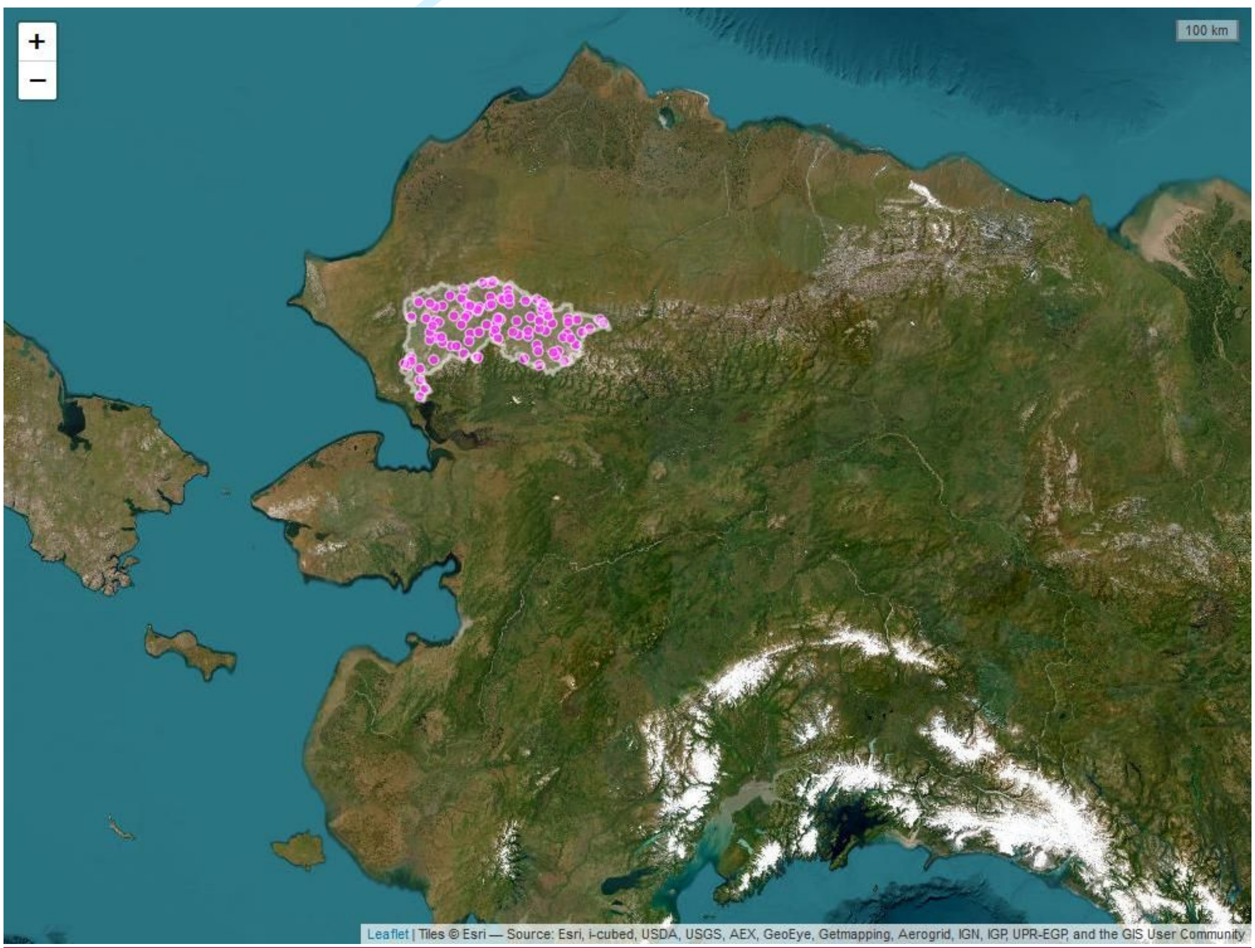

Figure 2. Screenshot of a *leaflet* interactive map showing the Noatak National Preserve boundary in northern Alaska, USA, and 100 random sample points within the preserve. Landsat time series data were extracted for each of these sample points. Base map from ESRI World Imagery.

Part 2: Format, clean, and summarize Landsat data in preparation for analysis

We load the Landsat data into R, format and clean the data, and then examine data availability. Here, we provide Landsat data for the 100 sample points as a dataset in *LandsatTS*; however, the dataset alternatively could be read into R as a data.table using the *fread()* function from the *data.table* package (Dowle and Srinivasan 2021). Once loaded into R, we format the dataset for analysis using *lsat_format_data()*, which formats column names and scales the band values, among other necessary formatting. We then clean the dataset using *lsat_clean_data()* to filter out clouds, snow, and water, as well as radiometric and geometric errors. For these field sites, *lsat_clean_data()* removed 78,625 of 99,600 observations (78.94%), including one sample point located in water. We then check the availability of clear-sky Landsat observations for the remaining 99 sample points using *lsat_summarize_data*(). On average (± 1 SD), each sample point had 212±48 clear-sky observations made between 1985 and 2022. The annual number of observations is typically small before the year 2000, as highlighted by the figure generated by the function (Figure 3).

Code Box 2: Format, clean, and summarize Landsat data in preparation for analysis

```
# Load required R packages
require(LandsatTS)
require(data.table)
require(tidyverse)
require(sf)
require(leaflet)
require(mapview)

# Load Landsat data for Noatak sites, or read in file using data.table::fread().
data(noatak.dt)

# Format the exported data
noatak.dt <- lsat_format_data(noatak.dt)

# Clean the data by filtering out clouds, snow, water, etc.
noatak.dt <- lsat_clean_data(noatak.dt)

# Summarize the availability of Landsat data for each pixel
lsat_summarize_data(noatak.dt)

# Continue to Code Box 3...
```

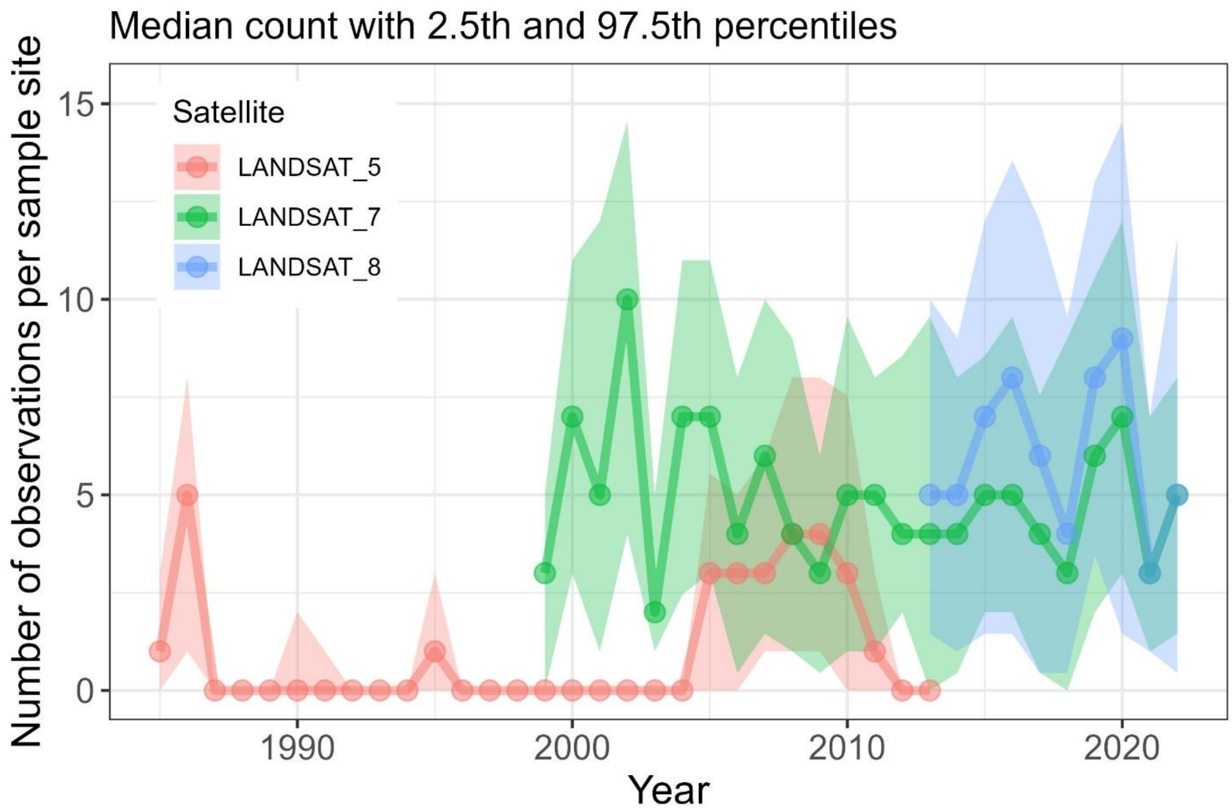

Figure 3. Annual availability of quality screened summer Landsat observations summarized across sample points in the Noatak National Preserve as returned by the function *lsat_summarize_data()*. Summaries are based on observations acquired between day of year 152 (beginning of June) and 273 (end of September). Note the limited availability of observations before the year 2000. Lines with points denote median counts while shaded bands encompass the 2.5th to 97.5th percentiles of counts among sample points.

Part 3: Generate cross-calibrated time series of annual maximum vegetation greenness

To generate time series of annual maximum vegetation greenness for each sample point, we (1) compute NDVI, (2) cross-calibrate NDVI among Landsat sensors, and then (3) estimate annual maximum NDVI (NDVImax) using phenological modeling. First, we calculate NDVI using *lsat_calc_spectral_index()*, which supports calculating a variety of commonly used spectral indices. There are systematic differences in NDVI among Landsat sensors, so next we calibrate NDVI from Landsat 5 TM and Landsat 8 OLI to match Landsat 7 ETM+, which has measurements that temporally overlap with the other two sensors. We cross-calibrate NDVI among sensors using *lsat_calibrate_poly()* to fit and apply polynomial regression models. As the number of field sites in this dataset is rather small, we use a pre-processed dataset of Landsat observations that were randomly sampled from across northern high-latitudes ecosystems and are included for this purpose with *LandsatTS*. The function generates and returns a series of graphs (Figure 4) and tabular data (Table 3) that help with evaluating model performance and can optionally be written to a user-specified directory. As desired, calibration visually (Figure 4) and statistically (Table 3) reduced the bias between Landsat 7 NDVI and Landsat 5 and 8 NDVI.

As a step towards estimating annual $NDVI_{max}$, we fit phenological models to the calibrated NDVI time series using *lsat_fit_phenological_curves()*. The function automatically returns a figure with Landsat observations and fitted phenological curves for nine random sample locations in the dataset (Figure 5). Each phenological curve characterizes the seasonal progression of NDVI using observations pooled over a multi-year period (here a 7-year moving window) and should be smooth and hump-shaped. Beware of phenological curves with long straight lines that could suggest inadequate seasonal distribution of data used when fitting the curves. Phenological models were not fit for three sites that were minimally vegetated (NDVI < 0.15) because it is challenging to extract a meaningful vegetation phenology signal under these conditions. After fitting phenological models for 22 field sites, we then generated growing season summary statistics, including estimates of $NDVI_{max}$, using *lsat_summarize_growing_seasons()*. The *lsat_evaluate_phenological_max()* can be used to output a figure that allows for visually assessing the performance of modelled $NDVI_{max}$ (Figure 6). In the case of the Noatak example dataset, modeled estimates of $NDVI_{max}$ tend to be biased slightly low (~1%) when only one or two observations are available from a growing season (Figure 6), yet there were rarely such few observations during the period from 2000 to 2021 (Figure 3). The final step following the cross-calibration and phenological modelling is the time series analysis.

Code Box 3: Cross-calibration and phenological modelling

```
# ... continuing from Code Box 2

# Compute the Normalized Difference Vegetation Index (NDVI)
noatak.dt <- lsat_calc_spectral_index(noatak.dt, si = 'ndvi')

# Cross-calibrate NDVI among sensors using polynomial regression
noatak.dt <- lsat_calibrate_poly(noatak.dt,
                             band.or.si = 'ndvi',
                             train.with.highlat.data = T,
                             overwrite.col = T)

# Fit phenological models (cubic splines) to each time series
noatak.pheno.dt <- lsat_fit_phenological_curves(noatak.dt, si = 'ndvi')

# Summarize growing season characteristics
noatak.gs.dt <- lsat_summarize_growing_seasons(noatak.pheno.dt, si = 'ndvi')

# Evaluate estimates of annual maximum NDVI
noatak.gs.eval.dt <- lsat_evaluate_phenological_max(noatak.pheno.dt, si = 'ndvi')

# Continue to Code Box 4...
```

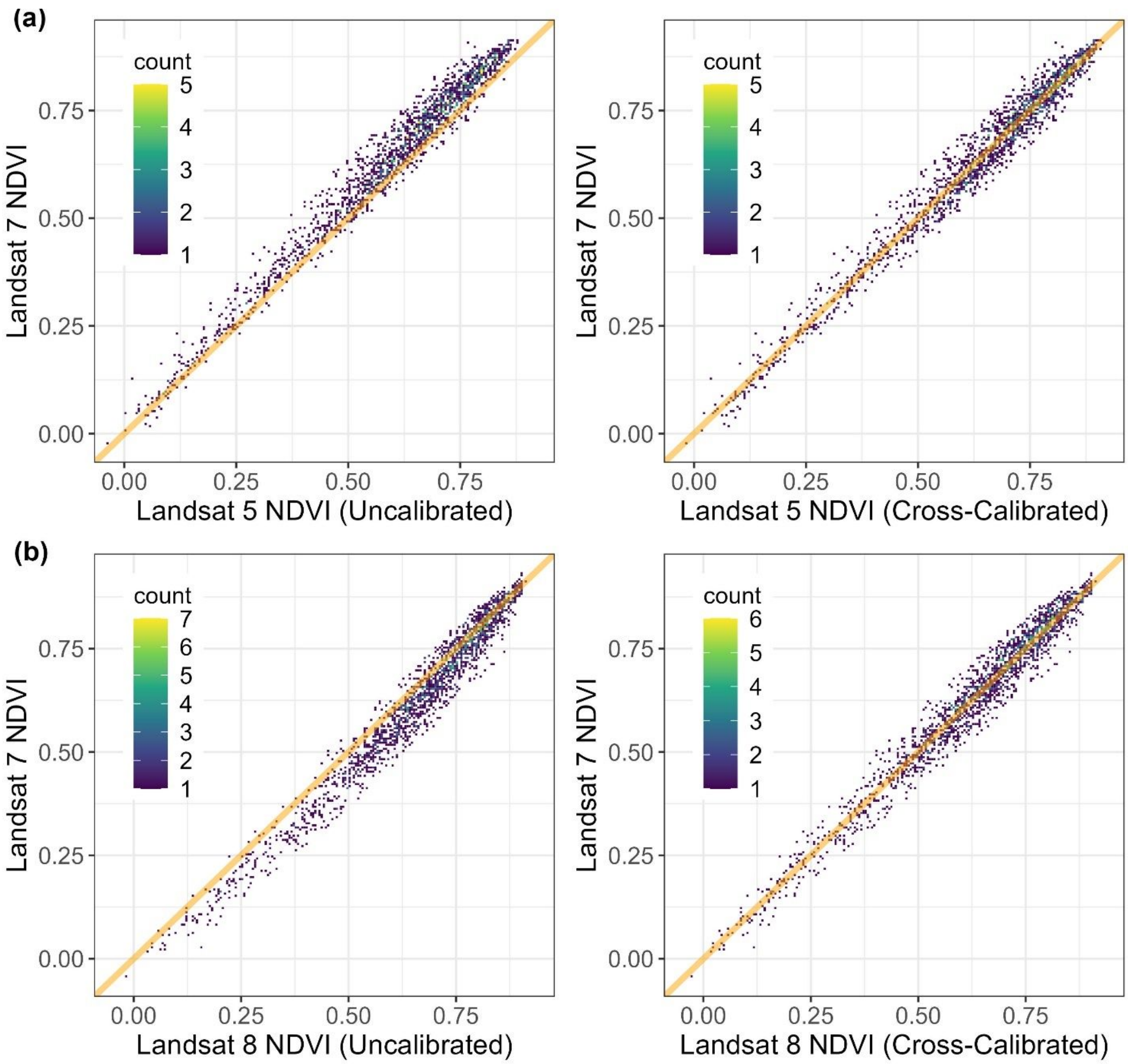

Figure 4. Relationships between Landsat 7 NDVI and both (a) Landsat 5 NDVI and (b) Landsat 8 NDVI using (left panels) original data and (right panels) data that were calibrated using polynomial regression models. Each point is a sample location from the Arctic – Boreal domain with temporally overlapping measurements from pairs of Landsat sensors. Orange diagonal lines depict 1:1 relationships. Model performance metrics are provided in Table 3. Cross-calibration substantially reduces biases between sensors.

Table 3. Summary of original biases, performance of polynomial regression models for cross-sensor calibration, and post-calibration biases in NDVI between Landsat 7 ETM+ and either Landsat 5 TM or Landsat 8 OLI. Each model was trained using 75% of available data selected at random and then cross-validated using the remaining 25% of data.

Satellite sensor	Number of sites		Original Data			Cross-Validated Error Metrics			
	Train	Eval.	RMSE	Median bias	Median % bias	r^2	RMSE	Median bias	Median % bias
Landsat 5 TM	5237	1746	0.052	-0.04	-6.1	0.974	0.032	<0.01	<0.1

Landsat 8 OLI	5927	1976	0.050	0.03	4.9	0.965	0.035	<0.01	<0.1

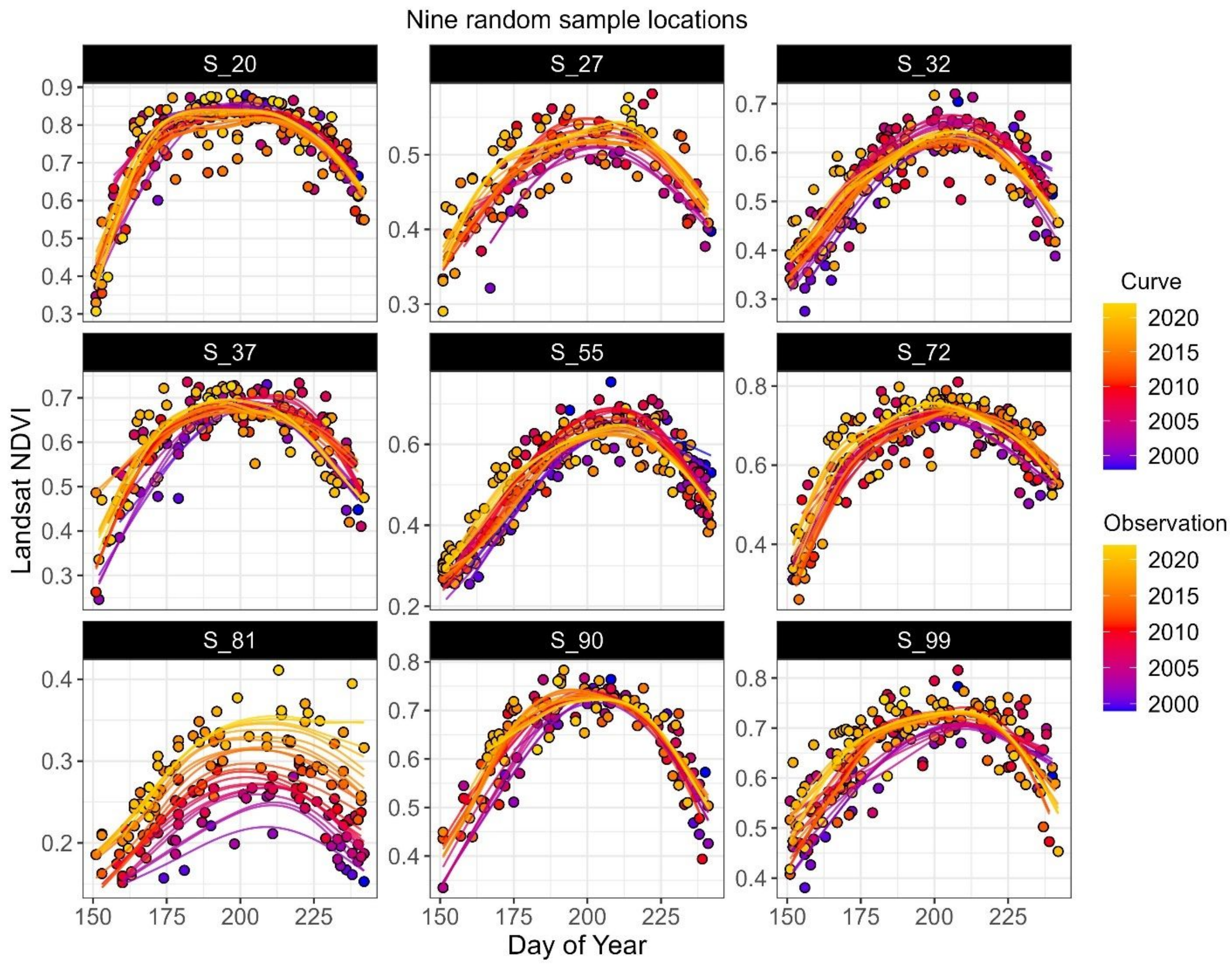

Figure 5. Seasonal progression of Landsat NDVI and phenological curves for nine random sample points in the Noatak National Preserve. Each dot is an observation that is colored by the year of acquisition ranging between 1985 and 2022. Each line represents a phenological curve that was fit to observations pooled over a 7-year window centered on the focal year as indicated by the color of the line. Color coding helps illustrate how individual curves are fit to observations. These figures can visually highlight long-term changes in phenology and can provide a quick visual assessment of how well curves are being fit to observations, especially when the function is run using the parameter *test.run* = TRUE.

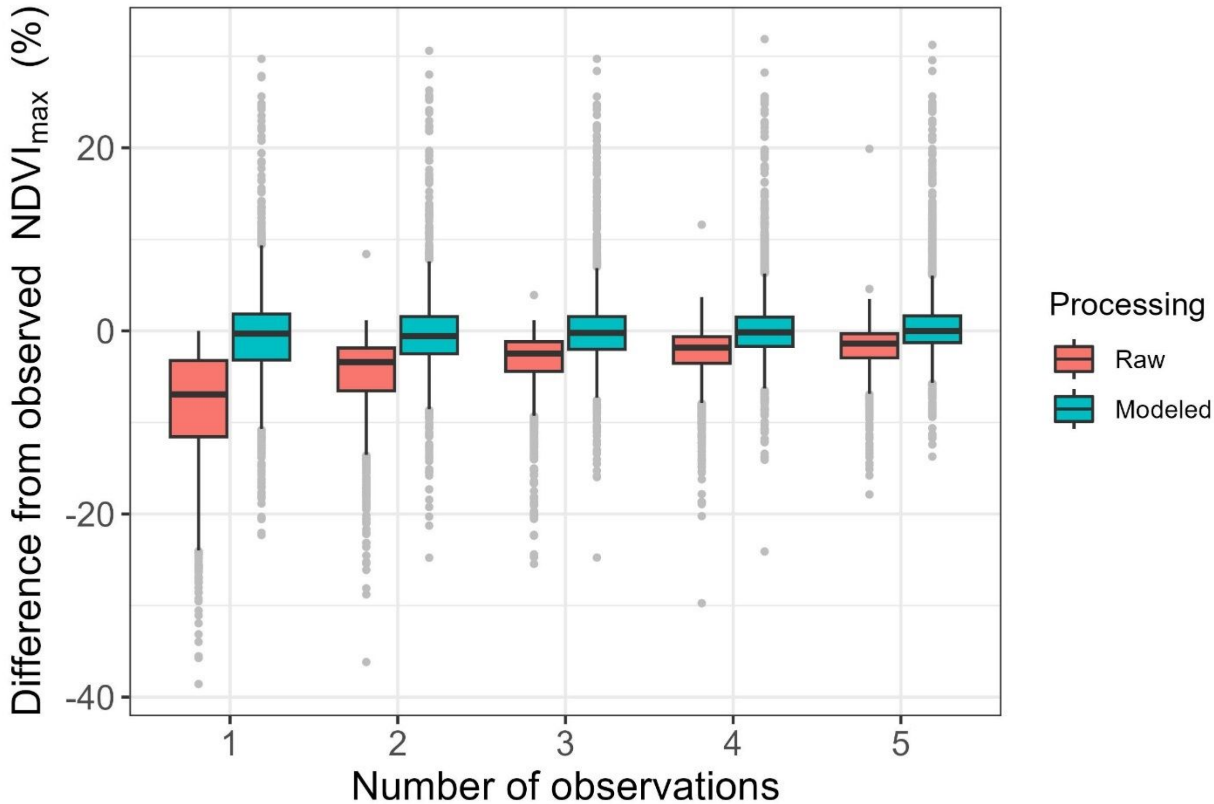

Figure 6. Raw estimates of annual maximum NDVI ($NDVI_{max}$) are biased low when only a few Landsat observations are available from a given growing season, whereas phenologically modeled estimates of $NDVI_{max}$ are minimally impacted by the availability of observations. The figure summarizes how raw and modeled estimates of $NDVI_{max}$ differ from observed $NDVI_{max}$ based on number of observations, as determined using *lsat_evaluate_phenological_max().*

Part 3: Analyze vegetation greenness time series

Finally, we evaluate the interannual trend in $NDVI_{max}$ from 2000 to 2022 for each sample point. We calculate temporal trends using the *lsat_calc_trend()* function that implements and summarizes non-parametric trend assessments (Table 4). Note how we use the "yrs" argument to restrict the time series analysis to the years between 2000-2022 to avoid using the low number of observations in the record prior to the turn of the millennium. We then create a histogram of recent $NDVI_{max}$ trends using *lsat_plot_trend_hist()* (Figure 7) and also create an interactive map showing the trend at each sample point (Figure 8). These figures indicate extensive greening across the study area in recent decades.

Code Box 4: Analyze and visualize vegetation greenness time series

```
# ... continuing from Code Box 3

# Compute temporal trend in annual NDVImax for each sample point
noatak.trend.dt <- lsat_calc_trend(noatak.gs.dt, si = 'ndvi.max', yrs = 2000:2022)

# Plot histogram of trends across sample points
lsat_plot_trend_hist(noatak.trend.dt, xlim = c(-21,21))
```

```
# Create an interactive map showing NDVI trends
colors.dt <- data.table(trend.cat = c("greening","no_trend","browning"),
                        trend.color = c("green","white","brown"))

noatak.trend.dt <- noatak.trend.dt[colors.dt, on = 'trend.cat']

noatak.trend.sf <- st_as_sf(noatak.trend.dt,
                            coords = c("longitude", "latitude"),
                            crs = 4326)

leaflet() %>%
  addProviderTiles('Esri.WorldImagery') %>%
  addPolylines(data = noatak.sf, color = 'white', weight = 3) %>%
  addCircleMarkers(data = noatak.trend.sf,
                   color = 'white',
                   weight = 1,
                   opacity = 0.9,
                   fillColor = ~trend.color,
                   fillOpacity = 0.5,
                   radius = ~sqrt(abs(total.change.pcnt))*3) %>%
  setView(-160, 68, zoom = 7) %>%
  addLegend('bottomright',
            colors = colors.dt$trend.color,
            labels = colors.dt$trend.cat,
            title = 'NDVImax trend',
            opacity = 1)

# End of code examples
```

Table 4. Abridged summary of $NDVI_{max}$ trends from 2000 to 2022 for each sample point (Sample ID) as generated using the function *lsat_calc_trend()*.Trends were assessed for each sample point by removing temporal autocorrelation and then applying a Mann-Kendall trend test (tau statistic and p-value provided). Slopes were calculated using the Theil-Sen slope estimators.

Sample ID	**Latitude**	**Longitude**	**N**	**Slope**	**Intercept**	**Tau**	**P-value**	**Total change**	**Total change (%)**
S_1	67.70765	-157.404	22	0.00109	0.5918	0.181	0.2639	0.025	4.2
S_10	68.23443	-158.416	23	0.00127	0.6144	0.091	0.5728	0.029	4.7
S_11	67.8104	-157.097	21	0.0017	0.6366	0.105	0.5376	0.039	6.1
S_12	67.81419	-160.017	23	0.00155	0.6943	0.108	0.4986	0.036	5.2
S_13	68.12915	-161.226	23	0.00209	0.5268	0.541	< 0.001	0.048	9.1
S_14	68.26632	-157.32	23	0.00067	0.2369	0.403	0.0095	0.015	6.3
S_15	67.87087	-156.911	22	0.00073	0.6307	0.01	0.9759	0.017	2.7
S_16	68.18229	-156.824	23	0.00048	0.6445	0.065	0.693	0.011	1.7
S_17	67.64494	-158.002	23	0.00314	0.6726	0.541	< 0.001	0.072	10.7
S_18	67.94227	-161.809	23	-0.00086	0.7419	-0.152	0.3377	-0.020	-2.7
S_19	67.76848	-162.447	23	0.00623	0.5918	0.784	< 0.001	0.025	4.2

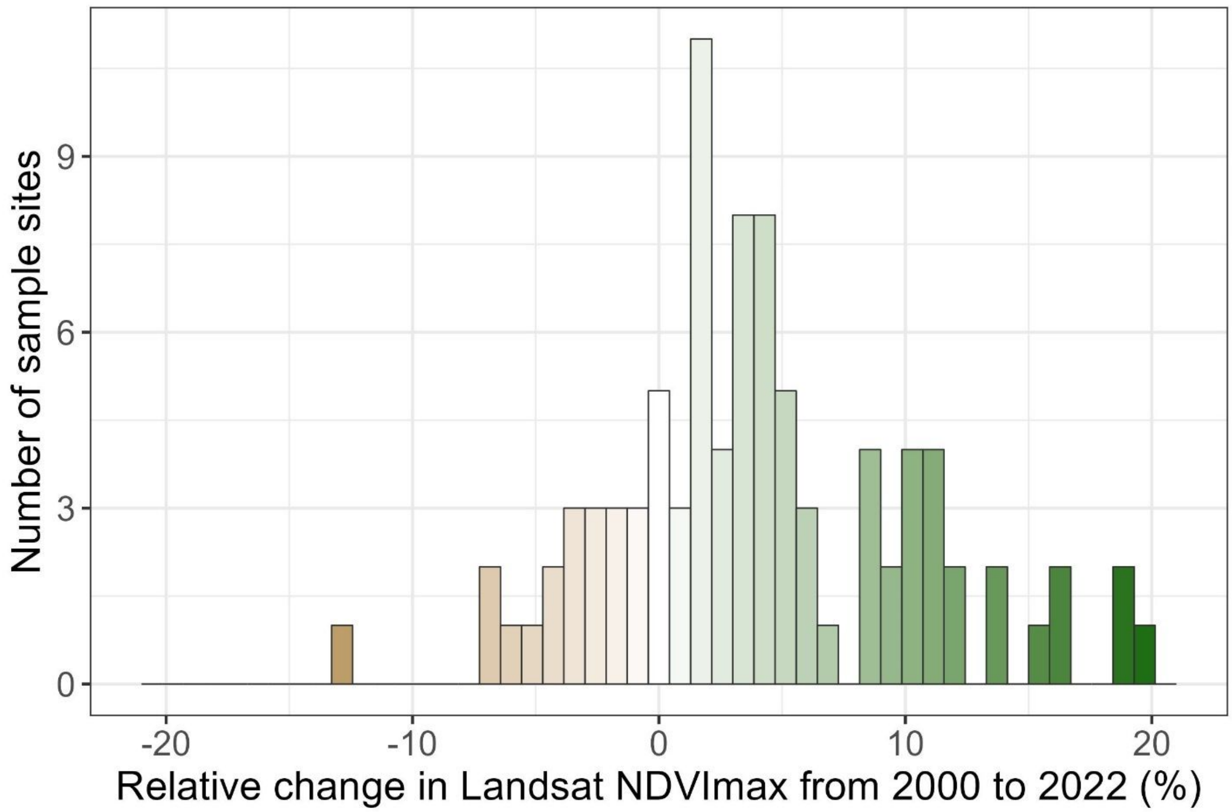

Figure 7. Histogram of relative change in Landsat $NDVI_{max}$ from 2000 to 2022 among sample points across the Noatak National Preserve. Relative changes in percent are calculated based on the Theil-Sen slope and intercept estimates (Table 4).

Review Only

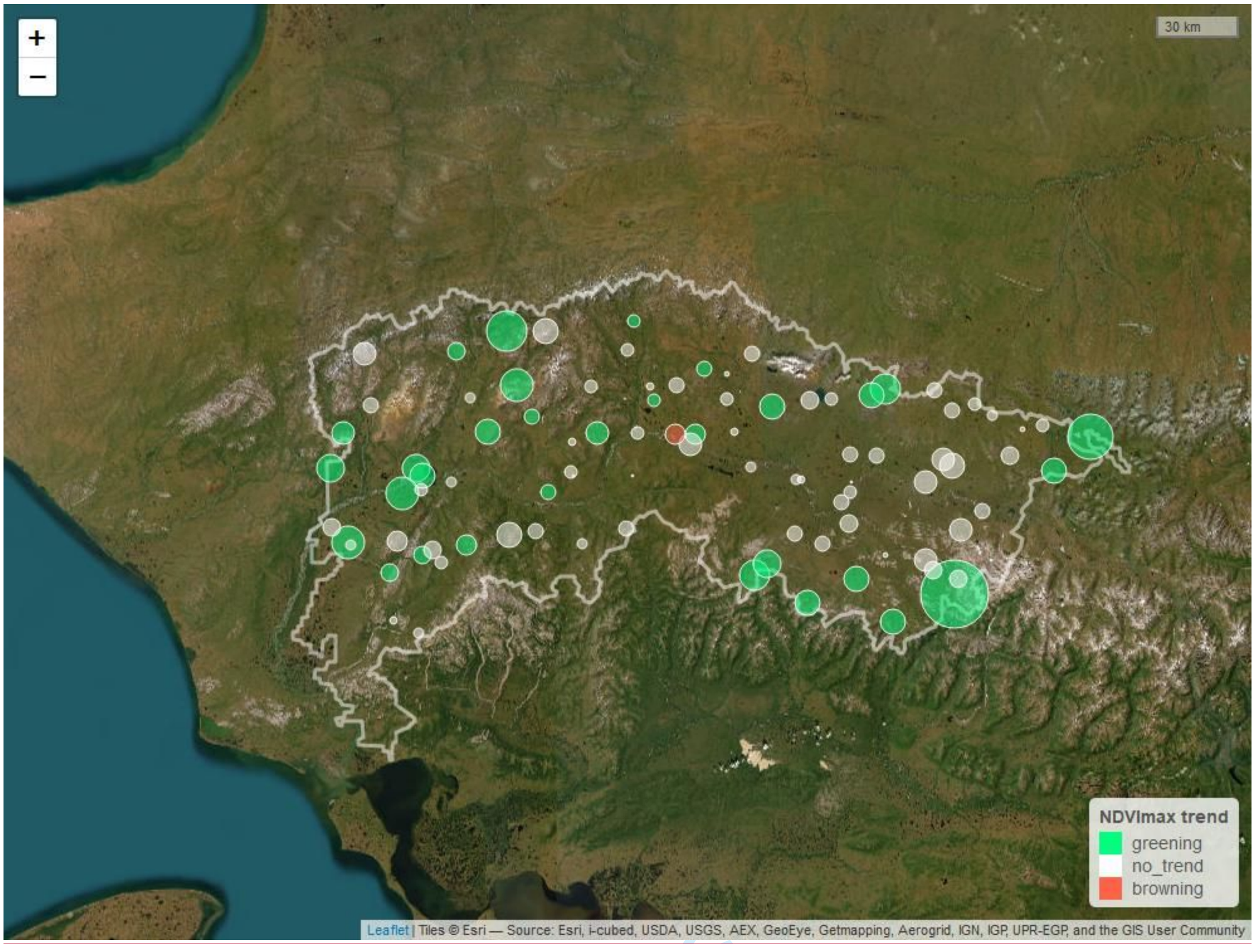

Figure 8. Screenshot of a *leaflet* interactive map showing the trends in $NDVI_{max}$ from 2000 to 2022 for sample points in the Noatak National Preserve. Base map from ESRI World Imagery.

Results and interpretation of the example analysis

Our analysis showed annual maximum vegetation greenness (i.e., $NDVI_{max}$) increased 5.5 ± 10.8% (mean ± 1 SD) from 2000 to 2022 across sample points in the Noatak National Preserve (Figure 7). During these years, vegetation greenness increased by at least 10% at 20% of sample points. Vegetation greenness systematically ($\alpha = 0.10$) increased at 32% of sample points, decreased at 1% of sample points, and exhibited no systematic change at the remaining 67% of sample points. Greening was especially prevalent in western parts of the preserve, as well as along in the northern foothills of the Brooks Range (Figure 8).

These remotely sensed changes suggest tundra productivity and biomass increased in recent decades across large parts of the Noatak National Preserve. These changes are consistent with observed warming-induced expansion of trees and tall shrubs in the preserve (Tape et al. 2006, Terskaia et al. 2020, Dial et al. 2022), as well as with rising summer temperatures increasing the productivity of existing vegetation in this cold tundra environment (Suarez et al. 1999, Berner et al. 2020, Dial et al. 2022). This preserve is also one of the most fire-prone regions in the Arctic and observed greening trends could partially be related to historical fires causing near-surface permafrost thaw, nutrient release, and subsequent shrub proliferation (Gaglioti et al. 2021). Greening in the preserve generally mirrors changes that have been observed more broadly across the Arctic tundra biome, though greening was more prevalent in the preserve than the broader Arctic (32% vs 27% of sample points) (Berner et al. 2020, Mekonnen et al. 2021).

This example analysis was based on Landsat data from 100 random sample points, yet nearly identical results were obtained when the analysis was performed using 1,000 sample points. Further insight into recent ecological changes could be garnered using a higher sample density with samples stratified by land cover type, ecological land unit, management unit, or other factors (e.g., Gaglioti et al. 2021, Berner and Goetz 2022). Nevertheless, Landsat data from even a relatively small random sample (n = 100) enabled robust inference about recent ecological changes that occurred over the past two decades within one of the most remote protected areas in the United States.

Package installation

The R package ~~*lsatTS*~~*LandsatTS* is publicly available through a GitHub code repository. Users will need to have installed the R software environment on their computer. The ~~*lsatTS*~~*LandsatTS* package is operating system agnostic and can be installed from within R using the *install_github()* function from the *devtools* package:

```
devtools::install_github("logan-berner/~~lsatTS~~LandsatTS")
```

The installation will compile the package from source code on the user's computer. As the ~~*lsatTS*~~*LandsatTS* package itself is exclusively written in R code, no additional software is required.

To use the data extraction and preparation functions, users will need an account on GEE, and to have installed and configured the *rgee* package to access GEE from R. Please see the GEE (https://earthengine.google.com/) and *rgee* (https://r-spatial.github.io/rgee/) websites for details on signing up for an account and configuring *rgee*, respectively.

All other external package dependencies are configured and automatically dealt with by *devtools* during the installation. ~~These required packages include (*lsatTS* tested with version cited):~~ These required packages include (*LandsatTS* tested with version cited): *crayon* v1.4.2 (Csárdi 2021), *data.table* v1.14.2 (Dowle and Srinivasan 2021), *dplyr* v1.0.7 (Wickham et al. 2021), *ggplot2* v3.3.5 (Wickham 2016), *ggpubr* v0.4.0 (Kassambara 2020), *magrittr* v2.0.1 (Bache and Wickham 2020), ~~*dplyr* v1~~*mapview* v2.10.0~~.7~~ ~~(Wickham et al. 2021)~~(Appelhans et al. 2021), ~~*tidyr* v1.1~~*purr* v0.3.4 ~~(Wickham 2021)~~(Henry and Wickham 2020), *R.utils* v2.11.0 (Bengtsson 2021), *ranger* v0.13.1 (Wright and Ziegler 2017), *sf* v1.0-4 (Pebesma 2018), ~~*crayon* v1.4.2 (Csárdi 2021), *mapview* v2.10.0 (Appelhans et al. 2021), *purr* v0.3.4 (Henry and Wickham 2020), *data.table* v1.14.2 (Dowle and Srinivasan 2021), *ggplot2* v3.3.5 (Wickham 2016), *R.utils* v2.11.0 (Bengtsson 2021),~~ *stats* v4.1.1 (R Core Team 2021), *stringr* v1.4.0 (Wickham 2019)~~, *ggpubr* v0.4.0 (Kassambara 2020), *ranger* v0.13.1 (Wright and Ziegler 2017),~~ , *tidyr* v1.1.4 (Wickham 2021), *zoo* v1.8.9 (Zeileis and Grothendieck 2005), ~~and~~ *zyp* v0.10-1.1 (Bronaugh and Werner 2019).

~~Data extraction~~

~~*lsatTS* enables~~Function descriptions

Below we provide a description of each function, with further details provided in the package manual that is available both within R and as Supplemental Material.

For Review Only

Export point~~-sample-based extraction of full~~-coordinate Landsat ~~data records~~time series from ~~GEE~~Google Earth Engine using ~~the application programming interface provided~~ lsat_export_ts()

The function *lsat_export_ts()* exports Landsat 5, 7 and 8 surface reflectance measurements for each sample location over a user-defined period by querying the ~~*rgee* package~~Landsat Collection 2 archived on GEE. Sample locations typically represent (1) center coordinates of field sites, (2) a census of all Landsat pixels from a small area of interest, or (3) a random sample from a large region. ~~Data extraction is conducted using the function *lsat_export_ts()*.~~ If the user wishes to extract Landsat data for all pixels in a small area of interest~~,~~ (e.g., 5 km x 5 km), then the central coordinates of each pixel can be obtained using *lstat_get_pixel_centers()* and then those sample locations are passed to *lsat_export_ts()*. ~~Please note *lsat_export_ts()* has not been tested for data extractions exceeding 10^5 Landsat pixels (~90 km^2). A recent analysis of the boreal forest biome focused on reflectance measurements acquired June through August from 1985 to 2019 for 10^5 Landsat pixels. This data extraction took about two weeks to run on GEE and yielded a total of ~41.6 million multispectral measurements that required ~15 Gb of hard drive storage (Berner and Goetz 2022). *lsatTS* enables large data extractions but is not infinitely scalable.~~

~~*Export point-coordinate Landsat time series from Google Earth Engine using lsat_export_ts()*~~

~~The function *lsat_export_ts()* exports time series of Landsat 5, 7 and 8 surface reflectance measurements for each sample location by querying the Landsat Collection 2 archived on GEE. Data are exported for user-defined time periods.~~ It is important to stress this function only works for sample locations (point coordinates) that must be supplied as a simple feature (*sf*) collection of point geometries.

The function issues one or more tasks to GEE that export the data in the form of comma separated value (CSV) files to the user's Google Drive. The number of tasks issued varies depending on the number of sample locations for which the Landsat record is to be extracted. Data extractions that involve ~~a large number of~~many sample locations are prone to errors and may exceed user limits set by GEE. Therefore, the function will chunk the sample locations into small groups (by default 250 sites) and for each chunk will issue a separate export task to GEE. The function returns a list of *rgee* task objects, which can be used to query the progress of the exports and subsequently retrieve the data from the user's Google Drive.

Please note that *lsat_export_ts()* has not been tested for data extractions exceeding 10^5 Landsat pixels (~90 km^2). It took about two weeks to extract four decades of summer Landsat data for 10^5 pixels sampled from across the boreal forest biome. This data extraction yielded ~41.6 million multispectral measurements that required ~15 Gb of hard drive storage (Berner and Goetz 2022). *LandsatTS* enables large data extractions but is not infinitely scalable.

Optional: Get central coordinates of pixels within a polygon using lsat_get_pixel_centers()

The function *lsat_get_pixel_centers()* facilitates extracting data for all Landsat pixels in a small area of interest (e.g., < 5 km x 5 km) by determining the central coordinates of all Landsat pixels that fall within a user-specified polygon. The user-specified polygon is supplied to the function as a simple feature collection. The function determines the Landsat Worldwide Reference System (WRS) scene whose center is closest to the center of the user-specified polygon. It then extracts the center coordinates for all pixels that overlap with the user-specified polygon from the first Landsat 8 scene on record available on GEE. A buffer can be specified to include additional

For Review Only

pixels beyond the polygon boundary. The function returns the pixel centers as a simple feature object that can then be passed to the *lsat_export_ts()* function for the extraction of the Landsat time series. Please note this function is not designed to be used for sampling polygons that would exceed tens of thousands of Landsat pixels. The number of pixels in large polygons can quickly become too difficult to handle in the subsequent export and processing workflow, and such polygons may also extend beyond the area of the Landsat scene (185 km x 180 km) used to determine the pixel centers. For large areas, we recommend a random or regular subsampling of point locations such as done in prior studies ~~(Berner et al. 2020, Berner and Goetz 2022)~~(Berner et al. 2020, Berner and Goetz 2022).

~~Data processing~~

~~Prepare~~Format data for analysis using lsat_~~general_prep~~format_data ()

The function *lsat_~~general_prep~~format_data()* takes the GEE exports generated by *lsat_export_ts()* and prepares the data for the subsequent *~~lsatTS~~LandsatTS* workflow. These preprocessing tasks include parsing coordinates and other information, renaming columns, and scaling band values. The GEE exports need to be passed to the function in the form of a *data.table* object. *lsat_~~general_prep~~format_data()* returns a *data.table* object that can then be passed on to *lsat_clean_data()* for the next step in the processing workflow. Please note that all *~~lsatTS~~LandsatTS* functions handling a *data.table* object require a column called “sample.id” that uniquely identifies each location. If this column is not called “sample.id”, please modify accordingly.

Clean surface reflectance data using lsat_clean_data()

The function *lsat_clean_data()* filters measurements to those made under clear-sky conditions. This function allows the user to filter measurements based on pixel quality flags and scene criteria. The USGS provides pixel quality flags based on the CFMask algorithm (Zhu et al. 2015) and information on each scene (e.g., cloud cover). The default settings for *lsat_clean_data()* will filter out measurements flagged as snow or water, as well as measurements acquired at high solar zenith angle (>60°), those with high geolocation uncertainty (>15 m), or those acquired as part of scenes with extensive cloud cover (>80%). Additionally, optional water masking is provided based on maximum surface water extent from the Landsat-based JRC Global Surface Water Dataset (Pekel et al. 2016). The main input supplied to *lsat_clean_data()* is a *data.table* of Landsat records for individual sample locations (specified by a sample.id column) - usually the direct output of *lsat_~~general_prep~~format_data()* - and returns cleaned records in the form of an updated *data.table*, along with a console message summarizing the number and percentage of measurements removed during cleaning (generally >70%).

Compute neighborhood mean surface reflectance using lsat_neighborhood_mean()

The function *lsat_neighborhood_mean()* computes the mean band-specific reflectance across a neighborhood of pixels for measurements at each period in time. This is helpful when each of the user’s sample locations ~~were~~was buffered to include a neighborhood of Landsat pixels (e.g., 3 x 3 pixels). If there are neighborhood pixels with no data (i.e., NA values), then the function omits those pixels and computes the mean across the remaining pixels. The main input to this function is a *data.table* of Landsat records for buffered sample locations. The function returns a new *data.table* with mean reflectance for each band at each point in time at every sample location. If used, the function should be called immediately after *lsat_clean_data()*.

For Review Only

Summarize data availability for each site using lsat_summarize_data~~_avail~~()

The function *lsat_summarize_data~~_avail~~()* takes a *data.table* of Landsat records and returns a summary *data.table* that provides information on the time period and number of observations available for each sample location. It also generates a figure showing the annual median (2.5th and 97.5th percentile) number of observations available from each satellite summarized across all sample locations. The figure is plotted to the current graphics device and can be saved by calling the function *ggsave()*.

Calculate spectral indices using lsat_calc_~~spec~~spectral_index()

The function *lsat_calc_~~spec~~spectral_index()* calculates a variety of common spectral indices. The function currently supports calculating 15 spectral indices, including the Normalized Difference Vegetation Index (NDVI), 2-band Enhanced Vegetation Index (EVI2), and others (Table 2). Note the function can only compute one spectral index at a time. As an input it requires a *data.table* with Landsat records and a string indicating the spectral index to be calculated. The function then returns the *data.table* updated with a new column containing the spectral index for each observation.

Table 2. Spectral indices that can be computed using the *lsat_calc_~~spec~~spectral_index()* function.

Name	Abbreviation	Formula	Citation
Enhanced Vegetation Index	EVI	$\frac{2.5(NIR - RED)}{NIR + 6 * RED - 7.5 * BLUE + 1}$	Huete et al. (2002)
Enhanced Vegetation Index (2-band)	EVI2	$\frac{2.5 * (NIR - RED)}{NIR + 2.5 * RED + 1}$	Jiang et al. (2008)
Moisture Stress Index	MSI	$\frac{SWIR1}{NIR}$	Rock et al. (1986)
Near Infrared Vegetation Index	NIRv	$\frac{NIR * (NIR - RED)}{NIR + RED}$	Badgley et al. (2017)
Normalized Burn Ratio	NBR	$\frac{NIR - SWIR2}{NIR + SWIR2}$	Key and Benson (1999)
Normalized Difference Infrared Index	NDII	$\frac{NIR - SWIR1}{NIR + SWIR1}$	Hardisky et al. (1983)
Normalized Difference Moisture Index	NDMI	$\frac{NIR - SWIR1}{NIR + SWIR1}$	Gao (1996)
Normalized Difference Vegetation Index (red)	NDVI	$\frac{NIR - RED}{NIR + RED}$	Rouse et al. (1974)
Normalized Difference Vegetation Index (green)	gNDVI	$\frac{NIR - GREEN}{NIR + GREEN}$	Gitelson and Merzlyak (1998)
Normalized Difference Vegetation Index (kernel)	kNDVI	$\tanh((\frac{NIR - RED}{NIR + RED})^2)$	Camps-Valls et al. (2021)
Normalized Difference Water Index	NDWI	$\frac{GREEN - NIR}{GREEN + NIR}$	McFeeters (1996)
Plant Senescence Reflectance Index	PSRI	$\frac{RED - BLUE}{NIR}$	Merzlyak et al. (1999)
Soil Adjusted Vegetation Index	SAVI	$1.5 * \frac{SWIR1 - RED}{SWIR1 + RED * 0.5} - \frac{SWIR2}{2}$	Huete (1988)
Soil Adjusted Total Vegetation Index	SATVI	$\frac{1.5 (NIR - RED)}{NIR + RED + 0.5}$	Marsett et al. (2006)
Wide Dynamic Range Vegetation Index	WDRVI	$\frac{NIR - RED}{0.2 * NIR + RED}$	~~(Gitelson 2004)~~Gitelson (2004)

For Review Only

Cross-calibrate spectral ~~band or index~~data across sensors using lsat_calibrate_rf()

The function *lsat_calibrate_rf()* will calibrate individual bands or spectral indices from Landsat 5 TM and Landsat 8 ~~ETM+~~OLI to match Landsat 7 ETM+ using random forest models following the approach developed by Berner et al. (2020). Further cross-sensor calibration is needed because there are systematic differences in individual bands and spectral indices among Landsat sensors that must be addressed when combining data from multiple sensors (Ju and Masek 2016, Roy et al. 2016, Berner et al. 2020, Berner and Goetz 2022). Here, the Landsat 7 ETM+ is used as a benchmark because it temporally overlaps with the other two sensors. Cross-calibration can only be performed on one band or spectral index at a time and requires having data from 100s to preferably many 1,000s of sample locations to train the random forest models. There is an option for users to train the random forest models using pre-processed Landsat data from ~6000 randomly sampled locations across the Arctic – Boreal domain.

The overall approach involves determining the median spectral reflectance at a sample location during a portion of the growing season using Landsat 7 and Landsat 5/8 data that were collected the same years. A random forest model is then trained to predict Landsat 7 reflectance from Landsat 5/8 reflectance. Random forest models are ensembles of regression trees (Breiman 2001) that here are trained using a fast implementation provided by the *ranger* package (Wright and Ziegler 2017). If the user's dataset includes both Landsat 5 and 8, then the function will train a random forest model for each sensor. The function evaluates model performance using both out-of-bag and cross-validated approaches. Please see Berner et al. (2020) for further details.

The main input to *lsat_calibrate_rf()* is a *data.table* of Landsat records for sample locations and a string specifying the name of the band or spectral index to be cross-calibrated. By default, *lsat_calibrate_rf()* will return a *data.table* with a new column containing the cross-calibrated data. ~~The~~If requested using the *write.output* parameter, the function creates a user-specified output directory that contains (1) trained random forest models, (2) a CSV file with model evaluation metrics, and (3) a multi-panel figure comparing sensors pre- and post-calibration. ~~Furthermore~~In any case, model evaluation metrics are returned to the console and the figure plotted in the active graphics device. If the default setting to add a new column with the cross-calibrated data is used, then either use those data in the subsequent functions (e.g., ndvi.xcal) or, once satisfied, manually overwrite the uncalibrated data to simplify subsequent column names.

Cross-calibrate spectral data across sensors using lsat_calibrate_poly()

The function *lsat_calibrate_poly()* behaves similarly to *lsat_calibrate_rf()* but fits polynomial regression models rather than random forest models. The function automatically fits first-, second- and third-order polynomial regression models (i.e., $Y = \beta_0 + \beta_1 X + \beta_2 X^2 + \beta_3 X^3$). It then automatically selects the most parsimonious fit using Bayesian Information Criterion (BIC), applies the most parsimonious model for cross-sensor calibration, and then returns regression model coefficients and cross-validation metrics. Initial testing showed *lsat_calibrate_poly()* and *lsat_calibrate_rf()* produce very similar results ($r^2 = 0.97$), have similar run times, and both effectively mitigate biases among Landsat sensors, yet an advantage of the more recently developed *lsat_calibrate_poly()* function is it generates regression model coefficients that can be more readily applied to other datasets or incorporated into other software (e.g., GEE).

For Review Only

Fit phenological curves to vegetation greenness time series using lsat_fit_phenological_curves()

The function *lsat_fit_phenological_curves()* provides information on the phenological timing of every Landsat observation relative to multi-year estimates of annual maximum vegetation greenness at each sample location. Specifically, the function models seasonal land surface phenology at each sample location using ~~flexibly~~ cubic splines iteratively fit to vegetation greenness (e.g., NDVI) time series within successive moving~~-~~ windows. The magnitude and timing of annual maximum vegetation greenness are determined for each ~~time~~ period by first pooling observations over years within each moving-window and then fitting cubic splines to observations that have been sorted by day of year. Often there are too few observations from an individual year to fit a reliable phenological curve, therefore the function enables users to pool observations over multiple years when fitting each cure. The default is a 7-year moving-window centered on the focal year, but the width of the moving window can be made shorter or longer if there are many or few observations in the data record. For each time period, a cubic spline is initially fit that describes vegetation greenness for each day of year during the growing season. To screen outliers, each observation of vegetation greenness is compared against the model fitted values for that day of year and if the deviation is greater than a user-specified difference (default is a 30% difference), then the observation is removed, and the cubic spline is re-fit. This is repeated until no observations exceed the user-specified threshold. The phenological status of each remaining observation is then determined relative to the modeled maximum vegetation greenness during the multi-year period. Additional details are provided in Berner et al. (2020).

The function takes as input a *data.table* with irregular time series of vegetation greenness observations at each sample location, as well as several parameters (e.g., moving window width, minimum number of observation needed to fit a cubic spline, cubic spline flexibility). The function returns a new *data.table* with phenological information for each remaining observation that occurred during a time period with adequate data for modeling surface phenology (i.e., typically fewer observations will be returned than are provided to the function). Among other output, the returned *data.table* provides for each observation the modeled estimates of (1) vegetation greenness for that day of year and for peak summer; (2) vegetation greenness for that day of year as a fraction of annual maximum vegetation greenness; (3) day of year when annual maximum vegetation greenness occurred; and (4)~~ and~~ expected difference in vegetation greenness between that day of year and peak summer. The function also returns a figure to the current graphic device that shows seasonal progression of Landsat observations and modeled surface phenology for a random subset of nine sample locations. The user can optionally output a CSV that includes for each sample location the vegetation greenness predicted for each day of year during each ~~time~~ period by the cubic splines. Furthermore, the function includes an optional "test run" mode that will run the function on a random subset of nine sample locations and return a figure showing model fits, thus allowing the user to quickly experiment with different parameter settings. Note the function was designed to characterize seasonal phenology in terrestrial ecosystems with a single growing season and thus may not be suitable for use in ecosystems with multiple growing seasons. Also, the function was designed for spectral indices that are typically positive (e.g., NDVI). If using a spectral index that is typically negative (e.g., NDWI) then multiply the index by -1 before running the *lsat_fit_phenological_curves()* and *lsat_summarize_growing_seasons()* functions and then back-transform afterwards.

For Review Only

Derive annual growing season metrics using lsat_summarize_growing_seasons()

The function *lsat_summarize_growing_seasons()* estimates several annual growing season metrics from vegetation greenness time series and modeled land surface phenology derived from Landsat satellite observations. The function's main input is the *data.table* generated by *lsat_fit_phenological_curves()* and user-specified parameters including the name of the spectral index and the phenological cut-off for an observation to be considered part of the growing season. Specifically, an observation is considered to be part of the growing season if the modeled vegetation greenness for that day of year is within a user-specified fraction of modeled annual maximum vegetation greenness (by default 0.75). The function returns a new *data.table* that includes for each sample location the annual mean, median, and 90th percentile vegetation greenness computed from observations during each growing season. The function also returns phenologically~~-~~ modeled estimates of the magnitude and timing (day of year) of annual maximum vegetation greenness. For each sample location, annual maximum vegetation greenness is estimated by first adjusting individual observations by the expected difference in vegetation greenness between that day of year and peak summer, and then taking the median of phenologically~~-~~ adjusted values within each growing season. Please see Berner et al. (2020) for additional details.

Assess estimates of maximum vegetation greenness using lsat_evaluate_phenological_max()

The function *lsat_evaluate_phenological_max()* assesses how estimates of annual maximum vegetation greenness vary with the number of Landsat observations when derived from raw observations and after phenological modeling. Raw estimates of annual maximum vegetation greenness are sensitive to the number of observations available from a growing season, but phenological modeling tends to substantially reduce this dependency (Berner et al. 2020). The main input to the function is a *data.table* with Landsat records and phenological information generated by *lsat_fit_phenological_curves()*. The function assumes the "actual" annual maximum vegetation greenness at a sample location is captured by having at least a user-specific number of observations (e.g., ≥ 7). ~~The~~For each site, the function extracts ~~site x~~ years with at least the user-specified number of growing season observations and then repeatedly compares how raw and phenologically~~-~~ modeled estimates of annual maximum vegetation greenness differ from actual annual maximum vegetation greenness as progressively smaller subsets of observations are used. The function returns a figure to the current graphic device that summarizes how raw and modeled estimates of annual maximum vegetation greenness differ from actual conditions when there are between 1 and n-1 Landsat observations from a single growing season. This lets the user determine how much annual estimates of maximum vegetation greenness are impacted by the number of available growing season observations.

~~**Data analysis**~~

Compute interannual trends in vegetation greenness using lsat_calc_trend()

The function *lsat_calc_trend()* computes a temporal trend in annual time series of vegetation greenness for each sample location over a user-specified ~~time~~ period. This function ~~iteratively~~ pre-whitens each time series (i.e., ~~remove~~removes temporal autocorrelation) (Yue et al. 2002) and then computes Mann-Kendall trend tests and Theil-Sen slope indicators as implemented by the *zyp.yuepilon()* function from the *zyp* package (Bronaugh and Werner 2019). The function takes as input a *data.table* with annual time series of vegetation greenness, or other spectral index, for each sample location. The function returns (1) a new *data.table* that summarizes the

For Review Only

interannual trend at each sample location; (2) a console message summarizing trends across all sample locations~~; and (3) a multi-panel figure summarizing interannual variability and trends in vegetation greenness.~~. Specifically, the new *data.table* summarizes for each sample location the trend slope, intercept, Kendall's tau, and p-value, as well as total absolute and relative change in vegetation greenness and other information (e.g., number of years with observations). The console message summarizes the mean (±1 SD) relative change in vegetation greenness across all sample locations, as well as the percentage of samples sites that greened, browned, or had no trend based on a user-specified critical value (default α = 0.10). ~~The multi-panel figure provides (a) a histogram of relative change in vegetation greenness among sample locations and (b) a time series of annual mean (± 1 SE) vegetation greenness for sample locations that greened, browned, or had no trend.~~

~~**Example application: Vegetation greenness trends for a landscape on Disko Island**~~

~~Here we provide an example analysis of interannual changes in vegetation greenness from 2000 to 2020 across a ~4 km^2 study area on Disko Island off the western coast of Greenland (Figure 2). The study area (approximate center 69.27°N, 53.46°W) is located on the eastern slopes of the Blæsedalen valley just east of Qeqertarsuaq (Godhavn). The close proximity of the valley to the University of Copenhagen's Arctic Station has made the area subject to much ecological and geological research, including multiple long-term monitoring projects and experiments (https://arktiskstation.ku.dk). Climatically, the site lies within the transition zone between the low and high Arctic, with basaltic soils on discontinuous permafrost (Xu et al. 2021) covered by erect dwarf shrub tundra (Walker et al. 2002). We characterize annual maximum vegetation greenness using the Normalized Difference Vegetation Index (NDVI$_{max}$) derived from Landsat satellite observations. Landsat NDVI$_{max}$ relates to vegetation productivity and aboveground biomass in tundra ecosystems (Johansen and Tømmervik 2014, Berner et al. 2018, Berner et al. 2020). Here, we focus on the period from 2000 to 2020 because there was limited Landsat data available prior to 2000 in this region, as shown below. We provide the scripts associated with this example as supplemental files and in this section guide the reader through the analysis code with example output figures and tables that are generated by the *lsatTS* functions (excluding Figure 2).~~

For Review Only

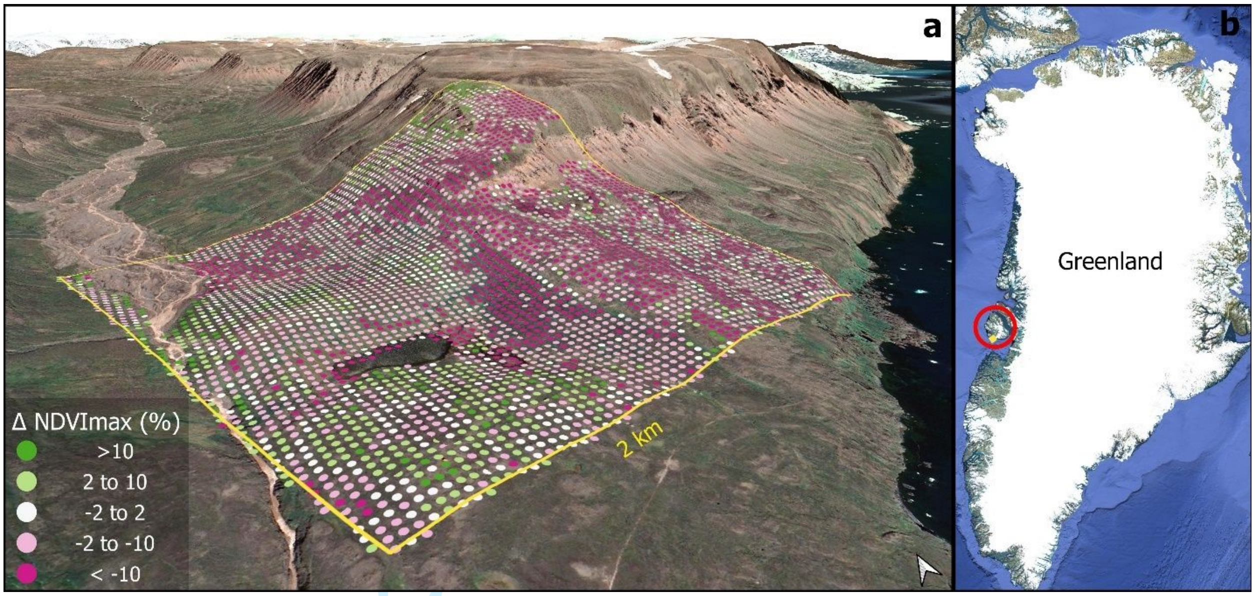

~~Figure 2. (a) Relative changes in Landsat annual maximum NDVI (NDVI$_{max}$) from 2000 to 2020 across the study area on Disko Island. (b) Location of study area off the western coast of Greenland. Figure created using QGIS (v3.20; QGIS.org 2021). Background imagery from Google Satellite © 2022 CNES / Airbus used with fair use permission. Underlying digital elevation model from the U.S. National Snow and Ice Data Center (Howat et al. 2014, Howat et al. 2015).~~

For Review Only

~~*Part 1: Export Landsat time series from Google Earth Engine*~~

~~First the user needs to export Landsat time series for sample locations in the study area using GEE (Code Box 1). For this they need to prepare the environment, set the boundaries of the study area and then retrieve the Landsat pixel center coordinates using the *lsat_get_pixel_centers()* function. Next, the Landsat records are exported for the pixel center locations using *lsat_export_ts()*. Here, we choose to export only Landsat observations in the between day of year 152 (beginning of June) and 273 (end of September). The user then waits for GEE to finish the exports. Progress can be monitored using the GEE task manager in the web browser (https://code.earthengine.google.com/tasks) or on the R console, using the *ee_monitoring()* function provided by *rgee*. For the example, it took ~2 days to export the 19 files (totaling ~692 MB) associated with this example analysis. The CSV files containing the raw exports then need to be copied from the user's Google Drive to the local machine that will carry out the subsequent processing using *lsatTS*. The files can be copied manually or using the ee_drive_to_local() function provided by *rgee*. Once the records are available locally, they need to be cleaned and processed into vegetation index time series as detailed in the next section.~~

~~Code Box 1: Export Landsat time series from Google Earth Engine~~

```
# Load required R packages
require(lsatTS)
require(rgee)
require(sf)
require(ggplot2)
require(data.table)

```

```
# Initialize Google Earth Engine
ee_Initialize()

# Create sf polygon of the study area
aoi.poly <- st_polygon(list(matrix(
  c(-332950,-2243300,
    -334950,-2243300,
    -334950,-2245300,
    -332950,-2245300,
    -332950,-2243300),
  ncol = 2,
  byrow = T)))

# Transform polygon to WGS84 lat long
aoi.poly <- aoi.poly %>%
  st_sfc(crs = 3413) %>%
  st_transform(crs = 4326) %>%
  st_as_sf()

# Get the central coordinates for each of the 4557 Landsat pixels in study area
aoi.pts <- lsat_get_pixel_centers(aoi.poly)

# Export summer Landsat surface reflectance measurements for each pixel to a folder
# called "earth_engine/lsat_disko" on the user's Google Drive.
lsat_export_ts(
  pixel_coords_sf = aoi.pts,
  startJulian = 152,
  endJulian = 273,
  prefix = 'disko',
  drive_export_dir = 'earth_engine/lsat_disko')

```

Plot histogram of

~~Part 2: Derive~~ vegetation greenness ~~time series from the raw Landsat data~~

~~To derive the vegetation greenness time series from the raw exports of Landsat time series, the records first need to be imported to R as a data.table object, re-formatted~~trends using lsat_~~general_prep() and cleaned with lsat_clean_data() to filter out clouds, snow, and water, as well as radiometric and geometric errors (Code Box 2). For the study area on Disko Island, lsat_clean_data() removed 1,817,683 of 2,452,693 observations (74.11%) in the data cleaning process. The availability of Landsat observations for all point locations ("sample.ids") in the remaining dataset can then be visualized using lsat_summarize_data_avail(). In the case of the pixel centers across the study area on Disko Island, the number of observations is poor before the year 2000, as highlighted by the graph that is automatically generated by the function (Figure 3). Therefore, we later limit the analysis of vegetation greenness to the years between 2000 and 2020. Finally, the NDVI is calculated using the lsat_calc_spec_index(). The dataset is then ready for the sensor cross-calibration and phenological modelling.~~ plot_trend_hist()

~~Code Box 2: Derived~~ The function *lsat_plot_trend_hist()* creates a histogram depicting the total percent change in vegetation greenness ~~time series from the raw Landsat data~~

```
# Import CSV exported with GEE as data.table
data.files <- list.files('~/earth_engine/lsat_disko', full.names = T)
```

```
lsat.dt <- do.call("rbind", lapply(data.files, fread))

# (Re-)format the imported raw data
lsat.dt <- lsat_general_prep(lsat.dt)

# Clean data by filtering clouds, snow, and water, as well as radiometric and
geometric errors.
lsat.dt <- lsat_clean_data(lsat.dt)

# Summarize the availability of Landsat data for each pixel
lsat_summarize_data_avail(lsat.dt)

# Compute the Normalized Difference Vegetation Index (NDVI)
lsat.dt <- lsat_calc_spec_, or other spectral index(lsat.dt, si = 'ndvi')
```

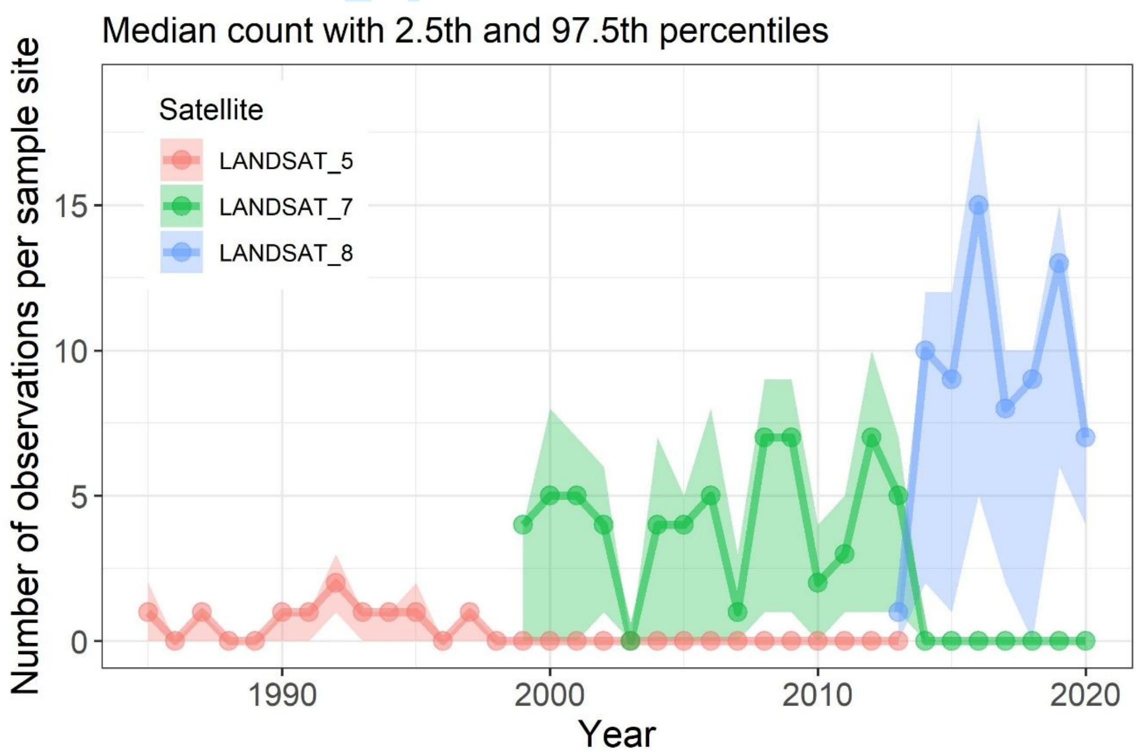

~~Figure 3. Availability of quality-screened Landsat observations across years for sample locations in the study area on Disko Island as returned by the *lsat_summarize_data_avail()* function. Summaries are based on observations acquired between day-of-year 152 (beginning of June) and 273 (end of September). , Note the limited availability of observations before the year 2000. Lines with points denote median counts while shaded error bands encompass the 2.5th to 97.5th percentiles of counts~~ among sample locations.

~~*Part 3: Cross-sensor calibration and phenological modelling*~~

~~The derived NDVI time series need to be calibrated across the different Landsat sensors, and then $NDVI_{max}$ estimated using the phenological modelling approach (Code Box 3). We start by cross-calibrating the time series using *lsat_calibrate_rf()*. As the number of observations in~~

~~the Disko Island dataset~~ The function takes the *data.table* that is ~~too small to calibrate the random forest models, we use the pre-processed dataset of high latitude observations included with *lsatTS*. The function saves the models in a specified~~ output ~~directory and generates a series of graphs (Figure 4) and tabular data (Table 3) that help with evaluating model performance. As desired, the calibration reduced the median bias between the Landsat 7 observations and the Landsat 5 and 8 observations visually (Figure 4) and statistically (Table 3). Next, as a step towards estimating annual NDVI~~~~$_{max}$~~~~, we fit phenological models to the calibrated NDVI time series using *lsat_fit_phenological_curves()*. The~~ by the function ~~automatically~~ *lsat_calc_trend()* and returns a figure ~~with Landsat observations and fitted phenological curves for nine random sample locations in the dataset (Figure 5). Each phenological curve characterizes the seasonal progression of NDVI using observations pooled over a multi-year period (here an 11-year moving window) and should be smooth and hump-shaped. Beware of phenological curves with long straight lines that could suggest inadequate seasonal distribution of data used when fitting the curves. Once the models are fitted, the summary statistics (including the estimated NDVI~~~~$_{max}$~~~~) are extracted using *lsat_summarize_growing_seasons()*. The *lsat_evaluate_phenological_max()* can be used to output a figure that allows for visually assessing the performance of modelled NDVI~~~~$_{max}$~~ ~~(Figure 6). In the case of this Disko Island dataset, modeled estimates of NDVI~~~~$_{max}$~~ ~~tend to be biased slightly low (~1%) when only one or two observations are available from a growing season (Figure 6), yet there were rarely such few observations during the period from 2000 to 2020 (Figure 3). The final step following the cross-calibration and phenological modelling is the time series analysis.~~

~~Code Box 3: Cross-calibration and phenological modelling~~

```
# Cross-calibrate NDVI among sensors using random forest models
# Outputs in Figure 4 and Table 3.
Lsat.dt <- lsat_calibrate_rf(
  lsat.dt,
  band.or.si = 'ndvi',
  train.with.highlat.data = T,
  outdir = 'output/ndvi_xcal_smry/',
  overwrite.col = T)

# Fit phenological models (cubic splines) to time series at
# each sample location (Figure 5)
lsat.pheno.dt <- lsat_fit_phenological_curves(lsat.dt, si = 'ndvi')

# Summarize spectral characteristics for each growing season
lsat.gs.dt <- lsat_summarize_growing_seasons(lsat.pheno.dt, si = 'ndvi')

# Evaluate the estimates of annual maximum NDVI (Figure 6)
lsat.eval.dt <- lsat_evaluate_phenological_max(lsat.pheno.dt, si = 'ndvi')
```

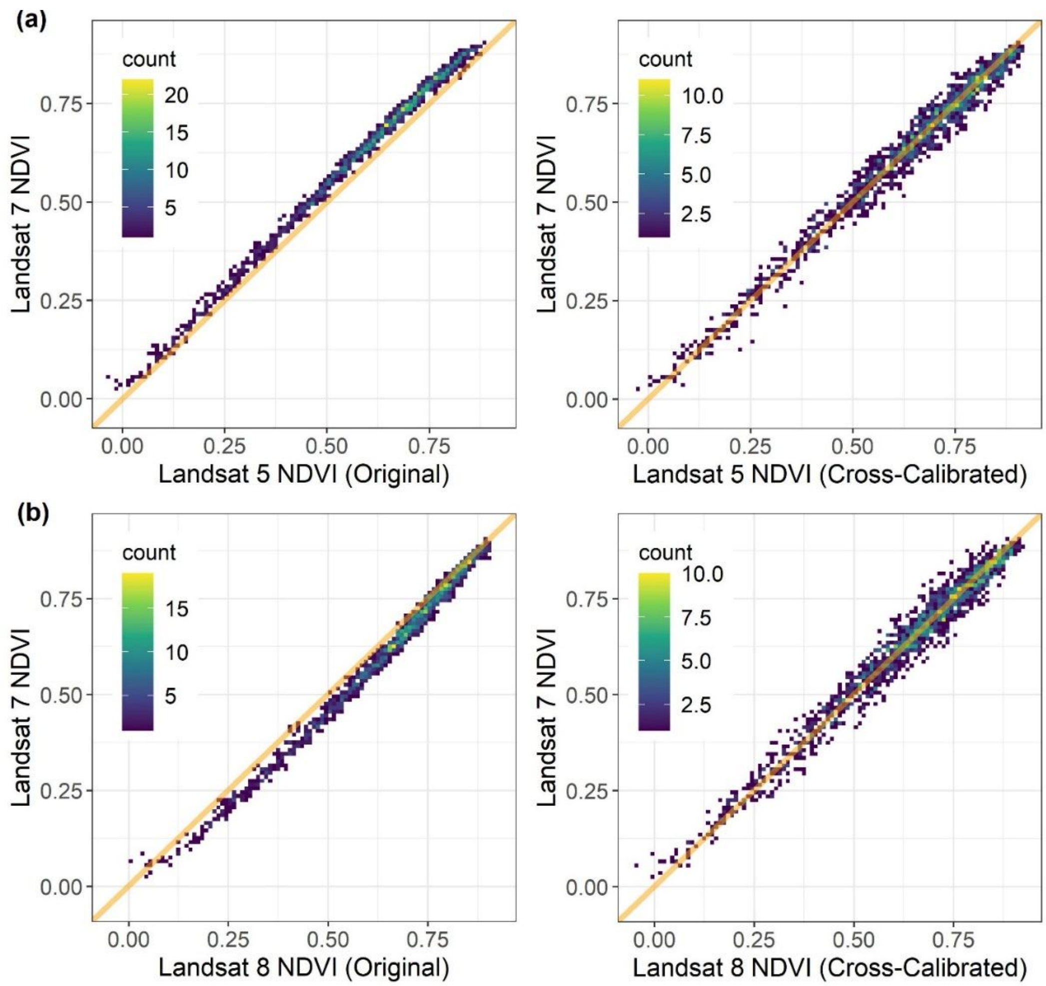

~~Figure 4. Relationships between Landsat 7 NDVI and both (a) Landsat 5 NDVI and (b) Landsat 8 NDVI using (left panels) original data and (right panels) data that were cross-calibrated with random forest models. Each point is a sample location from the Arctic – Boreal domain where there were temporally overlaps measurements from pairs Landsat satellites. Orange diagonal lines depict 1:1 relationships. Model performance metrics are provided in Table 3. Note that cross-calibration substantially reduces biases between sensors but does increase scatter.~~

~~Table 3. Summary of original biases, performance of random forest models for cross-sensor calibration, and post-calibration biases in NDVI between Landsat 7 ETM and either Landsat 5 TM or Landsat 8 ETM+. Error metrics were derived internally by the random forest using out-of-bag (OOB, i.e., withheld) data and further assessed using cross-validation, which yielded nearly identical results albeit with further information on post-calibration biases.~~

~~Satellite sensor~~	~~Original Data~~		~~OOB Error Metrics~~			~~Cross-Validated Error Metrics~~				
	~~Median bias~~	~~Median % bias~~	~~r^2~~	~~RMSE~~	~~N~~	~~r^2~~	~~RMSE~~	~~N~~	~~Median bias~~	~~Median % bias~~
~~Landsat 5 TM~~	~~-0.04~~	~~-6.1~~	~~0.98~~	~~0.03~~	~~4315~~	~~0.98~~	~~0.03~~	~~1438~~	~~+0.001~~	~~+0.1~~
~~Landsat 8 ETM+~~	~~+0.03~~	~~+4.6~~	~~0.97~~	~~0.03~~	~~4881~~	~~0.97~~	~~0.03~~	~~1627~~	~~-0.001~~	~~-0.1~~

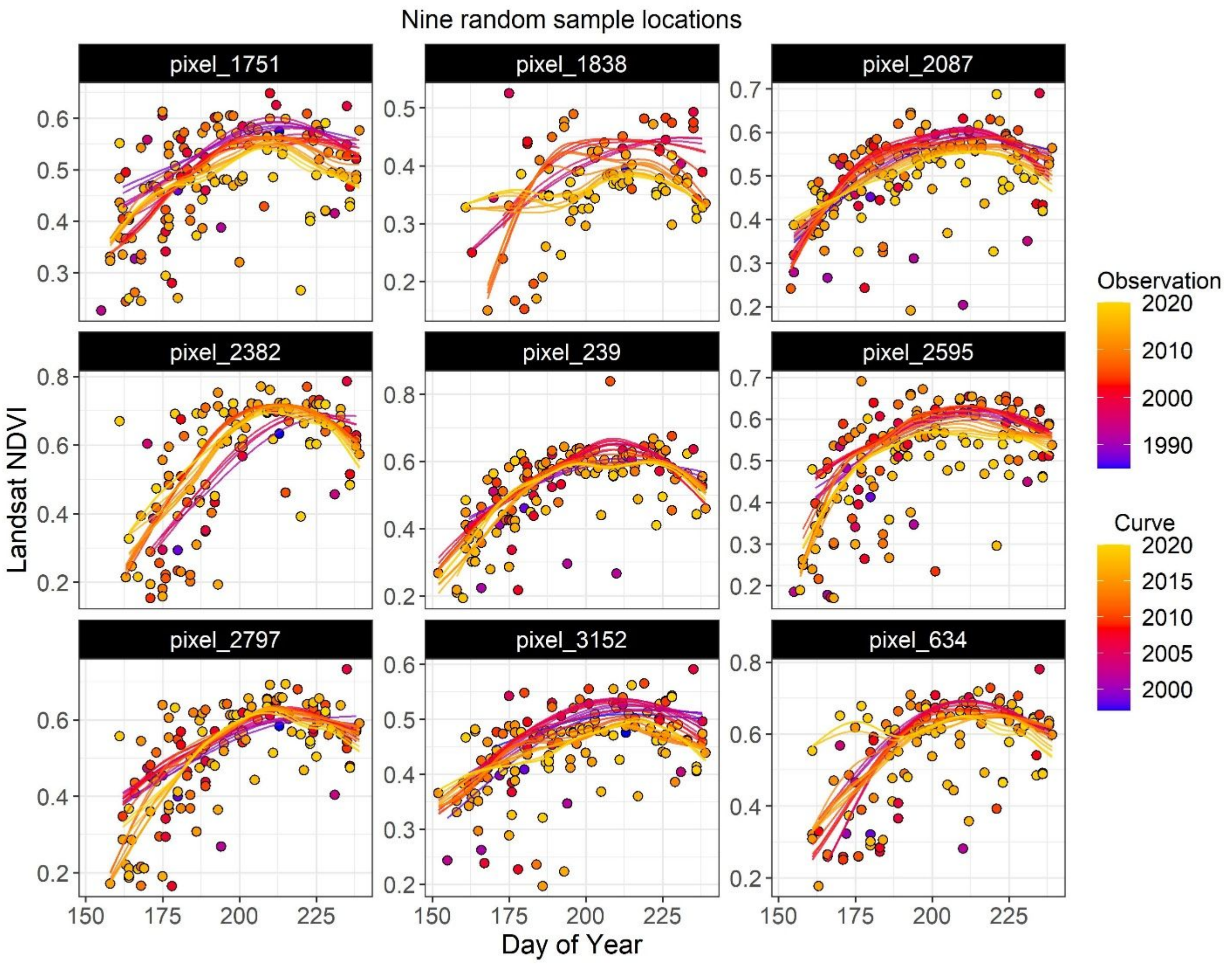

~~Figure 5. Seasonal progression of Landsat NDVI and phenological curves for nine random sample locations from the study area on Disko Island. Each point is an observation sorted by the day of year it was acquired and colored by the year of acquisition. Each phenological curve was fit to observations pooled over an 11-year window centered on each focal year.~~

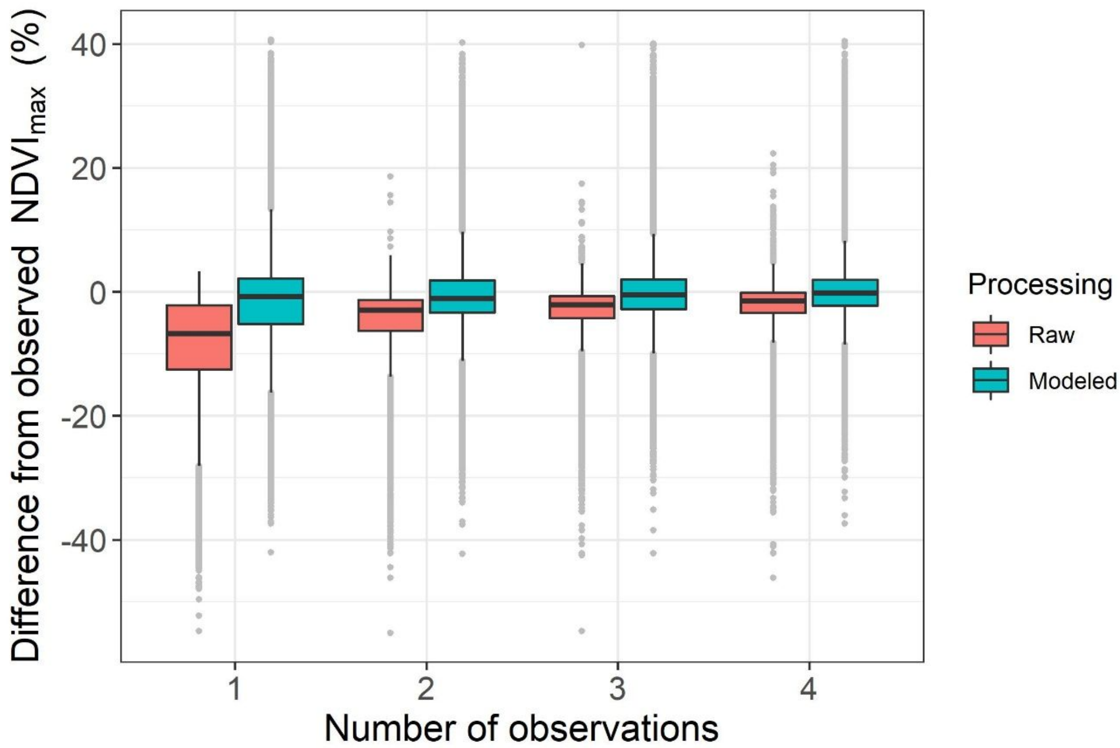

~~Figure 6. Raw estimates of annual maximum NDVI (NDVI$_{max}$) are biased low when few Landsat observations are available from a given growing season, whereas phenologically modeled estimates of NDVI$_{max}$ are minimally impacted by the availability of observations. The figure summarizes how raw and modeled estimate of NDVI$_{max}$ differ from observed NDVI$_{max}$ based on number of observations, as determined using *lsat_evaluate_phenological_max()*.~~

~~*Part 3: Analyze vegetation greenness time series*~~

~~Finally, the trend in the NDVI$_{max}$ across years for each sample location (pixel center) in our study area on Disko Island is calculated using the *lsat_calc_trend()* function (Code Box 4). Note how we use the "yrs" argument to restrict the time series analysis to the years between 2000-2020 to avoid using the low number of observations in the record prior the turn of the millennium. Figure 7 shows a histogram of precent change in NDVI$_{max}$ across the study area and a time series of annual mean NDVI$_{max}$ by trend category, both of which are generated by the function. These figures indicate extensive browning across the study area in recent decades.~~

~~Code Box 4: Analyze vegetation greenness time series~~
that is plotted to the current graphics device.

Conclusions

The *LandsatTS*

```
# Compute temporal trend in NDVImax (Figure 7)
lsat.trend.dt <- lsat_calc_trend(lsat.gs.dt, si = 'ndvi.max', yrs = 2000:2020)
```

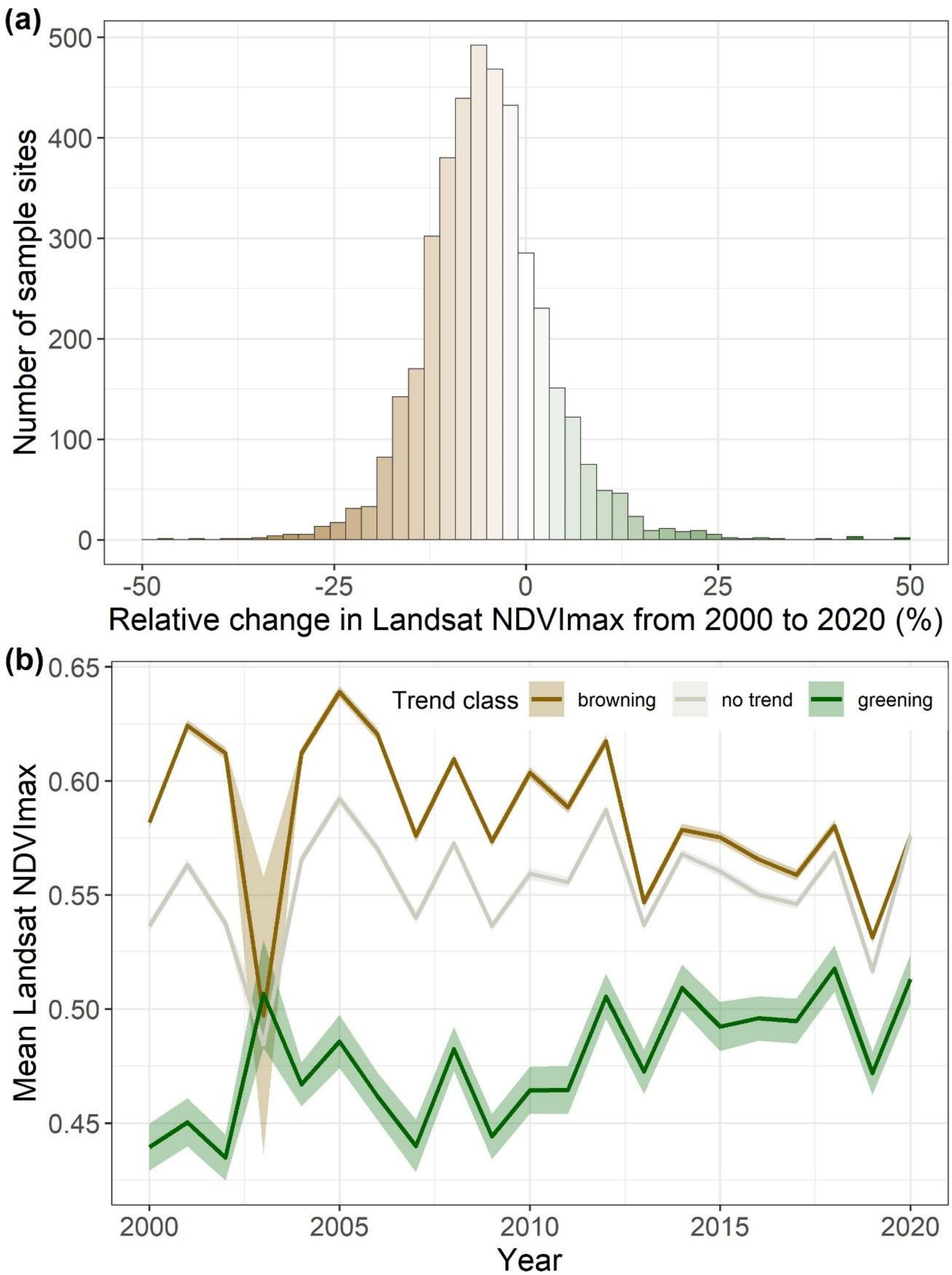
(a)
Number of sample sites
0
100
200
300
400
500
-50
-25
0
25
50
Relative change in Landsat NDVImax from 2000 to 2020 (%)
(b)
Mean Landsat NDVImax
0.45
0.50
0.55
0.60
0.65
Trend class
browning
no trend
greening
2000
2005
2010
2015
2020
Year

~~Figure 7. (a) Histogram of relative change in Landsat $NDVI_{max}$ from 2000 to 2020 among sample locations in the study area on Disko Island. Landsat $NDVI_{max}$ decreased (browned) across much of the study area over the past two decades. (b) Annual mean Landsat $NDVI_{max}$ from 2000 to 2020 for sample locations grouped by their concomitant temporal trend. Trends were assessed for each sample location by removing temporal autocorrelation and then applying a Mann-Kendall trend test. Error bands depict ±1 standard error.~~

~~*Results from the example study*~~

~~This example analysis showed that from 2000 to 2020, annual maximum vegetation greenness (i.e., $NDVI_{max}$) systematically decreased (α = 0.10; browned) across 51% of the study area on Disko Island, whereas vegetation greenness systematically increased (α = 0.10; greened) across 3% of this study area (Figure 2a and 8). There were no systematic changes across the remaining 46% of the study area (Figure 2a and 8). Overall, vegetation greenness decreased by an average of 5.7 ± 8.4% (± 1 SD) during this period. The predominance of browning in this study area contrasts with widespread greening in the Arctic (Myers-Smith et al. 2020, Frost et al. 2021), where Landsat observations indicate that average Arctic vegetation greenness increased 3.9% from 2000 to 2020 (Berner et al. 2020, Mekonnen et al. 2021). Nevertheless, browning in this study area is broadly consistent with findings from recent pan-Arctic analyses using Landsat (Berner et al. 2020) and MODIS (Frost et al. 2021) satellite data that show regional browning in southwestern Greenland. The causes of browning in southwestern Greenland warrant further investigation but are potentially linked to hotter and dried conditions suppressing shrub and other vegetation growth and, in some areas, with defoliation from moths (*Eurois occulta*) or browsing by muskoxen (*Ovibos moschatus*) (Forchhammer 2017, Gamm et al. 2018, Prendin et al. 2020). This analysis demonstrates a general workflow that can be used to not only explore long-term changes in vegetation greenness across focal landscapes, but also to perform sample-based analyses across large geographic domains.~~

~~**Conclusion**~~

~~The *lsatTS*~~ package for R facilitates ~~the extraction~~extracting and processing ~~of~~ Landsat surface reflectance time series, as well as generating and analyzing metrics of vegetation greenness and other spectral indices. We demonstrated the functionality of this software by analyzing multidecadal changes in vegetation greenness across ~~a tundra landscape on Disko Island off~~ the ~~west coast of Greenland~~Noatak National Preserve, USA, but would like to highlight that these tools are also well suited for sample-based analyses of vegetation dynamics across ~~large~~ geographic regions ~~such as whole~~ranging from individual field sites to entire terrestrial biomes (e.g., Berner et al. 2020, Berner and Goetz 2022). To date, ~~*lsatTS*~~*LandsatTS* has been used for ecological studies focused on the Arctic tundra and boreal forest biomes, but many of the functions could be used for studies focused on lower latitude ecosystems, especially ecosystems ~~with~~without a ~~single~~multi-modal growing season. Overall, this software provides a suite of functions to enable broader use of Landsat satellite data for assessing and monitoring Earth's land surface over the past four decades in a sample-based framework suitable for local to global geographic extents.

Acknowledgements

We acknowledge support from the National Aeronautics and Space Administration (NASA) Arctic Boreal Vulnerability Experiment (ABoVE) under Grant No. 80NSSC19M0112 to S.J.G.

For Review Only

and the NASA New Investigator Program (NIP) under Grant No. 80NSSC21K1364 to L.T.B. This study was also supported by the National Science Foundation Navigating the New Arctic Big Idea under Grant No. 2127273 to L.T.B. and S.J.G. The contributions from J.J.A and S.N. to this study were funded by the Independent Research Fund of Denmark (grant 7027-00133B) and the EU Horizon 2020 CHARTER project (Grant Agreement Number: 869471). Landsat 5 (doi.org/10.5066/P9IAXOVV), Landsat 7 (doi.org/10.5066/P9C7I13B), and Landsat 8 (doi.org/10.5066/P9OGBGM6) surface reflectance data courtesy of the U.S. Geological Survey.

References

Appelhans, T., F. Detsch, C. Reudenbach, and S. Woellauer. 2021. mapview: Interactive Viewing of Spatial Data in R. R package version 2.10.0. https://CRAN.R-project.org/package=mapview.

Aybar, C., Q. Wu, L. Bautista, R. Yali, and A. Barja. 2020. rgee: An R package for interacting with Google Earth Engine. Journal of Open Source Software **5**:2272.

Bache, S. M., and H. Wickham. 2020. magrittr: A Forward-Pipe Operator for R. R package version 2.0.1. https://CRAN.R-project.org/package=magrittr.

Badgley, G., C. B. Field, and J. A. Berry. 2017. Canopy near-infrared reflectance and terrestrial photosynthesis. Science Advances **3**:e1602244.

Bengtsson, H. 2021. R.utils: Various Programming Utilities. R package version 2.11.0. https://CRAN.R-project.org/package=R.utils.

Berner, L. T., and S. J. Goetz. 2022. Satellite observations document trends consistent with a boreal forest biome shift. Global Change Biology ~~**00**:1-18~~**28**:3275–3292.

Berner, L. T., P. Jantz, K. D. Tape, and S. J. Goetz. 2018. Tundra plant aboveground biomass and shrub dominance mapped across the North Slope of Alaska. Environmental Research Letters **13**:035002.

Berner, L. T., R. Massey, P. Jantz, B. C. Forbes, M. Macias-Fauria, I. H. Myers-Smith, T. Kumpula, G. Gauthier, L. Andreu-Hayles, B. Gaglioti, P. J. Burns, P. Zetterberg, R. D'Arrigo, and S. J. Goetz. 2020. Summer warming explains widespread but not uniform greening in the Arctic tundra biome. Nature communications **11**:4621.

Bhatt, U. S., D. A. Walker, M. K. Raynolds, J. E. Walsh, P. A. Bieniek, L. Cai, J. C. Comiso, H. E. Epstein, G. V. Frost, and R. Gersten. 2021. Climate drivers of Arctic tundra variability and change using an indicators framework. Environmental Research Letters **16**:055019.

Boyd, M. A., L. T. Berner, P. Doak, S. J. Goetz, B. M. Rogers, D. Wagner, X. J. Walker, and M. C. Mack. 2019. Impacts of climate and insect herbivory on productivity and physiology of trembling aspen (Populus tremuloides) in Alaskan boreal forests. Environmental Research Letters **14**:085010.

Boyd, M. A., L. T. Berner, A. C. Foster, S. J. Goetz, B. M. Rogers, X. J. Walker, and M. C. Mack. 2021. Historic declines in growth portend trembling aspen death during a contemporary leaf miner outbreak in Alaska. Ecosphere **12**:e03569.

Breiman, L. 2001. Random Forests. Machine Learning **45**:5-32.

Bronaugh, D., and A. Werner. 2019. zyp: Zhang + Yue-Pilon trends package. R package version 0.10-1.1. https://CRAN.R-project.org/package=zyp.

Camps-Valls, G., M. Campos-Taberner, Á. Moreno-Martínez, S. Walther, G. Duveiller, A. Cescatti, M. D. Mahecha, J. Muñoz-Marí, F. J. García-Haro, and L. Guanter. 2021. A unified vegetation index for quantifying the terrestrial biosphere. Science Advances **7**:eabc7447.

Cheng, J., B. Karambelkar, and Y. Xie. 2022. leaflet: Create Interactive Web Maps with the JavaScript 'Leaflet' Library. R package version 2.1.1. https://CRAN.R-project.org/package=leaflet.

Csárdi, G. 2021. crayon: Colored Terminal Output. R package version 1.4.2. https://CRAN.R-project.org/package=crayon.

For Review Only

Dial, R. J., C. T. Maher, R. E. Hewitt, and P. F. Sullivan. 2022. Sufficient conditions for rapid range expansion of a boreal conifer. Nature **608**:546-551.

dos Santos, A. 2017. landsat8: Landsat 8 Imagery Rescaled to Reflectance, Radiance and/or Temperature. R package version 0.1-10. https://CRAN.R-project.org/package=landsat8.

Dowle, M., and A. Srinivasan. 2021. data.table: Extension of `data.frame`. R package version 1.14.2. https://CRAN.R-project.org/package=data.table.

~~Forchhammer, M. 2017. Sea-ice induced growth decline in Arctic shrubs. Biology Letters **13**.~~

~~Frost, G. V., M. J. Macander, U. S. Bhatt, H. E. Epstein, L. T. Berner, J. W. Bjerke, B. C. Forbes, S. J. Goetz, M. J. Lara, T. Park, G. K. Phoenix, M. K. Raynolds, H. Tømmervik, and D. A. Walker. 2021. Tundra greenness [in "State of the Climate in 2020"]. Bulletin of the American Meteorological Society **102**:S290–S292.~~

Foster, A. C., J. A. Wang, G. V. Frost, S. J. Davidson, E. Hoy, K. W. Turner, O. Sonnentag, H. Epstein, L. T. Berner, A. H. Armstrong, M. Kang, B. M. Rogers, E. Campbell, K. R. Miner, K. M. Orndahl, L. L. Bourgeau-Chavez, D. A. Lutz, N. French, D. Chen, J. Du, T. A. Shestakova, J. K. Shuman, K. Tape, A.-M. Virkkala, C. Potter, and S. Goetz. 2022. Disturbances in North American boreal forest and Arctic tundra: impacts, interactions, and responses. Environmental Research Letters **17**:113001.

Gaglioti, B., L. T. Berner, B. M. Jones, K. M. Orndahl, A. P. Williams, L. Andreu-Hayles, R. D'Arrigo, S. J. Goetz, and D. H. Mann. 2021. Tussocks enduring or shrubs greening: Alternate responses to changing fire regimes in the Noatak River Valley, Alaska. Journal of Geophysical Research: Biogeosciences **126**:e2020JG006009.

~~Gamm, C. M., P. F. Sullivan, A. Buchwal, R. J. Dial, A. B. Young, D. A. Watts, S. M. Cahoon, J. M. Welker, and E. Post. 2018. Declining growth of deciduous shrubs in the warming climate of continental western Greenland. Journal of Ecology **106**:640-654.~~

Gao, B.-C. 1996. NDWI—A normalized difference water index for remote sensing of vegetation liquid water from space. Remote Sensing of Environment **58**:257-266.

Gitelson, A. A. 2004. Wide dynamic range vegetation index for remote quantification of biophysical characteristics of vegetation. Journal of plant physiology **161**:165-173.

Gitelson, A. A., and M. N. Merzlyak. 1998. Remote sensing of chlorophyll concentration in higher plant leaves. Advances in Space Research **22**:689-692.

~~Goetz, S. J., and S. D. Prince. 1999. Modelling Terrestrial Carbon Exchange and Storage: Evidence and Implications of Fuctional Convergence in Light-use Efficiency. Advances in Ecological Research **28**:57-92.~~

Gorelick, N., M. Hancher, M. Dixon, S. Ilyushchenko, D. Thau, and R. Moore. 2017. Google Earth Engine: Planetary-scale geospatial analysis for everyone. Remote Sensing of Environment **202**:18-27.

Goslee, S. 2011. Analyzing remote sensing data in R: The Landsat Package. The Journal of Statistial Software **43**.

Hansen, M. C., P. V. Potapov, R. Moore, M. Hancher, S. A. Turubanova, A. Tyukavina, D. Thau, S. V. Stehman, S. J. Goetz, T. R. Loveland, A. Kommareddy, A. Egorov, L. Chini, C. O. Justice, and J. R. G. Townshend. 2013. High-Resolution Global Maps of 21st-Century Forest Cover Change. science **342**:850.

Hardisky, M., V. Klemas, and M. Smart. 1983. The influence of soil salinity, growth form, and leaf moisture on the spectral radiance of Spartina alterniflora. Photogrammetric Engineering & Remote Sensing **49**:77-83.

Helman, D. 2018. Land surface phenology: What do we really 'see' from space? Science of the Total Environment **618**:665-673.

Henry, L., and H. Wickham. 2020. purrr: Functional Programming Tools. R package version 0.3.4. https://CRAN.R-project.org/package=purrr.

~~Howat, I., A. Negrete, and B. Smith. 2015. MEaSUREs Greenland Ice Mapping Project (GIMP) Digital Elevation Model, Version 1. NASA National Snow and Ice Data Center Distributed Active Archive Center. doi: https://doi.org/10.5067/NV34YUIXLP9W. [2021-11-23], Boulder, Colorado USA.~~

~~Howat, I. M., A. Negrete, and B. E. Smith. 2014. The Greenland Ice Mapping Project (GIMP) land classification and surface elevation data sets. The Cryosphere **8**:1509-1518.~~

Huete, A., K. Didan, T. Miura, E. P. Rodriguez, X. Gao, and L. G. Ferreira. 2002. Overview of the radiometric and biophysical performance of the MODIS vegetation indices. Remote Sensing of Environment **83**:195-213.

Huete, A. R. 1988. A soil-adjusted vegetation index (SAVI). Remote Sensing of Environment **25**:295-309.

Jia, G. J., H. E. Epstein, and D. A. Walker. 2003. Greening of arctic Alaska, 1981–2001. Geophysical Research Letters **30**:2067.

Jiang, Z., A. R. Huete, K. Didan, and T. Miura. 2008. Development of a two-band enhanced vegetation index without a blue band. Remote Sensing of Environment **112**:3833-3845.

~~Johansen, B., and H. Tømmervik. 2014. The relationship between phytomass, NDVI and vegetation communities on Svalbard. International Journal of Applied Earth Observation and Geoinformation **27**:20-30.~~

Ju, J., and J. G. Masek. 2016. The vegetation greenness trend in Canada and US Alaska from 1984–2012 Landsat data. Remote Sensing of Environment **176**:1-16.

Kassambara, A. 2020. ggpubr: 'ggplot2' Based Publication Ready Plots. R package version 0.4.0. https://CRAN.R-project.org/package=ggpubr.

Key, C. H., and N. C. Benson. 1999. The Normalized Burn Ratio (NBR): A Landsat TM radiometric measure of burn severity. United States Geological Survey, Northern Rocky Mountain Science Center.(Bozeman, MT).

Kong, D., T. R. McVicar, M. Xiao, Y. Zhang, J. L. Peña-Arancibia, G. Filippa, Y. Xie, and X. Gu. 2022. phenofit: An R package for extracting vegetation phenology from time series remote sensing. Methods in Ecology and Evolution **13**:1508-1527.

Lai, J., C. J. Lortie, R. A. Muenchen, J. Yang, and K. Ma. 2019. Evaluating the popularity of R in ecology. Ecosphere **10**:e02567.

Marsett, R. C., J. Qi, P. Heilman, S. H. Biedenbender, M. C. Watson, S. Amer, M. Weltz, D. Goodrich, and R. Marsett. 2006. Remote sensing for grassland management in the arid southwest. Rangeland Ecology & Management **59**:530-540.

McFeeters, S. K. 1996. The use of the Normalized Difference Water Index (NDWI) in the delineation of open water features. International Journal of Remote Sensing **17**:1425-1432.

Mekonnen, Z. A., W. J. Riley, L. T. Berner, N. J. Bouskill, M. S. Torn, G. Iwahana, A. L. Breen, I. H. Myers-Smith, M. G. Criado, Y. Liu, E. S. Euskirchen, S. J. Goetz, M. C. Mack, and R. F. Grant. 2021. Arctic tundra shrubification: a review of mechanisms and impacts on ecosystem carbon balance. Environmental Research Letters **16**:053001.

Merzlyak, M. N., A. A. Gitelson, O. B. Chivkunova, and V. Y. Rakitin. 1999. Non-destructive optical detection of pigment changes during leaf senescence and fruit ripening. Physiologia plantarum **106**:135-141.

Myers-Smith, I. H., J. T. Kerby, G. K. Phoenix, J. W. Bjerke, H. E. Epstein, J. J. Assmann, C. John, L. Andreu-Hayles, S. Angers-Blondin, P. S. A. Beck, L. T. Berner, U. S. Bhatt, A. D. Bjorkman, D. Blok, A. Bryn, C. T. Christiansen, J. H. C. Cornelissen, A. M. Cunliffe, S. C. Elmendorf, B. C. Forbes, S. J. Goetz, R. D. Hollister, R. de Jong, M. M. Loranty, M. Macias-Fauria, K. Maseyk, S. Normand, J. Olofsson, T. C. Parker, F.-J. W. Parmentier, E. Post, G. Schaepman-Strub, F. Stordal, P. F. Sullivan, H. J. D. Thomas, H. Tømmervik, R. Treharne, C. E. Tweedie, D. A. Walker, M. Wilmking, and S. Wipf. 2020. Complexity revealed in the greening of the Arctic. Nature Climate Change **10**:106-117.

For Review Only

National Academies of Sciences. 2018. Thriving on Our Changing Planet: A Decadal Strategy for Earth Observation from Space. The National Academies Press, Washington, DC.

~~Pastick, N. J., M. T. Jorgenson, S. J. Goetz, B. M. Jones, B. K. Wylie, B. J. Minsley, H. Genet, J. F. Knight, D. K. Swanson, and J. C. Jorgenson. 2019. Spatiotemporal remote sensing of ecosystem change and causation across Alaska. Global Change Biology **25**:1171-1189.~~

Pebesma, E. J. 2018. Simple features for R: standardized support for spatial vector data. The R Journal **10**:439-446.

Pekel, J.-F., A. Cottam, N. Gorelick, and A. S. Belward. 2016. High-resolution mapping of global surface water and its long-term changes. Nature **540**:418-422.

~~Prendin, A. L., M. Carrer, M. Karami, J. Hollesen, N. Bjerregaard Pedersen, M. Pividori, U. A. Treier, A. Westergaard-Nielsen, B. Elberling, and S. Normand. 2020. Immediate and carry-over effects of insect outbreaks on vegetation growth in West Greenland assessed from cells to satellite. Journal of Biogeography **47**:87-100.~~

~~QGIS.org. 2021. QGIS Geographic Information System. QGIS Association. http://www.qgis.org.~~

Potapov, P., M. C. Hansen, A. Pickens, A. Hernandez-Serna, A. Tyukavina, S. Turubanova, V. Zalles, X. Li, A. Khan, F. Stolle, N. Harris, X.-P. Song, A. Baggett, I. Kommareddy, and A. Kommareddy. 2022. The Global 2000-2020 Land Cover and Land Use Change Dataset Derived From the Landsat Archive: First Results. Frontiers in Remote Sensing **3**.

Powell, S. L., W. B. Cohen, S. P. Healey, R. E. Kennedy, G. G. Moisen, K. B. Pierce, and J. L. Ohmann. 2010. Quantification of live aboveground forest biomass dynamics with Landsat time-series and field inventory data: A comparison of empirical modeling approaches. Remote Sensing of Environment **114**:1053-1068.

R Core Team. 2021. R: A Language and Environment for Statistical Computing. R Foundation for Statistical Computing, Vienna, Austria.

Raynolds, M. K., D. A. Walker, H. E. Epstein, J. E. Pinzon, and C. J. Tucker. 2012. A new estimate of tundra-biome phytomass from trans-Arctic field data and AVHRR NDVI. Remote Sensing Letters **3**:403-411.

Rock, B., J. Vogelmann, D. Williams, A. Vogelmann, and T. Hoshizaki. 1986. Remote detection of forest damage. BioScience **36**:439-445.

Rouse, J., R. Haas, J. Schell, and D. Deering. 1974. Monitoring vegetation systems in the Great Plains with ERTS. NASA special publication **351**:309-317.

Roy, D. P., V. Kovalskyy, H. K. Zhang, E. F. Vermote, L. Yan, S. S. Kumar, and A. Egorov. 2016. Characterization of Landsat-7 to Landsat-8 reflective wavelength and normalized difference vegetation index continuity. Remote Sensing of Environment **185**:57-70.

Sexton, J. O., X.-P. Song, M. Feng, P. Noojipady, A. Anand, and C. Huang. 2013. Global, 30-m resolution continuous fields of tree cover: landsat-based rescaling of MODIS vegetation continuous fields with lidar-based estimates of error. Int J Digit Earth **6**.

~~Tucker, C. J. 1979. Red and photographic infrared linear combinations for monitoring vegetation. Remote Sensing of Environment **8**:127-150.~~

Suarez, F., D. Binkley, M. W. Kaye, and R. Stottlemyer. 1999. Expansion of forest stands into tundra in the Noatak National Preserve, northwest Alaska. Ecoscience **6**:465-470.

Tape, K., M. Sturm, and C. Racine. 2006. The evidence for shrub expansion in Northern Alaska and the Pan-Arctic. Global Change Biology **12**:686-702.

Terskaia, A., R. J. Dial, and P. F. Sullivan. 2020. Pathways of tundra encroachment by trees and tall shrubs in the western Brooks Range of Alaska. Ecography **43**:769-778.

Verdonen, M., L. T. Berner, B. C. Forbes, and T. Kumpula. 2020. Periglacial vegetation dynamics in Arctic Russia: decadal analysis of tundra regeneration on landslides with time series satellite imagery. Environmental Research Letters **15**:105020.

For Review Only

Walker, ~~D. A., W. A. Gould, H. A. Maier, and M. K. Raynolds. 2002. The Circumpolar Arctic Vegetation Map: AVHRR-derived base maps, environmental controls, and integrated mapping procedures. International Journal of Remote Sensing **23**:4551-4570.~~

~~Walker,~~ X. J., H. D. Alexander, L. T. Berner, M. A. Boyd, M. M. Loranty, S. M. Natali, and M. C. Mack. 2021. Positive response of tree productivity to warming is reversed by increased tree density at the Arctic tundra-taiga ecotone. Canadian Journal of Forest Research **51**:1323-1338.

Wang, J. A., and M. A. Friedl. 2019. The role of land cover change in Arctic-Boreal greening and browning trends. Environmental Research Letters **14**:125007.

Wickham, H. 2016. ggplot2: Elegant Graphics for Data Analysis. Springer-Verlang New York.

Wickham, H. 2019. stringr: Simple, Consistent Wrappers for Common String Operations. R package version 1.4.0. https://CRAN.R-project.org/package=stringr.

Wickham, H. 2021. tidyr: Tidy Messy Data. R package version 1.1.4. https://CRAN.R-project.org/package=tidyr.

Wickham, H., R. Francois, H. Lionel, and K. Müller. 2021. dplyr: A Grammar of Data Manipulation. R package version 1.0.7. https://CRAN.R-project.org/package=dplyr.

~~Woodcock, C. E., R. Allen, M. Anderson, A. Belward, R. Bindschadler, W. Cohen, F. Gao, S. N. Goward, D. Helder, E. Helmer, R. Nemani, L. Oreopoulos, J. Schott, P. S. Thenkabail, E. F. Vermote, J. Vogelmann, M. A. Wulder, R. Wynne, and T. Landsat Sci. 2008. Free access to Landsat imagery. science **320**:1011-1011.~~

Wright, M. N., and A. Ziegler. 2017. Ranger: a fast implementation of random forests for high dimensional data in C++ and R. Journal of statistical software **77**:1-17.

Wulder, M., R. Skakun, W. Kurz, and J. White. 2004. Estimating time since forest harvest using segmented Landsat ETM+ imagery. Remote Sensing of Environment **93**:179-187.

Wulder, M. A., T. R. Loveland, D. P. Roy, C. J. Crawford, J. G. Masek, C. E. Woodcock, R. G. Allen, M. C. Anderson, A. S. Belward, W. B. Cohen, J. Dwyer, A. Erb, F. Gao, P. Griffiths, D. Helder, T. Hermosilla, J. D. Hipple, P. Hostert, M. J. Hughes, J. Huntington, D. M. Johnson, R. Kennedy, A. Kilic, Z. Li, L. Lymburner, J. McCorkel, N. Pahlevan, T. A. Scambos, C. Schaaf, J. R. Schott, Y. Sheng, J. Storey, E. Vermote, J. Vogelmann, J. C. White, R. H. Wynne, and Z. Zhu. 2019. Current status of Landsat program, science, and applications. Remote Sensing of Environment **225**:127-147.

~~Xu, W., A. Prieme, E. J. Cooper, M. A. Mörsdorf, P. Semenchuk, B. Elberling, P. Grogan, and P. L. Ambus. 2021. Deepened snow enhances gross nitrogen cycling among Pan-Arctic tundra soils during both winter and summer. Soil Biology and Biochemistry **160**:108356.~~

Wulder, M. A., J. G. Masek, W. B. Cohen, T. R. Loveland, and C. E. Woodcock. 2012. Opening the archive: How free data has enabled the science and monitoring promise of Landsat. Remote Sensing of Environment **122**:2-10.

Yue, S., P. Pilon, B. Phinney, and G. Cavadias. 2002. The influence of autocorrelation on the ability to detect trend in hydrological series. Hydrological processes **16**:1807-1829.

Zeileis, A., and G. Grothendieck. 2005. zoo: S3 Infrastructure for Regular and Irregular Time Series. Journal of statistical software **14**:1-27.

Zeng, L., B. D. Wardlow, D. Xiang, S. Hu, and D. Li. 2020. A review of vegetation phenological metrics extraction using time-series, multispectral satellite data. Remote Sensing of Environment **237**:111511.

Zhu, Z., S. Wang, and C. E. Woodcock. 2015. Improvement and expansion of the Fmask algorithm: cloud, cloud shadow, and snow detection for Landsats 4–7, 8, and Sentinel 2 images. Remote Sensing of Environment **159**:269-277.

For Review Only

Package 'LandsatTS'

January 20, 2023

Title An R package to facilitate retrieval, cleaning, cross-calibration, and phenological modeling of Landsat time-series data

Version 1.1.0

Description This software package facilitates sample-based time series analysis of surface reflectance and spectral indices derived from sensors on the Landsat satellites. The package includes functions that enable extraction of the full Landsat record for point sample locations or small study regions using Google Earth Engine directly accessed from R. Moreover, the package includes functions for (1) data cleaning, (2) cross-sensor calibration, (3) phenological modeling, and (4) time series analysis.

License Modified MIT

Encoding UTF-8

LazyData true

Roxygen list(markdown = TRUE)

RoxygenNote 7.2.2

Suggests testthat (>= 3.0.0)

Config/testthat/edition 3

Imports magrittr, dplyr, tidyr, rgee, sf, crayon, mapview, purrr, data.table, ggplot2, R.utils, stats, stringr, ggpubr, ranger, zoo, zyp

Depends R (>= 3.50)

For Review Only

R topics documented:

`lsat.example.dt` *Landsat surface reflectance for six sample sites in the Arctic*

Description

A dataset containing Landsat surface reflectance measurements and ancillary data for six sample sites in the Arctic. These data are used for the examples included with LandsatTS.

Usage

```
lsat.example.dt
```

Format

A data.table with 5296 rows and 23 variables

Source

Generated using example code provided in LandsatTS::lsat_export_ts()

For Review Only

`lsat_calc_spectral_index` *Calculate spectral indices*

Description

This function computes some widely used spectral vegetation indices. Only one index can be computed at a time. Current indices include the: Normalized Difference Vegetation Index (NDVI; Rouse et al. 1974), kernel NDVI (kNDVI; Camp-Valls et al. 2020), Green NDVI (gNDVI; Gitelson and Merzlyak 1998), Soil Adjusted Vegetation Index (SAVI; Huete 1998), Wide Dynamic Range Vegetation Index (WDRVI; Gitelson 2004), Enhanced Vegetation Index (EVI; Huete et al. 2002), 2-band EVI (EVI2; Jiang et al. 2008), Near Infrared Vegetation Index (NIRv; Badgley et al. 2017), Moisture Stress Index (MSI; Rock et al. 1986), Normalized Difference Water Index (NDWI; McFeeters 1996), Normalized Difference Moisture Index (NDMI; Gao 1996), Normalized Burn Ratio (NBR, Key and Benson 1999), Normalized Difference Infrared Index (NDII; Hardisky et al. 1983), Plant Senescence Reflectance Index (PSRI; Merzlyak et al. 1999), and the Soil-Adjusted Total Vegetation Index (SATVI; Marsett et al. 2006).

Usage

```
lsat_calc_spectral_index(dt, si)
```

Arguments

`dt`	Data.table containing surface reflectance data.
`si`	Character string specifying abbreviation of the desired spectral index.

Value

The input data.table with an appended column containing the spectral index.

Examples

```
data(lsat.example.dt)
lsat.dt <- lsat_format_data(lsat.example.dt)
lsat.dt <- lsat_clean_data(lsat.dt)
lsat.dt <- lsat_calc_spectral_index(lsat.dt, 'ndvi')
lsat.dt
```

For Review Only

lsat_calc_trend *Calculate non-parametric vegetation greenness trends*

Description

This function evaluates and summarizes interannual trends in vegetation greenness for sample sites over a user-specified time period. Potential interannual trends in vegetation greenness are assessed using Mann-Kendall trend tests and Theil-Sen slope indicators after prewhitening each time series. This trend assessment relies on the zyp.yuepilon() function from the zyp package, which provides further details.

Usage

```
lsat_calc_trend(dt, si, yrs, yr.tolerance = 1, nyr.min.frac = 0.66, sig = 0.1)
```

Arguments

dt	Data.table with columns including site, year, and the vegetation index of interest.
si	Spectral index for which to assess trend (e.g., NDVI).
yrs	A sequence of years over which to assess trends (e.g., 2000:2020).
yr.tolerance	The number of years that a site's first/last years of observations can differ from the start/end of the user-specified time period ('yrs') for a trend to be computed.
nyr.min.frac	Fraction of years within the time period for which observations must be available if a trend is to be computed.
sig	A p-value significance cutoff used to categories trends (e.g., 0.10)

Value

A list that includes: (1) a summary message about the mean relative change across sample sites; (2) a data.table summarizing the number and percentage of sites that fall into each trend category; (3) a data.table with trend statistics for each sample site.

Examples

```
data(lsat.example.dt)
lsat.dt <- lsat_format_data(lsat.example.dt)
lsat.dt <- lsat_clean_data(lsat.dt)
lsat.dt <- lsat_calc_spectral_index(lsat.dt, 'ndvi')
# lsat.dt <- lsat_calibrate_rf(lsat.dt, band.or.si = 'ndvi', write.output = F)
lsat.pheno.dt <- lsat_fit_phenological_curves(lsat.dt, si = 'ndvi')
lsat.gs.dt <- lsat_summarize_growing_seasons(lsat.pheno.dt, si = 'ndvi')
lsat.trend.dt <- lsat_calc_trend(lsat.gs.dt, si = 'ndvi.max', yrs = 2000:2020)
lsat.trend.dt
```

`lsat_calibrate_poly` *Cross-calibrate Landsat sensors using polynomial regression*

Description

There are systematic differences in spectral indices (e.g., NDVI) among Landsat 5, 7, and 8 (Landsat Collection 2). It is important to address these differences before assessing temporal trends in spectral data. Failure to address these differences can, for instance, introduce artificial positive trends into NDVI time-series that are based on measurements from multiple Landsat sensors (Ju and Masek 2016, Roy et al. 2016, Berner et al. 2020). This function cross-calibrates individual bands or spectral indices from Landsat 5/8 to match Landsat 7. Landsat 7 is used as a benchmark because it temporally overlaps with the other two sensors. Cross-calibration can only be performed on one band or spectral index at a time. The approach involves determining the typical reflectance at a sample during a portion of the growing season site using Landsat 7 and Landsat 5/8 data that were collected the same years. Polynomial regression models from first to third order are trained to predict Landsat 7 reflectance from Landsat 5/8 reflectance, the most parsimonious model is selected using BIC, and then that model is used to cross-calbirate the data. This approach is most suitable when working with data from 100s to preferably 1000s of sample samples.

The specific steps to cross-calibrating sensors include: (1) Identify the years when both Landsat 7 and Landsat 5/8 measured surface reflectance at a sample sample. (2) Pool the reflectance measurements across those years and compute 15-day moving median reflectance over the course of the growing season for each sensor and sampling sample. (3) Exclude 15-day periods with fewer than a specified number of measurements from both sets of sensors and then randomly select one remaining 15-day period from each sample sample. (4) Split the data into sets for model training and evaluation. (5) Train polynomial regression models that predict Landsat 7 reflectance based on Landsat 5/8 reflectance. Model order (1st to 3rd) is selected using BIC. (6) Apply the polynomial regression models to cross-calibrate measurements.

See Berner et al. (2020) for a full description of the approach.

Usage

```
lsat_calibrate_poly(
  dt,
  band.or.si,
  doy.rng = 152:243,
  min.obs = 5,
  train.with.highlat.data = F,
  frac.train = 0.75,
  trim = T,
  overwrite.col = F,
```

For Review Only

```
  write.output = F,
  outfile.id = band.or.si,
  outdir = NA
)
```

Arguments

`dt`	Data.table containing the band or spectral index to cross-calibrate.
`band.or.si`	Character string matching the column name of the band or spectral index to cross-calibrate.
`doy.rng`	Sequence of numbers specifying the Days of Year to use for model development.
`min.obs`	Minimum number of paired, seasonally-matched observations from Landsat 7 and Landsat 5/8 required to include a sampling sample.
`train.with.highlat.data`	(True/False) Should the RF models be trained using an internal high-latitude dataset that sampled the Arctic and Boreal biomes?
`frac.train`	Fraction of samples to use for training the random forest models. The remaining samples are used for model cross-validation.
`trim`	(True/False) If true, then for each sample site the percent difference in spectral indices between satellites is determined. The lowest 2.5 and highest 97.5 percentiles are then trimmed. This is meant to reduce potential differences that are not directly attributable to the sensors, but rather to exogenous factors.
`overwrite.col`	(True/False) Overwrite existing column or (by default) append cross-calibrated data as a new column?
`write.output`	(True/False) Should RF models and evaluation content be written to disk? Either way, evaluation table and figure are printed in the console.
`outfile.id`	Identifier used when naming output files. Defaults to the input band, but can be specified if needed such as when performing Monte Carlo simulations.
`outdir`	Output directory (created if necessary) to which multiple files will be written. The files include: (1) fitted random forest models as R objects, (2) evaluation data in a csv file, (3) summary of model cross-validation in a csv file, and (4) multi-panel scatter plot comparing sensors pre- and post-calibration in jpeg format. If cross-calibrating both Landsat 5 and 8, then the function returns files for both sensors.

For Review Only

Value

The input data.table with an appended column titled band.xcal, where "band" is your specified band or spectral index.

Examples

```
data(lsat.example.dt)
lsat.dt <- lsat_format_data(lsat.example.dt)
lsat.dt <- lsat_clean_data(lsat.dt)
lsat.dt <- lsat_calc_spectral_index(lsat.dt, 'ndvi')
lsat.dt <- lsat_calibrate_poly(lsat.dt, band.or.si = 'ndvi',
                               train.with.highlat.data = TRUE,
                               write.output = FALSE)
lsat.dt
```

`lsat_calibrate_rf` *Cross-calibrate Landsat sensors using Random Forests models*

Description

There are systematic differences in spectral indices (e.g., NDVI) among Landsat 5, 7, and 8 (Landsat Collection 2). It is important to address these differences before assessing temporal trends in spectral data. Failure to address these differences can, for instance, introduce artificial positive trends into NDVI time-series that are based on measurements from multiple Landsat sensors (Ju and Masek 2016, Roy et al. 2016, Berner et al. 2020). This function cross-calibrates individual bands or spectral indices from Landsat 5/8 to match Landsat 7. Landsat 7 is used as a benchmark because it temporally overlaps with the other two sensors. Cross-calibration can only be performed on one band or spectral index at a time. The approach involves determining the typical reflectance at a sample during a portion of the growing season site using Landsat 7 and Landsat 5/8 data that were collected the same years. A Random Forest model is then trained to predict Landsat 7 reflectance from Landsat 5/8 reflectance. To account for potential seasonal and regional differences between sensors, the Random Forest models also include as covariates the midpoint of each 15-day period (day of year), the spatial coordinates of each sample sample, and potentially other use-specified variables. This approach is most suitable when working with data from 100s to preferably 1000s of sample samples.

The specific steps to cross-calibrating sensors include: (1) Identify the years when both Landsat 7 and Landsat 5/8 measured surface reflectance at a sample sample. (2) Pool the reflectance measurements across those years and compute 15-day moving median reflectance over the course of the growing season for each sensor and sampling sample. (3) Exclude 15-day periods with fewer than a specified number of measurements from both sets of sensors and then randomly select one remaining 15-day period from each sample sample. (4) Split the data into sets for model training and evaluation. (5) Train Random Forest models that predict Landsat 7 reflectance based on Landsat 5/8 reflectance. The models also account for potential seasonal and regional differences between sensors by including as covariates the midpoint of each 15-day period (day of year) and the spatial coordinates of each sampling sample. The models are trained using the ranger function from the ranger package (Wright and Ziegler, 2017). (6) Apply the fitted Random Forest models to cross-calibrate measurements.

See Berner et al. (2020) for a full description of the approach.

Usage

```
lsat_calibrate_rf(
  dt,
  band.or.si,
  doy.rng = 152:243,
  min.obs = 5,
  train.with.highlat.data = F,
  add.predictors = NULL,
  frac.train = 0.75,
  trim = T,
  overwrite.col = F,
  write.output = F,
  outfile.id = band.or.si,
  outdir = NA
)
```

For Review Only

Arguments

`dt`	Data.table containing the band or spectral index to cross-calibrate.
`band.or.si`	Character string matching the column name of the band or spectral index to cross-calibrate.
`doy.rng`	Sequence of numbers specifying the Days of Year to use for model development.
`min.obs`	Minimum number of paired, seasonally-matched observations from Landsat 7 and Landsat 5/8 required to include a sampling sample.
`train.with.highlat.data`	(True/False) Should the RF models be trained using an internal high-latitude dataset that sampled the Arctic and Boreal biomes?
`add.predictors`	Vector of additional predictors to use in the Random Forest models. These should be time-invariant and match column names.
`frac.train`	Fraction of samples to use for training the random forest models. The remaining samples are used for model cross-validation.
`trim`	(True/False) If true, then for each sample site the percent difference in spectral indices between satellites is determined. The lowest 2.5 and highest 97.5 percentiles are then trimmed. This is meant to reduce potential differences that are not directly attributable to the sensors, but rather to exogenous factors.
`overwrite.col`	(True/False) Overwrite existing column or (by default) append cross-calibrated data as a new column?
`write.output`	(True/False) Should RF models and evaluation content be written to disk? Either way, evaluation table and figure are printed in the console.
`outfile.id`	Identifier used when naming output files. Defaults to the input band, but can be specified if needed such as when performing Monte Carlo simulations.
`outdir`	Output directory (created if necessary) to which multiple files will be written. The files include: (1) fitted random forest models as R objects, (2) evaluation data in a csv file, (3) summary of model cross-validation in a csv file, and (4) multi-panel scatter plot comparing sensors pre- and post-calibration in jpeg format. If cross-calibrating both Landsat 5 and 8, then the function returns files for both sensors.

For Review Only

Value

The input data.table with an appended column titled band.xcal, where "band" is your specified band or spectral index.

Examples

```
data(lsat.example.dt)
lsat.dt <- lsat_format_data(lsat.example.dt)
lsat.dt <- lsat_clean_data(lsat.dt)
lsat.dt <- lsat_calc_spectral_index(lsat.dt, 'ndvi')
lsat.dt <- lsat_calibrate_rf(lsat.dt, band.or.si = 'ndvi',
                             train.with.highlat.data = TRUE,
                             write.output = FALSE)
lsat.dt
```

`lsat_clean_data` *Clean Landsat surface reflectance data*

Description

This function enables users to filter out surface reflectance measurements that exhibit: (1) clouds, cloud shadows, snow, or water flagged by the CFMask algorithm; (2) surface water over the Landsat record; (2) impossibly high reflectance (>1.0) and abnormally low reflectance (<0.005); (3) scene cloud cover above a user-defined threshold; (4) geometric uncertainty above a user-defined threshold; (5) solar zenith angle above a user-defined threshold.

Usage

```
lsat_clean_data(
  dt,
  cloud.max = 80,
  geom.max = 30,
  sza.max = 60,
  filter.cfmask.snow = T,
  filter.cfmask.water = T,
  filter.jrc.water = T
)
```

For Review Only

Arguments

`dt`	Data.table generated by calling lsat_format_data().
`cloud.max`	Maximum allowable cloud cover in Landsat scene (percentage).
`geom.max`	Maximum allowable geometric uncertainty (meters).
`sza.max`	Maximum allowable solar zenith angle (degrees).
`filter.cfmask.snow`	(TRUE/FALSE) Remove measurements with CFmask flag = snow.
`filter.cfmask.water`	(TRUE/FALSE) Remove measurements with CFmask flag = water.
`filter.jrc.water`	(TRUE/FALSE) Remove sample sites that were ever innundated based on the maximum surface water extent variable from the JRC Global Surface Water Dataset.

Value

A data.table that includes Landsat measurements that met the quality control criteria.

Examples

```
data(lsat.example.dt)
lsat.dt <- lsat_format_data(lsat.example.dt)
lsat.dt <- lsat_clean_data(lsat.dt)
lsat.dt
```

`lsat_evaluate_phenological_max`
Evaluate estimates of annual phenological maximum

Description

Assess how the number of annual Landsat measurements impacts estimates of annual maximum vegetation greenness derived from raw measurements and phenological modeling. The algorithm computes annual maximum vegetation greenness using site x years with a user-specific number of measurements and then compares these with estimates derived when using progressively smaller subsets of measurements. This lets the user determine the degree to which annual estimates of maximum vegetation greenness are impacted by the number of available measurements.

Usage

```
lsat_evaluate_phenological_max(
  dt,
  si,
  min.frac.of.max = 0.75,
  zscore.thresh = 3,
  min.obs = 6,
  reps = 10,
  outdir = NA
)
```

Arguments

`dt`	Data.table output from lsat_fit_phenological_curves().
`si`	Character string specifying the spectral index (SI) to evaluate (e.g., NDVI).
`min.frac.of.max`	Numeric threshold (0-1) that defines the "growing season" as the seasonal window when the phenological curves indicate the SI is within a specified fraction of the maximum SI. In other words, an observation is considered to be from the "growing season" when the SI is within a user-specified fraction of the curve-fit growing season maximum SI.
`zscore.thresh`	Numeric threshold specifying the Z-score value beyond which individual measurements are filtered before computing the maximum SI.
`min.obs`	Minimum number of measurements needed for a site x year to be included in the evaluation (Default = 10).
`reps`	Number of times to bootstrap the assessment (Default = 10).
`outdir`	If desired, specify the output directory where evaluation data and figure should be written. If left as NA, then no output is only displayed in the console and not written to disk.

Value

A data.table and a figure summarizing how estimates of annnual maximum SI vary with the number of Landsat measurements made during each growing season.

For Review Only

Examples

```
data(lsat.example.dt)
lsat.dt <- lsat_format_data(lsat.example.dt)
lsat.dt <- lsat_clean_data(lsat.dt)
lsat.dt <- lsat_calc_spectral_index(lsat.dt, 'ndvi')
# lsat.dt <- lsat_calibrate_rf(lsat.dt, band.or.si = 'ndvi', write.output = FALSE)
lsat.pheno.dt <- lsat_fit_phenological_curves(lsat.dt, si = 'ndvi')
lsat_evaluate_phenological_max(lsat.pheno.dt, si = 'ndvi')
```

`lsat_export_ts` *Export reflectance time-series from the Landsat record using rgee*

Description

This function exports surface reflectance time series for a set of point-coordinates from the whole Landsat Collection 2 record using the Google Earth Engine. The resulting time-series can then be processed using the remainder of the lsatTS workflow.

For polygon geometries consider using lsat_get_pixel_centers() to generate pixel center coordinates for all pixels within a given polygon first.

Please note: Unlike other functions in this package, this function does NOT return the time-series as an object, instead it returns a list of the EE tasks issued for the export. The actual time-series are exported as CSV objects via the EE to the user's Google Drive. This way of exporting allows for a more efficient scheduling, larger exports, and does not require the R session to continue to run in the background while the requests are processed on the EE.

The progress of the exports can be monitored using the list of tasks returned in combination with ee_monitoring() from the rgee package, or simply by using the task overview in the web code-editor of the EE (https://code.earthengine.google.com).

Usage

```
lsat_export_ts(
  pixel_coords_sf,
  sample_id_from = "sample_id",
  chunks_from = NULL,
  this_chunk_only = NULL,
  max_chunk_size = 250,
  drive_export_dir = "lsatTS_export",
  file_prefix = "lsatTS_export",
  start_doy = 152,
  end_doy = 243,
  start_date = "1984-01-01",
  end_date = "today",
  buffer_dist = 0,
  scale = 30,
  mask_value = 0
)
```

For Review Only

Arguments

`pixel_coords_sf`
: Simple feature object of point coordinates for the sample.

`sample_id_from`
: The column name that specifies the unique sample identifier in pixel_coords_sf (defaults to "sample_id" as generated by lsat_get_pixel_centers).

`chunks_from`
: Column name in pixel_coords_sf to divide the exports into chunks. Over-rides chunk division by size (see max_chunk_size).

`this_chunk_only`
: Name of a specific chunk to be exported. Useful for re-exporting a single chunk should the export fail for some reason.

`max_chunk_size`
: Maximum number of sample coordinates to be exported in each chunk. Defaults to 250.

`drive_export_dir`
: Folder on the user's Google Drive to export the records to. Defaults to "lsatTS_export".

`file_prefix`
: Optional file_prefix for the exported files.

`start_doy`
: Optional first day of year to extract for. Defaults to 152.

`end_doy`
: Optional last day of year to extract for. Defaults to 243.

`start_date`
: Optional extraction start date (as string, format YYYY-MM-DD). Defaults to "1984-01-01".

`end_date`
: Optional extraction end date (as string, format YYYY-MM-DD). Defaults to today's date.

`buffer_dist`
: Buffer distance around sample coordinates. Wrapper for lsat_get_pixel_centers() to find all Landsat pixel centers around each point in pixel_coords_sf within the specified buffer distance (square)). Can be slow if the number of points is large. Defaults to 0 m.

`scale`
: scale for extraction. Defaults to 30 m nominal Landsat pixel size.

`mask_value`
: Optional masking value for global surface water mask. Defaults to 0.

Value

List of initiated rgee tasks.

Author(s)

Jakob J. Assmann and Richard Massey

Examples

```
# Using sf, dplyr and rgee
library(sf)
library(dplyr)
library(rgee)

# Initialize EE
ee_Initialize()

# Generate test points
test_points_sf <- st_sfc(st_point(c(-149.6026, 68.62574)),
                         st_point(c(-149.6003, 68.62524)),
                         st_point(c(-75.78057, 78.87038)),
```

For Review Only

```
                             st_point(c(-75.77098, 78.87256)),
                             st_point(c(-20.56182, 74.47670)),
                             st_point(c(-20.55376, 74.47749)), crs = 4326) %>%
  st_sf() %>%
  mutate(sample_id = c("toolik_1",
                       "toolik_2",
                       "ellesmere_1",
                       "ellesmere_1",
                       "zackenberg_1",
                       "zackenberg_2"),
         region = c("toolik", "toolik",
                    "ellesmere", "ellesmere",
                    "zackenberg", "zackenberg"))

# Export time-series using lsat_export_ts()
task_list <- lsat_export_ts(test_points_sf)

# Export time-series using with a chunk size of 2
task_list <- lsat_export_ts(test_points_sf, max_chunk_size = 2)

# Export time-series in chunks by column
task_list <- lsat_export_ts(test_points_sf, chunks_from = "region")
```

`lsat_fit_phenological_curves`   *Characterize land surface phenology using spectral vegetation index time series*

Description

This function characterizes seasonal land surface phenology at each sample site using flexible cubic splines that are iteratively fit to time series of spectral vegetation indices (e.g., NDVI). This function facilitates estimating annual maximum NDVI and other spectral vegetation indices with lsat_summarize_growing_seasons(). For each site, cubic splines are iteratively fit to measurements pooled over years within a moving window that has a user-specified width. Each cubic spline is iteratively fit, with each iteration checking if there are outliers and, if so, excluding outliers and refitting. The function returns information about typical phenology at a sample site and about the relative phenological timing of each individual measurenent. This function was designed for situations where the seasonal phenology is hump-shaped. If you are using a spectral index that is typically negative (e.g., Normalized Difference Water Index) then multiply the index by -1 before running this function, then back-transform your index after running the lsat_summarize_growing_seasons() function.

Usage

```
lsat_fit_phenological_curves(
  dt,
  si,
  window.yrs = 7,
  window.min.obs = 20,
  si.min = 0.15,
  spar = 0.78,
  pcnt.dif.thresh = c(-30, 30),
```

For Review Only

```
  weight = TRUE,
  spl.fit.outfile = FALSE,
  progress = TRUE,
  test.run = FALSE
)
```

Arguments

dt	Data.table with a multi-year time series a vegetation index.
si	Character string specifying the spectral index (e.g., NDVI) to use for determining surface phenology. This must correspond to an existing column in the data.table.
window.yrs	Number specifying the focal window width in years that is used when pooling data to fit cubic splines (use odd numbers).
window.min.obs	Minimum number of focal window observations necessary to fit a cubic spline.
si.min	Minimum value of spectral index necessary for observation to be used when fitting cubic splines. Defaults to 0.15 which for NDVI is about when plants are present. Note that si.min must be >= 0 because the underlying spline fitting function will error out if provided negative values.
spar	Smoothing parameter typically around 0.70 - 0.80 for this application. A higher value means a less flexible spline. Defaults to 0.78.
pcnt.dif.thresh	Vector with two numbers that specifcy the allowable negative and positive percent difference between individual observations and fitted cubic spline. Observations that differ by more than these thresholds are filtered out and the cubic spline is iteratively refit. Defaults to -30% and 30%.
weight	When fitting the cubic splines, should individual observations be weighted by their year of acquisition relative to the focal year? If so, each observation is weighted by exp(-0.25*n.yrs.from.focal) when fitting the cubic splines.
spl.fit.outfile	(Optional) Name of output csv file containing the fitted cubic splines for each sample site. Useful for subsequent visualization.
progress	(TRUE/FALSE) Print a progress report?
test.run	(TRUE/FALSE) If TRUE, then algorithm is run using a small random subset of data and only a figure is output. This is used for model parameterization.

Value

Data.table that provides, for each observation, information on the phenological conditions for that specific day of year during the focal period. These data can then be used to estimate annual maximum spectral index and other growing season metrics using lsat_summarize_growing_season(). A figure is also generated that shows observation points and phenological curves for nine random sample locations.

Examples

```
data(lsat.example.dt)
lsat.dt <- lsat_format_data(lsat.example.dt)
lsat.dt <- lsat_clean_data(lsat.dt)
lsat.dt <- lsat_calc_spectral_index(lsat.dt, 'ndvi')
lsat.dt <- lsat_calibrate_rf(lsat.dt, band.or.si = 'ndvi',
```

For Review Only

```
write.output = FALSE, train.with.highlat.data = TRUE)
lsat.pheno.dt <- lsat_fit_phenological_curves(lsat.dt, si = 'ndvi')
lsat.pheno.dt
```

`lsat_format_data` *Formats Landsat data for analysis*

Description

This function takes Landsat data exported from GEE and formats it for subsequent use. The function parses sample site coordinates and time period of each measurement, scales band values, and formats column names as needed for subsequent analysis using the LandsatTS package.

Usage

```
lsat_format_data(dt)
```

Arguments

`dt` Data.table with Landsat data exported from Google Earth Engine using lsat_export_ts().

Value

Data.table with formatted and scaled values.

Examples

```
data(lsat.example.dt)
lsat.dt <- lsat_format_data(lsat.example.dt)
lsat.dt
```

`lsat_get_pixel_centers` *Get Landsat 8 pixel centers for a polygon or a buffered point*

Description

A convenience helper function that determines the Landsat 8 grid (pixel) centers within a polygon plus an optional buffer. It can also be applied to a single point to retrieve all pixels within a buffer.

Does not work for large polygons. The default maximum number of pixels set by EE is 10000000 this should not be exceeded. Consider whether extraction for a large polygon is a good idea, if yes split the polygon into manageable chunks.

For the unlikely case that a polygon exceeds the boundaries of the Landsat tile closest to the polygon's center, the polygon is clipped at the boundaries of the Landsat tile and a warning is issued. Again, if this is the case, consider processing smaller polygons instead.

Please note: The approximation of the tile overlap with the polygon generates a warning by the sf package that the coordinates are assumed to be planar. This can be ignored.

For Review Only

Usage

```
lsat_get_pixel_centers(
  polygon_sf,
  pixel_prefix = "pixel",
  pixel_prefix_from = NULL,
  buffer = 15,
  plot_map = F,
  lsat_WRS2_scene_bounds = NULL
)
```

Arguments

`polygon_sf` Simple feature with a simple feature collection of type "sfc_POLYGON" containing a single polygon geometry. Alternatively, a simple feature containing a simple feature collection of type 'sfc_POINT' with a single point.

`pixel_prefix` Prefix for the generated pixel identifiers (output column "sample_id"). Defaults to "pixel".

`pixel_prefix_from` Optional, a column name in the simple feature to specify the pixel_prefix. Overrides the "pixel_prefix" argument.

`buffer` Buffer surrounding the geometry to be included. Specified in m. Defaults to 15 m - the nominal half-width of a Landsat pixel.

`plot_map` Optional, default is FALSE. If TRUE the retrieved pixel centers and the polygon are plotted on a summer Landsat 8 image (grey-scale red band) using mapview. If a character is supplied an additional output to a file is generated (png, pdf, and jpg supported, see mapview::mapshot). Note: Both slow down the execution of this function notably, especially for large polygons! Only use in interactive R sessions.

`lsat_WRS2_scene_bounds` File path to the Landsat WRS2 path row scene boundaries. If not specified the boundaries are downloaded to a temporary file when the function is executed for the first time during a session. To avoid future downloads, the file may be downloaded manually and it's file path specified using this argument. The file can be found here: https://prd-wret.s3.us-west-2.amazonaws.com/assets/palladium/production/atoms/files/WRS-2_bound_world_0.kml See also: https://www.usgs.gov/core-science-systems/nli/landsat/landsat-shapefiles-and-kml-files

Value

sf object of point geometries for Landsat 8 pixel centers within the polygon or the buffer around the point coordinate specified. For use in lsat_export_ts().

Author(s)

Jakob J. Assmann

Examples

```
# Using sf, dplyr, rgee and purr
library(sf)
library(dplyr)
```

For Review Only

```
library(rgee)
library(purrr)

# Initialize EE
ee_Initialize()

# Specify a region to retrieve pixel centers for
test_poly_sf <- list(matrix(c(-138.90125, 69.58413,
              -138.88988, 69.58358,
              -138.89147, 69.58095,
              -138.90298, 69.57986,
              -138.90125, 69.58413),
            ncol = 2, byrow = TRUE)) %>%
           st_polygon() %>%
           st_sfc(crs = 4326) %>%
           st_sf()

# Retrieve pixel centers and plot to mapview
pixels <- lsat_get_pixel_centers(test_poly_sf, plot_map = TRUE)


## Ge pixel centers for multiple regions
# Create multi-polygon sf
ellesmere <- st_polygon(list(matrix(c(-75.78526, 78.86973,
                                      -75.78526, 78.87246,
                                      -75.77116, 78.87246,
                                      -75.77116, 78.86973,
                                      -75.78526, 78.86973),
                                      ncol = 2, byrow = TRUE)))
zackenberg <- st_polygon(list(matrix(c(-20.56254, 74.47469,
                                    -20.56254, 74.47740,
                                    -20.55242, 74.47740,
                                    -20.55242, 74.47469,
                                    -20.56254, 74.47469),
                                  ncol = 2, byrow = TRUE)))
toolik <- st_polygon(list(matrix(c(-149.60686, 68.62364,
                                   -149.60686, 68.62644,
                                   -149.59918, 68.62644,
                                   -149.59918, 68.62364,
                                   -149.60686, 68.62364),
                                   ncol = 2, byrow = TRUE)))
test_regions_sf <- st_sfc(ellesmere, zackenberg, toolik, crs = 4326) %>%
  st_sf() %>%
  mutate(region = c("ellesmere", "zackenberg", "toolik"))

# Split and map lsat_get_pixel_centers using dplyr and purrr
pixel_list <- test_regions_sf %>%
   split(.$region) %>%
   map(lsat_get_pixel_centers,
       pixel_prefix_from = "region") %>%
   bind_rows()
```

`lsat_neighborhood_mean` *Compute Neighborhood Average Landsat Surface Reflectance*

For Review Only

Description

For each band, this function computes average surface reflectance across neighboring voxels at a sample site. Use this function when working with Landsat data extracted for buffered points. Also, make sure to have previously cleaning the individual observations using lsat_clean_data().

Usage

```
lsat_neighborhood_mean(dt)
```

Arguments

`dt`	A data.table containing coincident surface reflectance measurements for multiple Landsat pixels at each sample site.

Value

A data.table with average surface reflectance

`lsat_plot_trend_hist` *Create a histogram summarizing relative temporal changes in a spectral index across all sample sites.*

Description

Create a histogram summarizing relative temporal changes in a spectral index across all sample sites.

Usage

```
lsat_plot_trend_hist(dt, xlim = c(-30, 30))
```

Arguments

`dt`	A data.table output from lsat_calc_trend()
`xlim`	Numeric vector specifying the minimum and maximum values for the histogram x-axis.

Value

A histogram generated by ggplot2

Examples

```
data(lsat.example.dt)
lsat.dt <- lsat_format_data(lsat.example.dt)
lsat.dt <- lsat_clean_data(lsat.dt)
lsat.dt <- lsat_calc_spectral_index(lsat.dt, 'ndvi')
# lsat.dt <- lsat_calibrate_rf(lsat.dt, band.or.si = 'ndvi', write.output = F)
lsat.pheno.dt <- lsat_fit_phenological_curves(lsat.dt, si = 'ndvi')
lsat.gs.dt <- lsat_summarize_growing_seasons(lsat.pheno.dt, si = 'ndvi')
lsat.trend.dt <- lsat_calc_trend(lsat.gs.dt, si = 'ndvi.max', yrs = 2000:2020)
lsat_plot_trend_hist(lsat.trend.dt)
```

For Review Only

`lsat_summarize_data` *Summarize availability of Landsat data for each sample site*

Description

This little function summarizes the temporal period and availability of observations at each sample site.

Usage

```
lsat_summarize_data(dt)
```

Arguments

`dt`	Data.table with columns named "sample.id" and "year".

Value

Data.table summarizing for each sample site the first, last, and number of years with observations, the minimum and maximum number of observations in a year, and the total number of observations across years. Also returns a figure showing the median (2.5 and 97.5 percentiles) number of observations per sample site across years for each Landsat satellite.

Examples

```
data(lsat.example.dt)
lsat.dt <- lsat_format_data(lsat.example.dt)
lsat.dt <- lsat_clean_data(lsat.dt)
lsat_summarize_data(lsat.dt)
```

For Review Only

`lsat_summarize_growing_seasons` *Summarize growing season characteristics using spectral vegetation indices*

Description

This function not only computes mean, median, and 90th percentile of a spectral index (SI) using observations for a user-specified "growing season," but also estimates the annual maximum SI and associated day of year using phenology modeling and growing season observations.

Usage

```
lsat_summarize_growing_seasons(
  dt,
  si,
  min.frac.of.max = 0.75,
  zscore.thresh = 3
)
```

Arguments

`dt`	Data.table generated by the function lsat_fit_phenological_curves().
`si`	Character string specifying the spectral vegetation index to summarize (e.g., NDVI).
`min.frac.of.max`	Numeric threshold (0-1) that defines the "growing season" as the seasonal window when the phenological curves indicate the SI is within a specified fraction of the maximum SI. In other words, an observation is considered to be from the "growing season" when the SI is within a user-specified fraction of the curve-fit growing season maximum SI.
`zscore.thresh`	Numeric threshold specifying the Z-score value beyond which individual observations are filtered before summarizing growing season SI.

Value

Data.table summarizing annual growing season conditions based on a spectral index.

Examples

```
data(lsat.example.dt)
lsat.dt <- lsat_format_data(lsat.example.dt)
lsat.dt <- lsat_clean_data(lsat.dt)
lsat.dt <- lsat_calc_spectral_index(lsat.dt, 'ndvi')
# lsat.dt <- lsat_calibrate_rf(lsat.dt, band.or.si = 'ndvi', write.output = F)
lsat.pheno.dt <- lsat_fit_phenological_curves(lsat.dt, si = 'ndvi')
lsat.gs.dt <- lsat_summarize_growing_seasons(lsat.pheno.dt, si = 'ndvi')
lsat.gs.dt
```

`noatak.dt` *Example Landsat data for the Noatak National Preserve*

Description

This dataset provides Landsat time series data for 100 random sample locations within the Noatak National Preserve, USA. These data were extracted from Google Earth Engine using the lsat_export_ts() function.

Usage

```
data("noatak.dt")
```

Format

A data frame with 99600 observations on the following 23 variables.

`'system:index'` a character vector

`CLOUD_COVER` a numeric vector

`COLLECTION_NUMBER` a numeric vector

`DATE_ACQUIRED` a IDate

`GEOMETRIC_RMSE_MODEL` a numeric vector

For Review Only

`LANDSAT_PRODUCT_ID` a character vector

`LANDSAT_SCENE_ID` a character vector

`PROCESSING_LEVEL` a character vector

`QA_PIXEL` a numeric vector

`QA_RADSAT` a numeric vector

`SPACECRAFT_ID` a character vector

`SR_B1` a numeric vector

`SR_B2` a numeric vector

`SR_B3` a numeric vector

`SR_B4` a numeric vector

`SR_B5` a numeric vector

`SR_B6` a numeric vector

`SR_B7` a numeric vector

`SUN_ELEVATION` a numeric vector

`chunk_id` a character vector

`max_extent` a numeric vector

`sample_id` a character vector

`.geo` a character vector

Source

Generate as example data for Berner et al. (2023)

References

Landsat data are provided by the United States Geological Survey

For Review Only

`noatak.sf` *Noatak National Preserve Simple Feature*

Description

This dataset provides the spatial boundary of the Noatak National Preserve, USA, as a multipolygon simple feature.

Usage

```
data("noatak.sf")
```

Format

A simple feature data frame with 1 observations on the following 20 variables.

`OBJECTID` a numeric vector

`UNIT_CODE` a character vector

`GIS_Notes` a character vector

`UNIT_NAME` a character vector

`DATE_EDIT` a character vector

`STATE` a character vector

`REGION` a character vector

`GNIS_ID` a character vector

`UNIT_TYPE` a character vector

`CREATED_BY` a character vector

`METADATA` a character vector

`PARKNAME` a character vector

`CreationDa` a character vector

`Creator` a character vector

`EditDate` a character vector

`Editor` a character vector

`GlobalID` a character vector

`Shape_Leng` a numeric vector

`Shape_Area` a numeric vector

`geometry` a sfc_MULTIPOLYGON

Source

Downloaded from https://irma.nps.gov/DataStore/Reference/Profile/2296705

References

US National Park Service. 2022. Administrative Boundaries of National Park System Units - National Geospatial Data Asset (NGDA) NPS National Parks Dataset. NPS - Land Resources Division. https://irma.nps.gov/DataStore/Reference/Profile/2296705

Examples

```
data(noatak.sf)
plot(noatak.sf)
```

For Review Only

Index

For Review Only